A Global View of Sediment Transport in Alluvial Systems

Kolumban Hutter* Ioana Luca†

*Bergstrasse 5, 8044 Zürich, Switzerland, hutter@vaw.baug.ethz.ch,
†Dept. Math. Methods and Models, Univ. Politehnica of Bucharest,
Splaiul Independentei 313, 060042 Bucharest, Romania, iolucaro@yahoo.com

May 21, 2012

Abstract

Sediment transport arises in alluvial lake-river systems in two different forms: (i) as bed load, comprising the moving detritus of the river bed and of the shallow, often only near-shore regions, and (ii) the suspended sediment load of the finer fractions. In river hydraulics the latter are often neglected; so, the bed load transport is treated without back-coupling with the wash-load. This is justified on decadal time scales. In the deeper parts of lakes wind-induced shearing in the benthic boundary layer hardly mobilizes the bed material, which stays immobile for most time and may be set in motion only interruptedly. However, the particle laden fluid transports the suspended material, which is advected and may on longer time scales settle in deposition-prone regions. In general, the deposition to and erosion from the basal surface occur concurrently. This environmental interplay is studied in this article.

The slurry - a mixture of the bearer fluid and particles of various sizes – is treated as a mixture of class I, in which mass, momentum and energy balances for the mixture as a whole are formulated to describe the geophysical fluid mechanical setting, whilst the suspended solid particles move through the bearer medium by diffusion. The governing equations of this problem are formulated, at first for a compressible, better non-density preserving, mixture. They thus embrace barotropic and baroclinic processes. These equations, generally known as Navier-Stokes-Fourier-Fick (NSFF) fluids, are subjected to turbulent filter operations and complemented by zeroth and first order closure schemes. Moreover, simplified versions, e.g. the (generalized) Boussinesq, shallow water and hydrostatic pressure assumptions are systematically derived and the corresponding equations presented in both conservative and non-conservative forms. Beyond the usual constitutive postulates of NSFF–fluids and turbulent closure schemes the non-buoyant suspended particles give rise to settling velocities; these depend on the particle size, expressed by a nominal particle diameter. A review of the recent hydraulic literature of terminal settling velocities is given. It shows that the settling velocity depends on the particle diameter and on the particle Reynolds number.

A separate section is devoted to the kinematic and dynamic boundary conditions on material and non-material singular surfaces as preparation for the mathematical-physical description of the sediment transport model, which follows from an analysis of jump transition conditions at the bed.

The simplest description of detritus transport does not use the concept of the motion of a thin layer of sediments. It treats it as a singular surface, which is equipped

with surface grains of various grain size diameters. Such a simplified theoretical level is also used in this article; it implies that solid mass exchange, as erosion and deposition of different particle size fractions, is the only physical quantity relevant in the description of the sediment transport. It entails formulation of surface mass balances of an infinitely thin detritus layer for the sediment and surface momentum balance of the mixture. The deposition rate of the various grain fractions, expressed as grain classes, follows from a parameterization of the free fall velocity of isolated particles in still water, but is in general coupled with the local flow and then follows from the solution of the hydrodynamic equations and the processes at the basal surface. The erosion rate is governed by two statements, (a) a fracture criterion determining the threshold value of a stress tensor invariant at the basal surface, which separates existence and absence regimes of erosion, and (b) determination of the amount of erosion beyond the threshold value of the mentioned stress invariant.

Contents

1 Description of the sediment transport model

The spatially one-dimensional model for the formation of deltas due to alluvial sediment progradation from straight rivers provides enlightening insight into the physical behaviour of the interacting processes which are exhibited by the sedimentary erosion and deposition in river-lake systems. Laboratory experiments demonstrated excellent agreement between the theoretical predictions of the two limiting forms of the evolving deltas - GILBERT-type 'triangular subaqeous slopes' under hypo- and homo-pycnal conditions and smoothly evolving weakly curved foreset depositions so generated by turbulent density-under currents. The laboratory experiments reflect realistic flow states, but the theory was shown to equally reproduce realistic conditions, when in a linear valley an elongated lake is formed by steady sediment deposits from a side tributary and when, under special conditions, it may relatively quickly again disintegrate. Practically of significance is also the development of the sediment regime in an elongated reservoir after its construction; large sediment input through the decades after dam erection may fill the reservoir and make flushing scenarios necessary through a bottom outlet or a side-pass tunnel. Qualitatively, these scenarios can also be described by the model.

It is, however, clear that multi-dimensionality of the sedimentary processes generally prevails in a river mouth and its vicinity, especially in mountainous lakes of complex geometry, see Figs. 1, 2. Moreover, the sediment loads generally occur in two different forms, as (i) bed load, comprising the moving grains of the alluvial river bed or the frontal part of the delta, formed and evolved by the coarser sediment fractions of the prograding processes, and (ii) the suspended sediment load of the finer fractions (usually clay and silt). Both participate in the formation of the bottom boundary and its evolution in time and space, on the one hand by deposition or settling processes of the suspended, non-buoyant fines according to the local water current, which they are exposed to, and, on the other hand, by motion cessation, re-suspension of the sliding, rolling and saltation particles of the bed load and their consequential transports in suspension.

It transpires that the settling and re-suspension of particles depend upon (i) the state of the water flow above the sediment bed and the wind induced barotropic or baroclinic current in the wider vicinity of the river mouth, and (ii) the grain size distribution of the alluvial sediments. In deposition processes of the suspension load, often also called *wash load*, the coarser grains will settle out first, followed by the smaller ones. So, the slurry-like upper water layer will be subject to persistent particle size segregation and consequential alteration and steepening of the grain size curve. It is evident that an adequate model for the suspended sediment load must be formulated as a mixture of a pure fluid with

Figure 1: Channelized entrance of the river Rhine (Alpen-Rhein) into Lake Constance at Fussach, near Bregenz, showing alternating sandbanks within the artificial channel and a large patch of suspended sediments in front of the river mouth. The island on the right frame is Lindau. Copyright: 'Tino Dietsche - airpics4you.ch'

a number of solid constituents, each representative of a specific grain size range, and expressed as a balance of mass of its size-range with FICKian parameterization of its flux and vanishing production rate.[1]

In much the same way the moving sediment bed is equally composed of grains of different sizes, generally coarser than those of the suspended load. The material in this moving layer may again be interpreted as a mixture of a number of particles in very narrow size ranges plus an interstitial fluid. Except for eruptive intermittent bursts over which an averaging of the particle motions and the fluid might be justified on time scales relevant for sediment transport, all these components have nearly the same velocity, but it turns out that nevertheless balance laws of mass and momenta for the constituents need to be formulated. Because of its small thickness the moving sediment layer may then be viewed as a singular surface equipped with mass and momentum for which two-dimensional mass and momentum balances are to be formulated. Its mass density changes by deposition of fines from the wash load and re-suspension of the eroded components from the moving bed.

The likely computational procedures for the moving sediment bed can be either a continuum approach as stipulated above, or application of molecular dynamics of the par-

[1]It is assumed that no fragmentation of particles into sizes other than those in the own size-range occurs.

Figure 2: Close-up to the mouth of the river Rhine (Alpen-Rhein) at Fussach, near Bregenz, showing the right river dam and the suspended sediments (wash-load) with the strong spatial variation of its concentration. Copyright: 'Tino Dietsche - airpics4you.ch'

ticles interacting with each other and with the fluid, better and more adequately known as **D**iscrete **E**lement **M**ethod (DEM). This approach has been carefully studied in a Ph.-D. thesis by VETSCH (2011) [49], but the method is presently not sufficiently advanced to warrant a detailed presentation here. Consequently, the text below will be based on the continuum approach, but, of course, with implementation of additional simplifying assumptions. One is the complexity of the mixture formulation. The most detailed situation prevails when each component is equipped with its own density, velocity and temperature. For each of them balances of mass, momenta and energy must then be accounted for. HUTTER & JÖHNK (2004) [17], p. 255, call this a *mixture of class III.* When heat exchange between the constituents is rapid, all constituents possess (nearly) the same temperature; then it suffices to only consider the energy balance of the mixture as a whole, involving a single temperature field, while balances of mass and momentum of all the constituents are kept. This defines a *mixture of class II.* Still a further simplification is possible, if for some reason all constituents except one arise in small concentrations and have nearly the same velocity as the dominant bearer fluid. Such conditions prevail for the salts defining the mineralisation or salinity of lake or ocean water. In this case it may suffice to formulate also momentum balance for the mixture as a whole and to account for the variation of the concentrations of the constituent masses by their mass balances. This defines a *mixture of class I.* This is the principal conceptual formulation of the sediment transport as wash and bed loads for which the balances of momentum and energy are formulated for the

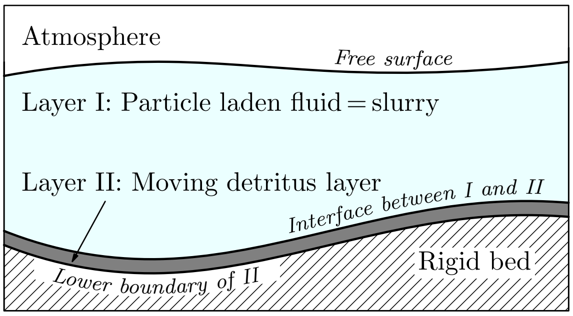

Figure 3: Lake domain divided into the large particle laden fluid part, I, and the moving detritus layer, II, with indicated boundaries: free surface, interface between I & II, and the lower boundary of the detritus layer where no grains move.

mixture as a whole, but balances of mass for each tracer individually and for the mixture as a whole.

Which mixture class ought to be applied depends on the sort and scale of application in focus. For hydraulic and possibly also geologic applications bed-load is likely restricted to near shore zones and the vicinity of river mouths. [Exceptions are, of course, large, very shallow lakes of, say, less than 5 m maximum depth (Neusiedler See, Austria/Hungary; Lake Taihu China; Northern part of Caspian Sea).] On the other hand, the suspended particle phase can be ignored in most interior parts of less shallow lakes for shorter, hydraulically relevant, e.g. decadal time scales, but ought to be considered for variations over geologically relevant time scales over centuries and millennia. In near shore zones and close to river mouths, particle laden mixtures will likely govern the wash and bed load transports.

The above description indicates that for certain questions, bed load movement or relatively rapid depositing or erosive detritus rates are localized to sub-regions of, but not subject to, the entire lake. In such cases application of *sub-structuring* or *nesting* is suggested, of which the use is as follows: Global, e.g. wind induced processes of the entire homogeneous or stratified lake are investigated with a judiciously simplified model (e.g. in which bed load movement is ignored) and a discretisation allowing determination of the current, (temperature and particle concentration[2]) fields within the entire lake, however, with values of the field variables only at the grid points of the relatively large meshes of the lake-scale global problem. A sub-region of the lake in the vicinity of the river mouth and the lowest part of the river is subsequently selected and the governing equations describing the dynamics of the upper-layer and the bed load are then discretized with a much finer net than the equations of the global, whole lake analysis. At the open, lake-ward boundaries the flux conditions must then be properly transferred as boundary values for the boundary value problem, valid in the sub-region within which the evaluation of the bottom topography in the river mouth region is determined.

In the subsequent analysis the lake domain will at least be subdivided into two layers,

[2]Often these fields may even be dropped and simply assumed to be frozen to the fluid particles.

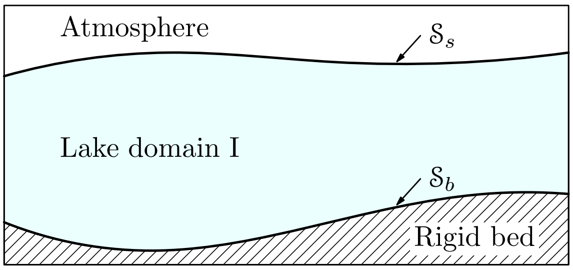

Figure 4: Lake domain bounded by the free surface $\mathcal{S}_s$ and the basal surface $\mathcal{S}_b$.

see Fig. 3. In the upper layer the lake water will be treated as a particle laden, possibly turbulent BOUSSINESQ fluid subject to the shallow water approximation.[3] This layer may, at a later stage be further sub-divided into sub-layers for computational reasons or in order to model stratification. The second layer is the domain of the sliding, rolling and saltating sediment, saturated by fluid. Its upper boundary will, in general, move or deform, and it defines the bathymetric profile of the lake bottom as a function of time and space. Its lower boundary marks the upper boundary of the rigid immobile solid bed. In comparison to the upper layer, this second layer is very thin, and it may well be thought to be describable by an infinitely thin sheet of which the physical properties must account for its finite thickness.[4] We will conceive layer II as a singular surface separating the rigid bed and layer I, see Fig. 4, being equipped with its own material properties and balance laws.

Layer I is interacting at its upper surface with the atmosphere; wind-shear transfers momentum to it, and solar irradiation may give rise to changes in the stratification. The interface between the two layers is non-material in general unless neither suspended material from layer I is deposited nor certain fractions of the bed-load in layer II are (re)-suspended into layer I. This fact makes adequate definition of the interface between the two layers difficult. Experience with laboratory experiments, however, shows that under given dynamical conditions immediately above the interface, grains above the corresponding minimum grain diameter do not erode, i.e. are not lifted into layer I (for a substantial amount of time), but stay within the detritus layer. This implies that an erosion inception condition which depends on the particle diameter must be established.

2 Governing equations in lake domain I

The field equations in lake domain I are formulated at this general level as those for turbulent motion of a BOUSSINESQ fluid of a mixture of class I. We briefly explain the derivation of these equations.

[3]The focus is not on strong internal baroclinic motion but rather on the reproduction of the current near the basal surface (e.g. the benthic boundary layer).

[4]In the theory of interfaces such sheets are called *diffuse interfaces.*

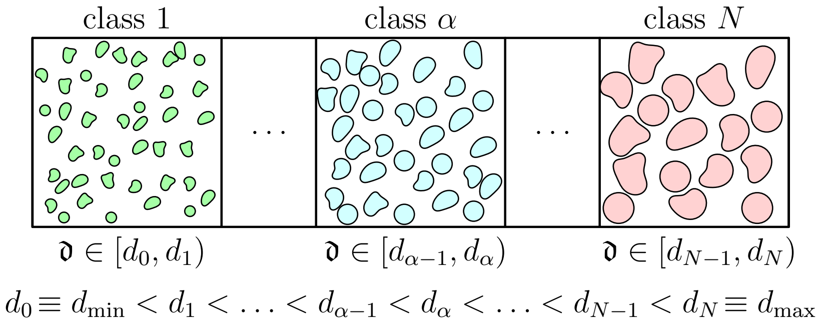

Figure 5: Partition of the interval $[d_{\min}, d_{\max})$, in which the nominal particle diameters range, into N disjoint subsets, each of them defining a particle class; $\mathfrak{d}$ is the nominal particle diameter.

2.1 Laminar flow

The solid particles surrounded by the bearer fluid possess nominal diameters in the interval $[d_{\min}, d_{\max})$, $d_{\min} < d_{\max}$. This interval is partitioned into N subintervals, and so particles in $[d_{\alpha-1}, d_\alpha)$ define the α-th particle class, see Fig. 5.[5] Such a class is modelled as a continuous body with its own motion and rheology. Thus, at the level of fine resolution (at which methods of direct numerical simulation are applicable) the slurry is modelled as a continuous mixture consisting of a fluid and N solid constituents (classes). Moreover, since the solid particles are dragged on by the fluid with nearly the same velocity as that of the fluid, a mixture of class I is an appropriate concept to be applied for the description of the slurry flow. The equations describing this flow take then the forms

- Balance of mass for the mixture

$$\frac{\mathrm{d}\,\rho}{\mathrm{d}\,t} + \rho\,\mathrm{div}\,\boldsymbol{v} = 0\,; \tag{1}$$

- Balance of momentum for the mixture

$$\rho \left\{ \frac{\mathrm{d}\,\boldsymbol{v}}{\mathrm{d}t} + 2\boldsymbol{\Omega} \times \boldsymbol{v} \right\} = -\mathrm{grad}\;p + \mathrm{div}\,\boldsymbol{\sigma}_E + \rho\boldsymbol{g}\,; \tag{2}$$

- Balance of mixture energy

$$\begin{aligned} \rho\,\frac{\mathrm{d}\epsilon}{\mathrm{d}\,t} &= -\mathrm{div}\,\boldsymbol{q} - p\,\mathrm{div}\,\boldsymbol{v} + \mathrm{tr}\,(\boldsymbol{\sigma}_E\boldsymbol{D})\,, \quad \text{or}^6 \\ \rho\,\frac{\mathrm{d}h}{\mathrm{d}\,t} - \frac{\mathrm{d}\,p}{\mathrm{d}\,t} &= -\,\mathrm{div}\,\boldsymbol{q} + \mathrm{tr}\,(\boldsymbol{\sigma}_E\boldsymbol{D})\,, \end{aligned} \tag{3}$$

[5] This is motivated by sieve experiments: one has a whole column of sieves, numbered $0, \ldots, \alpha, \ldots, N-1$, with the largest mesh size on top and the smallest at the bottom; class α ($\alpha = 1, \ldots, N$) consists of those particles which are collected by sieve $\alpha - 1$. It is tacitly understood that the sieve with number '0' is impermeable for all particles of sizes larger than a chosen minimum (say for clay and silt fractions which cannot pass very small holes simply because of cohesion coalescence).

in which h is the mixture enthalpy,

$$h \equiv \epsilon + \frac{p}{\rho}\,; \tag{4}$$

- Balance of tracer mass of constituent α

$$\rho\,\frac{\mathrm{d}\,c_\alpha}{\mathrm{d}\,t} = -\mathrm{div}\,\{\boldsymbol{j}_\alpha - \rho\,c_\alpha \boldsymbol{w}^s_\alpha\} + \phi^{(c_\alpha)}, \quad \alpha = 1, \ldots, N\,. \tag{5}$$

In these equations ρ is the mixture density, $\boldsymbol{v}$ is the barycentric velocity, p, $\boldsymbol{\sigma}_E$, ϵ, $\boldsymbol{q}$, are the pressure, the extra stress tensor, the internal energy and the heat flux vector, respectively, all referring to the mixture as a whole, $\boldsymbol{g}$ is the gravity vector, and $\boldsymbol{\Omega}$ ($|\boldsymbol{\Omega}| = 7.272 \times 10^{-5}\,[\mathrm{s}^{-1}]$) is the angular velocity of the rotation of the Earth. (As customary in Geophysical Fluid Dynamics, the EULER acceleration is ignored and the centripetal acceleration is thought to be incorporated in the gravity term.) Moreover, we use the notation

$$\frac{\mathrm{d}\,(\cdot)}{\mathrm{d}\,t} \equiv \frac{\partial\,(\cdot)}{\partial\,t} + (\mathrm{grad}\,(\cdot))\,\boldsymbol{v}\,, \quad \boldsymbol{D} \equiv \mathrm{sym}\,(\mathrm{grad}\,\boldsymbol{v}) = \tfrac{1}{2}(\boldsymbol{L} + \boldsymbol{L}^T) \text{ with } \boldsymbol{L} \equiv \mathrm{grad}\,\boldsymbol{v}\,, \tag{6}$$

as the substantive derivative following the barycentric motion, and the strain rate or rate of strain or stretching tensor $\boldsymbol{D}$ of the barycentric velocity, respectively. Finally, the balance law of tracer mass of constituent α, (5), requires special justification. It is easy to show that the mass balance law of constituent α, $\partial\rho_\alpha/\partial\,t + \mathrm{div}\,(\rho_\alpha \boldsymbol{v}_\alpha) = \phi^{(c_\alpha)}$, where ρ_α, $\boldsymbol{v}_\alpha$ and $\phi^{(c_\alpha)}$ are the density, the velocity and the mass production rate density of constituent α, can be written as

$$\rho\,\frac{\mathrm{d}\,c_\alpha}{\mathrm{d}\,t} = -\mathrm{div}\,\boldsymbol{\mathfrak{J}}_\alpha + \phi^{(c_\alpha)}\,, \tag{7}$$

in which $c_\alpha, \boldsymbol{\mathfrak{J}}_\alpha$ are the mass fraction or concentration and the diffusive-advective mass flux of constituent α, respectively:

$$c_\alpha \equiv \frac{\rho_\alpha}{\rho}\,, \quad \boldsymbol{\mathfrak{J}}_\alpha \equiv \rho c_\alpha (\boldsymbol{v}_\alpha - \boldsymbol{v})\,. \tag{8}$$

We recall that the constituent α is composed of particles of various diameters ranging in $[d_{\alpha-1}, d_\alpha)$. Thus, one may think of class α as a continuous mixture of a finite number of constituents. A possibility to account for this fact is to introduce the decomposition

$$\boldsymbol{\mathfrak{J}}_\alpha = \underbrace{\rho c_\alpha (\boldsymbol{v}_\alpha - \boldsymbol{v}^s_\alpha)}_{\equiv\, \boldsymbol{j}_\alpha} + \underbrace{\rho\,c_\alpha (\boldsymbol{v}^s_\alpha - \boldsymbol{v})}_{\equiv\, -\rho\,c_\alpha \boldsymbol{w}^s_\alpha}\,, \tag{9}$$

[6]Consider the term $p\,\mathrm{div}\,\boldsymbol{v}$ on the right-hand side of $(3)_1$. With the aid of (1) this takes the form

$$-p\,\mathrm{div}\,\boldsymbol{v} = \frac{p}{\rho}\frac{\mathrm{d}\,\rho}{\mathrm{d}\,t} = -\rho\frac{\mathrm{d}}{\mathrm{d}\,t}\left(\frac{p}{\rho}\right) + \frac{\mathrm{d}\,p}{\mathrm{d}\,t}\,.$$

Therefore, the balance of mixture energy may also be written as

$$\rho\frac{\mathrm{d}}{\mathrm{d}\,t}\left(\epsilon + \frac{p}{\rho}\right) - \frac{\mathrm{d}\,p}{\mathrm{d}\,t} = -\,\mathrm{div}\,\boldsymbol{q} + \mathrm{tr}\,(\boldsymbol{\sigma}_E \boldsymbol{D})\,,$$

suggesting the definition of the mixture enthalpy (4). In almost density preserving materials the term $p\,\mathrm{div}\,\boldsymbol{v}$ in $(3)_1$ and the term $\mathrm{d}\,p/\mathrm{d}\,t$ in $(3)_2$ are generally ignored, which implies $\mathrm{d}\epsilon/\mathrm{d}\,t \approx \mathrm{d}h/\mathrm{d}\,t$, which is the reason why one can often see in the literature both formulations using ϵ or h.

where $\boldsymbol{v}_\alpha^s$ is the velocity of a *representative* granular constituent (perhaps that one with greatest concentration or that with the mean diameter) of the mixture class α. Thus, $\boldsymbol{j}_\alpha$ is now the diffusive flux of the constituent α with respect to the representative particle in the class α. For this flux term a gradient type constitutive relation will be postulated in the spirit of FICK's law. The second term expresses the advected flux of the representative particle relative to the barycentric motion. For this advected flux a constitutive relation is postulated. In sediment transport work a rather restricted but courageous statement is made:

$$\boldsymbol{w}_\alpha^s = w_\alpha^s \boldsymbol{e}_z \iff \rho c_\alpha(\boldsymbol{v}_\alpha^s - \boldsymbol{v}) = -\rho c_\alpha w_\alpha^s \boldsymbol{e}_z \,, \tag{10}$$

where $w_\alpha^s > 0$ is the terminal free falling velocity of the selected representative particle in still water, and $\boldsymbol{e}_z$ is the unit vector against the gravity vector.[7] This is how $w_\alpha^s \boldsymbol{e}_z$ would enter formula (5). Of course, in reality this is not correct; perhaps as an approximation, non-vanishing horizontal components of $\boldsymbol{w}_\alpha^s$ are expected. A likely better choice may be

$$\boldsymbol{w}_\alpha^s = w_\alpha^s \left\{ \tan\theta \frac{\boldsymbol{v}_H}{\|\boldsymbol{v}_H\|} + \boldsymbol{e}_z \right\} \,, \tag{11}$$

where

$$\boldsymbol{v}_H \equiv \{\boldsymbol{v} - (\boldsymbol{v}\cdot\boldsymbol{e}_z)\boldsymbol{e}_z\}_{\mathcal{S}_b} \tag{12}$$

is the horizontal velocity at the basal surface $\mathcal{S}_b$, see Fig. 3, and θ is a tilt angle (approx. 0° or somewhat larger) to be determined. More generally, determination of the motion of a solid particle immersed in a moving fluid is a difficult specialized topic of interaction dynamics.

The above balance equations can also easily be transformed to *conservative form* by judiciously combining them with the balance equation of mass (1). Often these forms are better suited to numerical implementation. This yields[8]

- Balance of mass for the mixture

$$\frac{\partial \rho}{\partial t} + \operatorname{div}(\rho \boldsymbol{v}) = 0\,; \tag{13}$$

[7]For a non-buoyant particle α falling in still water we have $\boldsymbol{w}_\alpha^s \equiv -(\boldsymbol{v}_\alpha^s - \boldsymbol{v}) = w_\alpha^s \boldsymbol{e}_z$; here $\boldsymbol{v}_\alpha^s$ is the velocity of the solid particle, and $\boldsymbol{v} \approx \boldsymbol{0}$ is the velocity of the surrounding fluid at rest. When the grain stops to decelerate it has attained the so-called terminal settling velocity or free fall velocity.

[8](a) Using (1) yields for the left-hand side of (2)

$$\rho\frac{\mathrm{d}\boldsymbol{v}}{\mathrm{d}t} = \frac{\mathrm{d}\rho\boldsymbol{v}}{\mathrm{d}t} - \frac{\mathrm{d}\rho}{\mathrm{d}t}\boldsymbol{v} \overset{(1)}{=} \frac{\mathrm{d}\rho\boldsymbol{v}}{\mathrm{d}t} + (\rho\operatorname{div}\boldsymbol{v})\boldsymbol{v} = \frac{\partial\rho\boldsymbol{v}}{\partial t} + \operatorname{div}(\rho\boldsymbol{v}\otimes\boldsymbol{v}),$$

whilst the right-hand side remains unchanged.

(b) Using (1), for a scalar function f we obtain

$$\rho\frac{\mathrm{d}f}{\mathrm{d}t} = \frac{\mathrm{d}\rho f}{\mathrm{d}t} - \frac{\mathrm{d}\rho}{\mathrm{d}t}f \overset{(1)}{=} \frac{\mathrm{d}\rho f}{\mathrm{d}t} + (\rho\operatorname{div}\boldsymbol{v})f = \frac{\partial\rho f}{\partial t} + \operatorname{div}(\rho f\boldsymbol{v}),$$

which turns (3) and (5) into (15) and (16), respectively.

- Balance of momentum for the mixture

$$\frac{\partial(\rho \boldsymbol{v})}{\partial t} + \operatorname{div}(\rho \boldsymbol{v} \otimes \boldsymbol{v}) + 2\rho \boldsymbol{\Omega} \times \boldsymbol{v} = \operatorname{div}(-p\boldsymbol{I} + \boldsymbol{\sigma}_E) + \rho \boldsymbol{g}\,; \tag{14}$$

- Balance of mixture energy

$$\begin{aligned} &\frac{\partial(\rho\epsilon)}{\partial t} + \operatorname{div}(\rho\epsilon\boldsymbol{v}) = -\operatorname{div}\boldsymbol{q} - p\operatorname{div}\boldsymbol{v} + \operatorname{tr}(\boldsymbol{\sigma}_E\boldsymbol{D}) \quad \text{or} \\ &\frac{\partial(\rho h)}{\partial t} + \operatorname{div}(\rho h\boldsymbol{v}) - \left\{\frac{\partial p}{\partial t} + \operatorname{grad} p\cdot\boldsymbol{v}\right\} = -\operatorname{div}\boldsymbol{q} + \operatorname{tr}(\boldsymbol{\sigma}_E\boldsymbol{D})\,; \end{aligned} \tag{15}$$

- Balance of tracer mass α

$$\frac{\partial(\rho\, c_\alpha)}{\partial t} + \operatorname{div}(\rho\, c_\alpha \boldsymbol{v}) = -\operatorname{div}(\boldsymbol{j}_\alpha - \rho\, c_\alpha \boldsymbol{w}^s_\alpha) + \phi^{(c_\alpha)}\,, \quad \alpha = 1,\dots,N. \tag{16}$$

2.2 Turbulent motion

For the turbulent motion it is common usage to average equations (13)–(16) by applying adequate filter operations to the balance laws. If the filter operation is denoted by $\langle\cdot\rangle$, any field variable f can be composed of its average $\langle f \rangle$ and fluctuation f' according to

$$f = \langle f \rangle + f'\,, \quad f' \equiv f - \langle f \rangle\,. \tag{17}$$

If this decomposition is applied to all field variables and a statistical filter with the property $\langle\langle\cdot\rangle\rangle = \langle\cdot\rangle$ is chosen, the filter operation is called REYNOLDS averaging. For example, the averaged balance law of mass (13) takes the form

$$\frac{\partial\langle \rho \rangle}{\partial t} + \operatorname{div}(\langle \rho \rangle\langle \boldsymbol{v}\rangle) = -\operatorname{div}(\langle \rho' \boldsymbol{v}'\rangle)\,. \tag{18}$$

Evidently, the correlation $\langle \rho' \boldsymbol{v}' \rangle$ only arises because of density variations due to turbulence. The turbulent mass flux on the right-hand side of (18) is the only place of all averaged balance laws, where such a term arises. It is small for nearly density preserving fluids and will then be ignored.[9]

Rather than referring to the general balance laws (13)–(16) we consider the balance laws (i) corresponding to a generalized BOUSSINESQ fluid and (ii) those obtained with the assumption that the density fluctuations are negligibly small.

[9] If for the velocity the so-called FAVRE averaging operator is employed,

$$\{\boldsymbol{v}\} \equiv \frac{\langle \rho \boldsymbol{v}\rangle}{\langle \rho \rangle}\,, \tag{19}$$

then the averaged mass balance takes the form

$$\frac{\partial\langle \rho \rangle}{\partial t} + \operatorname{div}(\langle \rho \rangle\{\boldsymbol{v}\}) = 0\,. \tag{20}$$

So, Favre averaging would preserve the invariance of the balance of mass under filtering. However, this would also imply consequences in the remaining balance laws. A complete derivation using FAVRE averaging is e.g. given in LUCA et al. (2004) [26]. We prefer to stay with (18).

2.2.1 Model 1: Generalized BOUSSINESQ fluid

A BOUSSINESQ *fluid* is defined as a fluid for which density variations are ignored except in the gravity term of the momentum equation. Balance of mass then reduces to div $\boldsymbol{v} = 0$, agreeing with the continuity equation of density preserving continua. A somewhat more general assumption is as follows, see e.g. Hutter et al. [18]:

$$\begin{aligned}&\text{(i) } \rho = \rho_0(z) + \rho_d(\boldsymbol{x}, t),\\ &\text{(ii) } \rho_d(\boldsymbol{x}, t) \text{ is everywhere ignored except in the gravity term.}\end{aligned} \tag{21}$$

We call this the *generalized* BOUSSINESQ *assumption.* In (21), $\rho_0(z)$ is a static density field, which in a lake usually represents the stable stratification induced by radiation. For $\rho_0(z) =$ constant, (21) reduces to the classical BOUSSINESQ assumption. Owing to $(21)_{(\mathrm{i})}$, with

$$p = p_d + p_{st}, \quad p_{st} \equiv g \int_0^z \rho_0(\xi) \mathrm{d}\xi \,, \tag{22}$$

where g is the gravity constant, we introduce the dynamic, p_d, and the 'quasi-static', p_{st}, pressures, which implies

$$-\mathrm{grad}\; p = -\mathrm{grad}\; p_d - \rho_0(z)\, \boldsymbol{g} \,. \tag{23}$$

With (21)–(23), the physical balance laws (1)–(3), (5) subjected to the generalized BOUSSINESQ assumption take the forms

- Balance of mass for the mixture

$$\mathrm{div}\, \rho_0 \boldsymbol{v} = 0 \,; \tag{24}$$

- Balance of momentum for the mixture

$$\rho_0 \left\{ \frac{\mathrm{d}\,\boldsymbol{v}}{\mathrm{d}\,t} + 2\boldsymbol{\Omega} \times \boldsymbol{v} \right\} = -\mathrm{grad}\; p_d + \mathrm{div}\, \boldsymbol{\sigma}_E + (\rho - \rho_0)\boldsymbol{g} \,; \tag{25}$$

- Balance of mixture energy

$$\rho_0 \frac{\mathrm{d}\,\epsilon}{\mathrm{d}\,t} = -\mathrm{div}\, \boldsymbol{q} - p\, \mathrm{div}\, \boldsymbol{v} + \mathrm{tr}\, (\boldsymbol{\sigma}_E \boldsymbol{D}) \quad \text{or} \quad \rho_0 \frac{\mathrm{d}\,h}{\mathrm{d}\,t} - \frac{\mathrm{d}\,p}{\mathrm{d}\,t} = -\mathrm{div}\, \boldsymbol{q} + \mathrm{tr}\, (\boldsymbol{\sigma}_E \boldsymbol{D}) \,; \tag{26}$$

- Balance of tracer mass of constituent α

$$\rho_0 \frac{\mathrm{d}\,c_\alpha}{\mathrm{d}\,t} = -\mathrm{div}\, \{\boldsymbol{j}_\alpha - \rho_0\, c_\alpha \boldsymbol{w}^s_\alpha\} + \phi^{(c_\alpha)}, \quad \alpha = 1, \ldots, N \,, \tag{27}$$

or in the alternative, conservative forms, see (13)–(16),

- Balance of mass for the mixture

$$\mathrm{div}\, \rho_0 \boldsymbol{v} = 0 \,; \tag{28}$$

- Balance of momentum for the mixture

$$\frac{\partial\,(\rho_0 \boldsymbol{v})}{\partial\, t} + \operatorname{div}(\rho_0 \boldsymbol{v}\otimes\boldsymbol{v}) + 2\rho_0\boldsymbol{\Omega}\times\boldsymbol{v} = \operatorname{div}(-p_d\boldsymbol{I} + \boldsymbol{\sigma}_E) + (\rho-\rho_0)\boldsymbol{g}\,; \tag{29}$$

- Balance of mixture energy

$$\begin{gathered}\frac{\partial\,(\rho_0\epsilon)}{\partial\, t} + \operatorname{div}(\rho_0\epsilon\boldsymbol{v}) = -\operatorname{div}\boldsymbol{q} - p\operatorname{div}\boldsymbol{v} + \operatorname{tr}(\boldsymbol{\sigma}_E\boldsymbol{D}) \quad \text{or}\\ \frac{\partial\,(\rho_0 h)}{\partial\, t} + \operatorname{div}(\rho_0 h\boldsymbol{v}) - \left\{\frac{\partial\, p}{\partial t} + \operatorname{grad} p\cdot\boldsymbol{v}\right\} = -\operatorname{div}\boldsymbol{q} + \operatorname{tr}(\boldsymbol{\sigma}_E\boldsymbol{D})\,;\end{gathered} \tag{30}$$

- Balance of tracer mass of constituent α

$$\frac{\partial(\rho_0\, c_\alpha)}{\partial\, t} + \operatorname{div}(\rho_0\, c_\alpha\boldsymbol{v}) = -\operatorname{div}(\boldsymbol{j}_\alpha - \rho_0 c_\alpha \boldsymbol{w}^s_\alpha) + \phi^{(c_\alpha)}, \quad \alpha = 1,\dots,N\,. \tag{31}$$

We mention that for relatively shallow basins the term involving $\mathrm{d}\,p/\mathrm{d}\,t$ in $(26)_2$ and $(30)_2$ is ignored in the enthalpy formulations.

The turbulent analogues to the balance laws (24)–(31) are obtained if these laws are subjected to the filter operation $\langle\cdot\rangle$. In this process, $\rho_0, \boldsymbol{g}, \boldsymbol{\Omega}$ do not possess fluctuations, so that $\langle\rho_0\rangle = \rho_0$, $\langle\boldsymbol{g}\rangle = \boldsymbol{g}$, $\langle\boldsymbol{\Omega}\rangle = \boldsymbol{\Omega}$. When omitting the angular brackets, the Reynolds averaged equations then take the forms

- Balance of mass for the mixture

$$\operatorname{div}\rho_0\boldsymbol{v} = 0\,; \tag{32}$$

- Balance of momentum of the mixture

$$\begin{aligned}\rho_0\,\frac{\mathrm{d}\boldsymbol{v}}{\mathrm{d}\,t} + 2\rho_0\boldsymbol{\Omega}\times\boldsymbol{v}\left(= \frac{\partial\,(\rho_0\boldsymbol{v})}{\partial\, t} + \operatorname{div}(\rho_0\boldsymbol{v}\otimes\boldsymbol{v}) + 2\rho_0\boldsymbol{\Omega}\times\boldsymbol{v}\right) =&\\ -\operatorname{grad}\, p_d + \operatorname{div}\boldsymbol{R} + (\rho-\rho_0)\boldsymbol{g}\,;&\end{aligned} \tag{33}$$

- Balance of mixture energy

$$\begin{gathered}\rho_0\frac{\mathrm{d}\epsilon}{\mathrm{d}\,t}\left(= \frac{\partial(\rho_0\epsilon)}{\partial\, t} + \operatorname{div}(\rho_0\epsilon\boldsymbol{v})\right) = -p\operatorname{div}\boldsymbol{v} - \operatorname{div}\boldsymbol{Q}_\epsilon + \phi^{(T)},\\ \rho_0\frac{\mathrm{d}\,h}{\mathrm{d}\,t} - \frac{\mathrm{d}\,p}{\mathrm{d}\,t}\left(= \frac{\partial(\rho_0 h)}{\partial\, t} + \operatorname{div}(\rho_0 h\boldsymbol{v}) - \frac{\mathrm{d}\,p}{\mathrm{d}\,t}\right) = -\operatorname{div}\boldsymbol{Q}_h + \phi^{(T)} + \operatorname{div}\boldsymbol{\mathcal{P}}\,;\end{gathered} \tag{34}$$

- Balance of tracer mass of constituent α

$$\rho_0\frac{\mathrm{d}\,c_\alpha}{\mathrm{d}\,t}\left(= \frac{\partial(\rho_0 c_\alpha)}{\partial\, t} + \operatorname{div}(\rho_0 c_\alpha\boldsymbol{v})\right) = -\operatorname{div}\{\boldsymbol{J}_\alpha - \rho_0 c_\alpha\boldsymbol{w}^s_\alpha\} + \phi^{(c_\alpha)}. \tag{35}$$

In these equations $\mathrm{d}f/\mathrm{d}\,t$ is the substantive derivative of f following the averaged turbulent velocity. Furthermore, the non-conservative and conservative forms have been written together to save space. The quantities[10]

$$\begin{gathered}\boldsymbol{R} \equiv \langle\boldsymbol{\sigma}_E\rangle - \rho_0 \langle\boldsymbol{v}' \otimes \boldsymbol{v}'\rangle , \quad \boldsymbol{Q}_\epsilon \equiv \langle\boldsymbol{q}\rangle + \rho_0 \langle\epsilon' \boldsymbol{v}'\rangle , \quad \boldsymbol{Q}_h \equiv \langle\boldsymbol{q}\rangle + \rho_0 \langle h' \boldsymbol{v}'\rangle , \\ \phi^{(T)} \equiv \mathrm{tr}\,(\langle\boldsymbol{\sigma}_E\rangle\langle\boldsymbol{D}\rangle) + \mathrm{tr}\,\langle\boldsymbol{\sigma}'_E\boldsymbol{D}'\rangle - \langle p' \mathrm{div}\,\boldsymbol{v}'\rangle , \quad \boldsymbol{\mathcal{P}} \equiv \langle p'\boldsymbol{v}'\rangle , \\ \boldsymbol{J}_\alpha \equiv \langle\boldsymbol{j}_\alpha\rangle + \rho_0 \langle c'_\alpha \boldsymbol{v}'\rangle - \rho_0 \langle c'_\alpha \boldsymbol{w}^{s'}_\alpha\rangle ,\end{gathered} \tag{36}$$

represent

(i) the total stress $\boldsymbol{R}$ (modulo the pressure) as a combination of the averaged extra stress tensor $\langle\boldsymbol{\sigma}_E\rangle$ and the REYNOLDS stress tensor $-\rho_0 \langle\boldsymbol{v}' \otimes \boldsymbol{v}'\rangle$ due to turbulence;

(ii) the total heat flux $\boldsymbol{Q}_\epsilon$, $\boldsymbol{Q}_h$ as the sum of the averaged 'laminar' heat flux $\langle\,\boldsymbol{q}\,\rangle$ and the energy flux due to turbulence in the internal energy, $\rho_0\langle\epsilon'\boldsymbol{v}'\rangle$, and the enthalpy, $\rho_0\langle h'\boldsymbol{v}'\rangle$ formulation, respectively;

(iii) the averaged internal energy/enthalpy production rate density $\phi^{(T)}$ due to the power of working $\mathrm{tr}\,\langle\boldsymbol{\sigma}_E\rangle\langle\boldsymbol{D}\rangle$ of the mean motion and the correlations $\mathrm{tr}\,\langle\boldsymbol{\sigma}'_E\boldsymbol{D}'\rangle$, $\langle p'\mathrm{div}\,\boldsymbol{v}'\rangle$;

(iv) the average pressure work $\boldsymbol{\mathcal{P}}$ (note that it only arises in the enthalpy formulation of the energy equation and that it can in principle be combined with the heat flux term $\boldsymbol{Q}_h$);

(v) the total mass flux of constituent α comprising the averaged laminar mass flux $\langle\boldsymbol{j}_\alpha\rangle$, turbulent mass flux $\rho_0 \langle c'_\alpha\boldsymbol{v}'\rangle$ and turbulent mass flux due to non-buoyant particle flow $\rho_0 \langle c'_\alpha \boldsymbol{w}^{s'}_\alpha\rangle$.

It is the goal of turbulence theory to propose closure relations for the quantities (36). We refrain to do this here and pass to the presentation of another model, for which, however, we give closure relations.

2.2.2 Model 2: Small density fluctuation assumption

One can find in the literature yet another set of averaged field equations which are stated as such but without any or little motivation. It can be motivated by considering the density fluctuation ρ' in the decomposition $\rho = \langle\rho\rangle + \rho'$ so small, that it is everywhere ignored. Of course, this strictly requires that $|\rho'| \ll \langle\rho\rangle$ and that any correlation $|\langle\rho' a'\rangle|$ is smaller than $|\langle a'b'\rangle|$ $(b' \neq \rho')$. We therefore propose the following

Small density-fluctuation-turbulence assumption: *Consider a non-density preserving fluid subjected to turbulent motions for which turbulent density fluctuations ρ' are negligibly small, such that*

$$|\rho'| \ll \langle\rho\rangle , \quad |\langle\rho' a'\rangle| \ll |\langle a'b'\rangle| \quad (b' \neq \rho') \tag{37}$$

can be dropped from the equations.

[10]For these formulae we employ the symbol $\langle\cdot\rangle$ of filter operation to emphasize the role of the averaged laminar quantities and averages of turbulent correlation quantities.

With this assumption the density function $\rho(\mathbf{x}, t)$ can be everywhere approximated by

$$\rho(\mathbf{x}, t) \approx \langle \rho(\mathbf{x}, t) \rangle . \tag{38}$$

Omitting the angular brackets $\langle \cdot \rangle$, with this approximation applied to the mixture mass density, the averaged balance laws as deduced from (13)–(16) can be written as

- Balance of mass for the mixture

$$\frac{\partial \rho}{\partial t} + \operatorname{div}(\rho \boldsymbol{v}) = 0 ; \tag{39}$$

- Balance of momentum for the mixture

$$\frac{\partial (\rho \boldsymbol{v})}{\partial t} + \operatorname{div}(\rho \boldsymbol{v} \otimes \boldsymbol{v}) + 2\rho \boldsymbol{\Omega} \times \boldsymbol{v} = -\operatorname{grad} p + \operatorname{div} \boldsymbol{R} + \rho \boldsymbol{g} ; \tag{40}$$

- Balance of mixture energy

$$\begin{aligned} \frac{\partial (\rho \epsilon)}{\partial t} + \operatorname{div}(\rho \epsilon \boldsymbol{v}) &= -p \operatorname{div} \boldsymbol{v} - \operatorname{div} \boldsymbol{Q}_\epsilon + \phi^{(T)} \quad \text{or} \\ \frac{\partial (\rho\, h)}{\partial t} + \operatorname{div}(\rho\, h \boldsymbol{v}) - \frac{\mathrm{d}\, p}{\mathrm{d}\, t} &= -\operatorname{div} \boldsymbol{Q}_h + \operatorname{div} \boldsymbol{\mathcal{P}} + \phi^{(T)} ; \end{aligned} \tag{41}$$

- Balance of tracer mass of constituent α

$$\frac{\partial (\rho\, c_\alpha)}{\partial t} + \operatorname{div} \rho\, c_\alpha \boldsymbol{v} = -\operatorname{div}(\boldsymbol{J}_\alpha - \rho\, c_\alpha \boldsymbol{w}^s_\alpha) + \phi^{(c_\alpha)} , \tag{42}$$

with the definitions

$$\begin{gathered} \boldsymbol{R} \equiv \langle \boldsymbol{\sigma}_E \rangle - \rho \langle \boldsymbol{v}' \otimes \boldsymbol{v}' \rangle , \quad \boldsymbol{Q}_\epsilon \equiv \langle \boldsymbol{q} \rangle + \rho \langle \epsilon' \boldsymbol{v}' \rangle , \quad \boldsymbol{Q}_h \equiv \langle \boldsymbol{q} \rangle + \rho \langle h' \boldsymbol{v}' \rangle , \\ \phi^{(T)} \equiv \operatorname{tr}(\langle \boldsymbol{\sigma}_E \rangle \langle \boldsymbol{D} \rangle) + \operatorname{tr} \langle \boldsymbol{\sigma}'_E \boldsymbol{D}' \rangle - \langle p' \operatorname{div} \boldsymbol{v}' \rangle , \quad \boldsymbol{\mathcal{P}} \equiv \langle p' \boldsymbol{v}' \rangle , \\ \boldsymbol{J}_\alpha \equiv \langle \boldsymbol{j}_\alpha \rangle + \rho \langle c'_\alpha \boldsymbol{v}' \rangle - \rho \langle c'_\alpha \boldsymbol{w}^{s'}_\alpha \rangle . \end{gathered} \tag{43}$$

In the subsequent analysis we will use equations (39)–(42), for which we assume the following closure relations:

(i) As in physical limnology, we take

$$\begin{gathered} \epsilon = c_v (T - T_0) + \epsilon_0 , \quad h = c_p (T - T_0) + h_0 , \\ c_v = \text{specific heat at constant volume} , \quad c_p = \text{specific heat at constant pressure} , \end{gathered} \tag{44}$$

where T is the absolute temperature, as expressions for the internal energy and enthalpy in the respective formulations; the specific heats c_v, c_p are assumed constant. For a thermodynamic justification of (44) or its generalization, see Appendix A.

(ii) The density ρ is taken as

$$\rho = \rho_w(T,s) + \left(\sum_{\alpha=1}^{N} c_\alpha\right)\rho_s\,, \tag{45}$$

in which $\rho_w(T,s)$ is the water density at temperature T and constant salinity s, and $\rho_s \approx 2100\,\mathrm{kg\,m^{-3}}$ is the buoyancy corrected density of the suspended sediment. Explicit formulae are e.g. given in (I, 10, p. 344ff)[11]. If the contribution of the mineralization is negligibly small, then

$$\begin{aligned} \rho_w = \rho_w(T) &= \rho^* \left(1 - \tilde{\alpha}(T-T^*)^2\right)\,, \\ \rho^* = 1000\,\mathrm{kg\,m^{-3}}\,, \quad T^* &= 277^\circ\,\mathrm{K}\,, \quad \tilde{\alpha} = 6.493\times 10^6\,\mathrm{K^{-2}}\,, \end{aligned} \tag{46}$$

is a useful quadratic approximation; ρ^* is the reference density of water at 4°C.

It was already mentioned that in very deep lakes of depth larger than approximately 500 m (Lake Baikal, Lake Tanganijka, Caspian Sea) the pressure dependence in the thermal equation of state should not be ignored. This implies that (45) is replaced by

$$\rho = \rho_w(T,s,p) + \left(\sum_{\alpha=1}^{N} c_\alpha\right)\rho_s\,, \tag{47}$$

in which the contribution of the pressure to ρ_w requires that the energy equation is used in the enthalpy formulation.

(iii) The specific energy production $\phi^{(T)}$, also called dissipation rate density, is deduced by assuming the Newtonian law for the dissipative stresses $\boldsymbol{\sigma}_E$. Thus, with $\boldsymbol{\sigma}_E = 2\rho\nu_\ell \boldsymbol{D}$, where ν_ℓ is the 'laminar' kinematic viscosity, $(43)_4$ yields

$$\begin{aligned} \phi^{(T)} &= \underbrace{4\rho\nu_\ell\, II_{\langle \boldsymbol{D}\rangle}}_{\substack{\text{dissipation rate due}\\ \text{to the mean velocity}}} + \underbrace{4\rho\nu_\ell\,\langle II_{\boldsymbol{D}'}\rangle}_{\substack{\text{turbulent dissipation}\\ \text{rate } \rho\varepsilon}} - \langle p' \mathrm{div}\, \boldsymbol{v}'\rangle = \\ &= \rho\,(4\nu_\ell II_{\langle \boldsymbol{D}\rangle} + \varepsilon) - \langle p' \mathrm{div}\, \boldsymbol{v}'\rangle\,, \end{aligned} \tag{48}$$

in which $II_{\boldsymbol{A}} \equiv \frac{1}{2}(\boldsymbol{A}\cdot\boldsymbol{A})$ is the second invariant of $\boldsymbol{A}$. Moreover, for $\langle p'\mathrm{div}\,\boldsymbol{v}'\rangle$ we assume

$$\langle p' \mathrm{div}\, \boldsymbol{v}'\rangle = \zeta_p \langle p\rangle\, \mathrm{div}\,\langle \boldsymbol{v}\rangle\,, \quad \zeta_p \approx 0\,, \tag{49}$$

while the turbulent dissipation rate ε will be later discussed, see (vii) below in this section.

(iv) For suspended particles of size range α we ignore fragmentation into other size ranges, so that we assume $\phi^{(c_\alpha)} = 0$.

[11] We shall refer to specific pages of [18] as (I, ...).

(v) The second order tensor $\boldsymbol{R}$, and vectors $\boldsymbol{Q}_\epsilon$, $\boldsymbol{Q}_h$, $\boldsymbol{J}_\alpha$ ($\alpha = 1, \dots, N$) are combinations of the averaged laminar and the turbulent fluxes of momentum, energy and species masses, given by the following gradient type parameterizations:[12]

$$
\begin{aligned}
\frac{1}{\rho}\boldsymbol{R} &= 2\nu_\ell \boldsymbol{D} - \langle \boldsymbol{v}' \otimes \boldsymbol{v}' \rangle = -\tfrac{2}{3} k \boldsymbol{I} + 2\left(\nu_\ell + \nu_t\right)\boldsymbol{D}, \\
\frac{1}{\rho^*[c_v]}\boldsymbol{Q}_\epsilon &= -\chi_\ell^{(T)} \operatorname{grad} T + \frac{\rho\, c_v}{\rho^*[c_v]}\langle T' \boldsymbol{v}' \rangle = -\left(\chi_\ell^{(T)} + \frac{\nu_t}{\sigma_T}\right)\operatorname{grad} T, \\
\frac{1}{\rho^*[c_p]}\boldsymbol{Q}_h &= -\chi_\ell^{(T)} \operatorname{grad} T + \frac{\rho\, c_p}{\rho^*[c_p]}\langle T' \boldsymbol{v}' \rangle = -\left(\chi_\ell^{(T)} + \frac{\nu_t}{\sigma_T}\right)\operatorname{grad} T\,, \qquad (50)\\
\frac{1}{\rho^*}\boldsymbol{J}_\alpha &= -\chi_\ell^{(c_\alpha)} \operatorname{grad} c_\alpha + \frac{\rho}{\rho^*}\langle c'_\alpha \boldsymbol{v}' \rangle - \frac{\rho}{\rho^*}\langle c'_\alpha \boldsymbol{w}^{s'}_\alpha \rangle = \\
&\quad -\left(\chi_\ell^{(c_\alpha)} + \frac{\nu_t}{\sigma_{c_\alpha}}\right)\operatorname{grad} c_\alpha - \frac{\rho}{\rho^*}\langle c'_\alpha \boldsymbol{w}^{s'}_\alpha \rangle, \quad \alpha = 1, \dots, N\,.
\end{aligned}
$$

In $(50)_1$, k is the turbulent kinetic energy per unit mass[13] and ν_t is the turbulent kinematic viscosity; they will be parameterized below in this section. The quantities $[c_v]$ and $[c_p]$ arising in $(50)_{2,3}$ are typical values of the specific heats c_v, c_p. Then, in $(50)_{2-4}$ the FOURIER law for the heat flux $\boldsymbol{q}$ and the FICK law for the diffusive flux $\boldsymbol{j}_\alpha$ are understood, which explains the 'laminar' difussivities $\chi_\ell^{(T)}$, $\chi_\ell^{(c_\alpha)}$. Moreover, σ_T and σ_{c_α} are turbulent PRANDTL and SCHMIDT numbers; they are always assumed to be constant, which expresses a certain similarity between the diffusive processes of momentum, heat and species masses, which is generally not borne out experimentally. The coefficient of grad T in the representations $(50)_{2,3}$ is supposed to be the same; this choice is exact if $[c_v] = [c_p]$ is selected. Additionally, to differentiate the viscosities from the diffusivities in $(50)_{2,3,4}$ one often makes use of the replacements

$$
\begin{aligned}
\left(\chi_\ell^{(T)} + \frac{\nu_t}{\sigma_T}\right) &\longrightarrow D^{(T)} \\
\left(\chi_\ell^{(c_\alpha)} + \frac{\nu_t}{\sigma_{c_\alpha}}\right) &\longrightarrow D^{(c_\alpha)}
\end{aligned}
\qquad (51)
$$

and calls $D^{(T)}$ the thermal diffusivity and $D^{(c_\alpha)}$ the species diffusivities. We shall follow this custom. We will also use the interpretation

$$
\nu_\ell + \nu_t \longrightarrow \nu_t
$$

[12] a) Parameterization $(50)_4$ does not account for cross dependences of the form

$$
-\sum_{\beta=1}^{N} \lambda_{\alpha\beta}\left(\chi_\ell^{(c_\beta)} + \frac{\nu_t}{\sigma_{c_\beta}}\right)\operatorname{grad} c_\beta\,, \quad \alpha = 1, \dots, N\,,
$$

with $\lambda_{\alpha\beta} < 1$. Our selection in $(50)_4$ is $\lambda_{\alpha\beta} = \delta_{\alpha\beta}$. In principle the more general case is possible.

[13] For a solenoidal velocity field it is often customary to incorporate the contribution of the turbulent kinetic energy k in relation $(50)_1$ into the pressure term, or to ignore it.

in $(50)_1$ and call the new ν_t – the kinematic turbulent viscosity. Finally, in the parameterization $(50)_4$ of $\boldsymbol{J}_\alpha$ we may assume

$$\langle c'_\alpha \boldsymbol{w}^{s'}_\alpha \rangle = \zeta \langle c_\alpha \rangle \langle \boldsymbol{w}^s_\alpha \rangle\,, \quad \zeta \approx 0\,,$$

as is the custom in the literature. Summarizing, for $\boldsymbol{R}$, $\boldsymbol{Q}_\epsilon$, $\boldsymbol{Q}_h$, $\boldsymbol{J}_\alpha$ we have the following closure relations:

$$\begin{aligned} \boldsymbol{R} &= -\tfrac{2}{3}\rho k \boldsymbol{I} + 2\rho\nu_t \boldsymbol{D}\,, \\ \boldsymbol{Q}_\epsilon &= -\rho^*[c_v] D^{(T)} \operatorname{grad} T\,, \quad \boldsymbol{Q}_h = -\rho^*[c_p] D^{(T)} \operatorname{grad} T\,, \\ \boldsymbol{J}_\alpha &= -\rho^* D^{(c_\alpha)} \operatorname{grad} c_\alpha - \zeta\rho \langle c_\alpha \rangle \langle \boldsymbol{w}^s_\alpha \rangle\,, \quad \zeta \approx 0\,, \quad \alpha = 1, \dots, N\,. \end{aligned} \tag{52}$$

(vi) For $\boldsymbol{w}^s_\alpha$ we assume (10), where expressions of the particle settling velocity w^s_α are discussed below in (vii).

(vii) Now, given numerical values for the laminar viscosity ν_ℓ, specific heats c_v, c_p, and diffusivities $D^{(T)}$, $D^{(c_\alpha)}$, the above model equations (39) - (52) must still be complemented by closure relations for ν_t, k, ε, w^s_α. The way of approach how this is done depends on the sophistication which is applied to the turbulent parameterization. When applying classical zeroth order closure schemes, algebraic parameterization for ν_t, k and ε are given; for higher order closure relations one or two equation models or full REYNOLDS models are suggested. Next we refer to such closure relations for ν_t, k and ε and then we review parameterizations for the particle settling velocity w^s_α.

Zeroth order, algebraic parameterization for ν_t, k and ε In (I, 6.2.6, p. 201ff), PRANDTL's eddy viscosity formula [34] was generalized and a proposal for the turbulent kinetic energy was given. Moreover, since dimensionally $[\varepsilon] = [k^{3/2}]/[\ell]$, where ℓ is a mixing length introduced by PRANDTL, the following propositions may be meaningful:

$$\begin{aligned} &\text{(I, 6.55)} \quad \nu_t = 2\ell^2\sqrt{II_{\boldsymbol{D}}}, \\ &\text{(I, 6.56)} \quad k = c_k 4\ell^2 II_{\boldsymbol{D}}, \\ &\text{(I, 6.57)} \quad \varepsilon = c_\varepsilon 8\ell^2 II_{\boldsymbol{D}}^{3/2}, \end{aligned} \tag{53}$$

where the third expression follows from $\varepsilon = \text{const} \times k^{3/2}/\ell$. PRANDTL added a balance equation of the form (54), below, but this would correspond to a first order closure scheme. At zeroth order closure, ℓ is an adjustable constant scalar coefficient.

First order parameterization – the $(k - \varepsilon)$-model The most popular first order turbulence model is the so-called $(k-\varepsilon)$ *model*. Its full derivation is e.g. given by HUTTER & JÖHNK [17], Chap. 11, and a summary is given in I, 6. Here we give a short presentation of this model.

The most simple first order turbulent closure model is based on a differential equation for ℓ and was proposed by PRANDTL [34] as

$$\frac{\partial \ell}{\partial t} + \operatorname{div} \ell \boldsymbol{v} + 2\ell\sqrt{2} + \cdots = 0\,, \tag{54}$$

Table 1: Numerical values for the closure constants of the $(k - \varepsilon)$ model

$c_\mu = 0.09$	$c_1 = 0.126$	$c_2 = 1.92$	$c_3 \approx 0$	$\sigma_k = 1.4$	$\sigma_\varepsilon = 1.3$

including the unspecified '$\cdots$', but was not pursued any further by him. We shall neither elaborate on this and will directly pass on to the standard turbulent two-equation model, which is the $(k - \varepsilon)$ model. It uses evolution equations for the specific turbulent kinetic energy k and the specific turbulent dissipation rate ε, and is based on the fact that ν_t, k and ε fulfil the dimensional identity $[\nu_t] = [k^2]/[\varepsilon]$, suggesting the parameterization

$$\nu_t = c_\mu \frac{k^2}{\varepsilon}\,, \tag{55}$$

in which c_μ is a dimensionless scalar, determined by inverse methods from experiments, but interpreted as a 'universal' constant. For k and ε balance laws are established,

$$\frac{\partial k}{\partial t} + \operatorname{div}(k\boldsymbol{v}) = -\operatorname{div}\boldsymbol{\phi}^k + \pi^k\,, \quad \frac{\partial \varepsilon}{\partial t} + \operatorname{div}(\varepsilon\boldsymbol{v}) = -\operatorname{div}\boldsymbol{\phi}^\varepsilon + \pi^\varepsilon\,,$$

in which the flux, $\boldsymbol{\phi}^k$, $\boldsymbol{\phi}^\varepsilon$, and production, π^k, π^ε, quantities must be parameterized. For a Boussinesq fluid, these are proposed and adequately justified e.g. by Hutter & Jöhnk [17] and also listed in I, 6, equations (I, 6.63)–(I, 6.65), to which the reader is referred. The fluxes have gradient closure form

$$\boldsymbol{\phi}^k = -\frac{\nu_t}{\sigma_k}\operatorname{grad} k, \quad \boldsymbol{\phi}^\varepsilon = -\frac{\nu_t}{\sigma_\varepsilon}\operatorname{grad}\varepsilon\,, \tag{56}$$

and the production terms are given by

$$\begin{aligned} \pi^k &= \operatorname{div}(\nu_\ell \operatorname{grad} k) + 4\nu_t I\!I_{\boldsymbol{D}} - \varepsilon + \frac{\rho\alpha_T}{\rho^*}\frac{\nu_t}{\sigma_T}\,\boldsymbol{g}\cdot\operatorname{grad} T\,, \\ \pi^\varepsilon &= \operatorname{div}(\nu_\ell \operatorname{grad}\varepsilon) + 4c_1 k I\!I_{\boldsymbol{D}} - c_2\frac{\varepsilon^2}{k} + c_3\frac{\rho\alpha_T}{\rho^*}\frac{c_\mu}{\sigma_T}\,k\,\boldsymbol{g}\cdot\operatorname{grad} T\,, \end{aligned} \tag{57}$$

in which α_T is the coefficient of thermal expansion of water and c_3 is small but not well constrained. Numerical values for the various closure constants are given in Table 1.

Historically, the $(k-\varepsilon)$ model has originally been developed in the 1970s by Hanjalic & Launder [14], Jones & Launder [21] and Launder & Spalding [24]. Rodi [35],[36] describes its applicability in geophysics and hydraulic engineering. Apart from the $(k-\varepsilon)$ model, other two-equation models have also been proposed. The $(k-\ell)$ and $(k-\omega)$ models use, besides the turbulent kinetic energy, a length – the Prandtl mixing length, or the turbulent vorticity, ω, with dimension $[k/\ell^2]$. Expositions on these latter models are given by Rotta [37] and Wilcox [51], [52]. For Reynolds stress parameterization by Large Eddy Simulation (LES), see Appendix B.

Particle settling velocity The fall velocity w_α^s is the remaining quantity of the above model, which has not been specified so far. It is an exhaustively treated subject of hydraulic research and still a topic of active on-going work. Its introduction in (42) and earlier equations, e.g. (10), is the fall velocity of particles in a specified size range under dynamic conditions of laminar or turbulent flow. Studies on the settling velocity are generally restricted to spherical particles in still water; but it is well known that the fall velocity of a non-buoyant particle in a fluid depends on both the particle shape and the flow state in the ambient fluid. This complex non-linear interaction is out of reach and physically too difficult for our purposes. Consequently, authors on this subject identify w_α^s with the terminal velocity of a free falling particle in still water, generally restricted to spheres or (unspecified) natural sediment particles. Here, we adopt this restricted view as well.

The ensuing description is based on the study by Song et al. (2008) [42], who summarize earlier work and replace the different formulae by their own one. For an isolated spherical particle in a fluid at rest the settling velocity can be estimated by balancing the net gravitational force and the drag resistance,

$$\Delta\rho g \,\frac{\pi}{6}\,\mathfrak{d}_\alpha^3 = \frac{1}{2}\,\rho C_{\mathfrak{d}_\alpha}\,\frac{\pi}{4}\,\mathfrak{d}_\alpha^2 (w_\alpha^s)^2, \qquad \Delta \equiv \frac{\rho_s}{\rho} - 1, \tag{58}$$

where $\rho_s, \rho, g, \mathfrak{d}_\alpha, C_{\mathfrak{d}_\alpha}$ are the densities of the particle and the fluid, the acceleration due to gravity, the (nominal) diameter of a representative element in the sediment class α[14], and $C_{\mathfrak{d}_\alpha}$ is the drag coefficient; (58) can be written as

$$C_{\mathfrak{d}_\alpha} = \frac{4}{3}\,\frac{\Delta\, g\, \mathfrak{d}_\alpha}{(w_\alpha^s)^2}\,, \tag{59}$$

which is used to deduce the settling velocity w_α^s once the drag coefficient $C_{\mathfrak{d}_\alpha}$ is given as function of w_α^s. Thus, it is well known that, depending on the particle Reynolds number

$$Re_\alpha \equiv \frac{w_\alpha^s \mathfrak{d}_\alpha}{\nu}\,, \tag{60}$$

there are two asymptotic limits for the settling velocity: $C_{\mathfrak{d}_\alpha} = A/Re_\alpha$ when $Re_\alpha < 1$ (Stokes flow), and $C_{\mathfrak{d}_\alpha} = B$ when $10^5 < Re_\alpha < 2 \times 10^5$ (turbulent flow), where A and B are constants, see any book on fluid dynamics of viscous flow. Substituting these expressions into (59) implies

$$\begin{aligned} w_\alpha^s &= \frac{4}{3A}\,\frac{\Delta\, g\, \mathfrak{d}_\alpha^2}{\nu} \quad \text{for Stokes flow}\,, \\ w_\alpha^s &= \sqrt{\frac{4}{3B}\Delta\, g\, \mathfrak{d}_\alpha} \quad \text{for turbulent flow}\,. \end{aligned} \tag{61}$$

According to Song et al. [42] most of the existing quasi-theoretical or semi-empirical

[14]Such a representative element in class α has already been used when defining the advected mass flux $\rho c_\alpha \boldsymbol{w}_\alpha^s$. To simplify the notation, we use $\mathfrak{d}_\alpha$ for the diameter of this grain particle; note that $\mathfrak{d}_\alpha \in [d_{\alpha-1}, d_\alpha)$, so that $\mathfrak{d}_\alpha$ should not be confused with d_α.

formulae are based on the asymptotic solutions (61).[15] A smooth connection between the two asymptotic representations for $C_{\mathfrak{d}_\alpha}$ is e.g. reached by

$$C_{\mathfrak{d}_\alpha} = \left\{ \left(\frac{A}{Re_\alpha} \right)^{1/n} + B^{1/n} \right\}^n \tag{62}$$

(Cheng (1997) [8]). Indeed, as $Re_\alpha \to 0$, relation (62) implies $C_{\mathfrak{d}_\alpha} \approx A/Re_\alpha$; similarly, for $Re_\alpha \to \infty$, $C_{\mathfrak{d}_\alpha} \approx B$. Introducing the dimensionless particle diameter

$$\mathfrak{d}^*_\alpha \equiv \left(\frac{\Delta\, g}{\nu^2} \right)^{1/3} \mathfrak{d}_\alpha \tag{63}$$

into (59) and using the definition (60) for Re_α yields

$$C_{\mathfrak{d}_\alpha} = \frac{4}{3} \frac{(\mathfrak{d}^*_\alpha)^3}{(Re_\alpha)^2}\,. \tag{64}$$

Equating (62) to (64) leads to a quadratic equation for $(Re_\alpha)^{1/n}$, which can be solved; subsequently an explicit formula for w^s_α can be found via the definition of the Reynolds number. This is done by Song et al [42]. Their formula reads

$$w^s_\alpha = \frac{\nu}{\mathfrak{d}_\alpha} \left\{ \sqrt{\frac{1}{4}\left(\frac{A}{B}\right)^{2/n} + \left(\frac{4}{3}\frac{(\mathfrak{d}^*_\alpha)^3}{B}\right)^{1/n}} - \frac{1}{2}\left(\frac{A}{B}\right)^{1/n} \right\}^n . \tag{65}$$

Various values for A, B and n that have been used by different authors for spherical particles and natural sediments are given. However, comparison of results with experiments is not satisfactory, and the disparate values for A, B and n, obtained by different authors make application of (65) cumbersome.

As an alternative, Song et al. [42] restrict consideration to Stokes flow and choose $(61)_1$ to evaluate

$$Re_\alpha = \frac{w^s_\alpha \mathfrak{d}_\alpha}{\nu} = \frac{4}{3A}\,(\mathfrak{d}^*_\alpha)^3\,. \tag{66}$$

Somewhat surprisingly[16], they substitute this into (62), obtain

$$C_{\mathfrak{d}_\alpha} = \left\{ \left(\frac{\sqrt{3}A}{2(\mathfrak{d}^*_\alpha)^{3/2}} \right)^{2/n} + B^{1/n} \right\}^n , \tag{67}$$

and using (64) deduce the settling velocity

$$w^s_\alpha = \frac{\nu}{\mathfrak{d}_\alpha}\mathfrak{d}^*_\alpha \left\{ \left(\frac{3A}{4}\right)^{2/n} + \left(\frac{3B}{4}\,(\mathfrak{d}^*_\alpha)^3\right)^{1/n} \right\}^{-n/2} . \tag{68}$$

[15] McGauhey [27], Zanke [56], Concha and Almendra [9], Turton & Clark [45], Zhang [58], Julien [22], Soulsby [43], Cheng [8], Ahrens [1], Guo [13], Jimenez and Madsen [20], Brown & Lawler [6], She et al. [38], Camenen [7].

[16] Formula (62) was proposed by Cheng [8] to match both asymptotic limits for Stokes *and* turbulent flows.

SONG et al. [42] take experimental data by EGLUND and HANSEN [10] and CHENG [8] and determine A, B and n by least square error minimization; they found

$$A = 32.2\,, \quad B = 1.17\,, \quad n = 1.75\,,$$

and then, on substituting these into (68), obtained the following formula for w^s_α,

$$w^s_\alpha = \frac{\nu}{\mathfrak{d}_\alpha} (\mathfrak{d}^*_\alpha)^3 \left\{38.1 + 0.93\, (\mathfrak{d}^*_\alpha)^{12/7}\right\}^{-7/8}\,, \tag{69}$$

and listed alternative formulae of settling velocities by other scholars, viz.,

- ZHU & CHENG (1993) [59]

$$\begin{aligned} w^s_\alpha &= \frac{\nu}{\mathfrak{d}_\alpha} (\mathfrak{d}^*_\alpha)^3 \left\{ \frac{1}{\sqrt{144\cos^6\beta + \left(4.5\cos^3\beta + 0.9\sin^2\beta\right)(\mathfrak{d}^*_\alpha)^3} + 12\cos^3\beta} \right\}, \\ \beta &= \begin{cases} 0\,, & \mathfrak{d}^*_\alpha \leqslant 1\,, \\ \pi\{2 + 2.5(\log \mathfrak{d}^*_\alpha)^{-3}\}^{-1}\,, & \mathfrak{d}^*_\alpha > 1\,. \end{cases} \end{aligned} \tag{70}$$

- CHENG (1997) [8]

$$w^s_\alpha = \frac{\nu}{\mathfrak{d}_\alpha} \left(\sqrt{25 + 1.2(\mathfrak{d}^*_\alpha)^2} - 5\right)^{3/2}. \tag{71}$$

- AHRENS (2000) [1]

$$\begin{aligned} w^s_\alpha &= \frac{\nu}{\mathfrak{d}_\alpha} (\mathfrak{d}^*_\alpha)^{3/2} \left(C_1 (\mathfrak{d}^*_\alpha)^{3/2} + C_2\right)\,, \\ C_1 &= 0.055 \tanh\left[12(\mathfrak{d}^*_\alpha)^{-1.77} \exp\left(-0.0004(\mathfrak{d}^*_\alpha)^3\right)\right]\,, \\ C_2 &= 1.06 \tanh\left[0.01(\mathfrak{d}^*_\alpha)^{1.5} \exp\left(-120/(\mathfrak{d}^*_\alpha)^3\right)\right]\,. \end{aligned} \tag{72}$$

- GUO (2002) [13]

$$w^s_\alpha = \frac{\nu}{\mathfrak{d}_\alpha} (\mathfrak{d}^*_\alpha)^3 \left[24 + \frac{\sqrt{3}}{2} (\mathfrak{d}^*_\alpha)^{3/2}\right]^{-1}. \tag{73}$$

- SHE et al. (2005) [38]

$$w^s_\alpha = 1.05 \frac{\nu}{\mathfrak{d}_\alpha (\mathfrak{d}^*_\alpha)^{3/2}} \left[1 - \exp\left(-0.315(\mathfrak{d}^*_\alpha)^{0.765}\right)\right]^{2.2}. \tag{74}$$

Table 2 presents a comparison of calculated settling velocities using formulae (69)–(74) with the experimental data of ENGLUND & HANSEN (1972) [10] and CHENG (1997) [8]. The average value of the relative error E and the standard deviation σ, defined as[17]

$$E = \frac{1}{N} \sum_{i=1}^{N} \left| \frac{(w^s_\alpha)^{\text{comp}}}{(w^s_\alpha)^{\text{exp}}} - 1 \right| \times 100\%\,, \qquad \sigma = \sqrt{\frac{1}{N} \sum_{i=1}^{N} \left| \frac{(w^s_\alpha)^{\text{comp}}}{(w^s_\alpha)^{\text{exp}}} - 1 \right|^2} \times 100\%\,,$$

[17] N is the number of experimental points where values for $(w^s_\alpha)^{\text{exp}}$ have been measured.

are listed in columns 2 and 3 of Table 2. It corroborates the best performance for (69). Even more convincing results are shown in the graphs of [42]. We therefore recommend to use (69).

Table 2: Fit accuracy of formulae (69)–(74) against experimental data by Eglund & Hansen [10], Cheng [8].

Equation Nr	*Error* $E(\%)$	*Standard deviation* $\sigma(\%)$
(69)	6.36	9.10
(70)	7.02	11.30
(71)	6.96	10.96
(72)	16.93	16.84
(73)	6.87	10.56
(74)	16.34	16.49

All these parameterizations enjoy the property that w^s_α does not depend on the flow dynamics of the slurry. It is, however, intuitively clear that the turbulent intensity may inhibit the free fall velocity. A bold account of this property may be the following choice

$$w^s_\alpha = \exp\left[-\left(\frac{k}{\sigma_k}\right)^2\right]\frac{\nu}{\mathfrak{d}^*_\alpha}(\mathfrak{d}^*_\alpha)^3\left\{38.1 + 0.93(\mathfrak{d}^*_\alpha)^{12/7}\right\}^{-7/8}, \tag{75}$$

in which k is the turbulent kinetic energy and σ_k a standard deviation, chosen to be sufficiently small. This reduces the value of w^s_α whenever k is large, which is the case close to the free surface, in the metalimnion and immediately above the moving detritus. A dependence on the Richardson number would be a competing alternative.

2.3 Boussinesq and shallow water approximations in Model 2

In this section we simplify the equations characterizing Model 2 by using the Boussinesq assumption or/and the shallow water assumption. Thus, when written with respect to a Cartesian coordinate system with horizontal (x, y)-axes and vertical z-axis, the Reynolds averaged equations (39)–(42), now in non-conservative form,[18] are as follows:

- Balance of mass

$$\frac{\partial \rho}{\partial t} + \frac{\partial \rho u}{\partial x} + \frac{\partial \rho v}{\partial y} + \frac{\partial \rho w}{\partial z} = 0\,; \tag{76}$$

[18]This form is a bit more convenient when the equations are subjected to a scaling analysis appropriate for justifying the Boussinesq and shallow water approximations.

- Balance of momentum

$$\rho\left(\frac{\partial u}{\partial t}+u\,\frac{\partial u}{\partial x}+v\,\frac{\partial u}{\partial y}+w\frac{\partial u}{\partial z}+\tilde{f}w-fv\right)=-\frac{\partial p}{\partial x}+\frac{\partial R_{xx}}{\partial x}+\frac{\partial R_{xy}}{\partial y}+\frac{\partial R_{xz}}{\partial z}\,;$$
$$\rho\left(\frac{\partial v}{\partial t}+u\,\frac{\partial v}{\partial x}+v\,\frac{\partial v}{\partial y}+w\,\frac{\partial v}{\partial z}+fu\right)=-\frac{\partial p}{\partial y}+\frac{\partial R_{yx}}{\partial x}+\frac{\partial R_{yy}}{\partial y}+\frac{\partial R_{yz}}{\partial z}\,;$$
$$\rho\left(\frac{\partial w}{\partial t}+u\,\frac{\partial w}{\partial x}+v\,\frac{\partial w}{\partial y}+w\,\frac{\partial w}{\partial z}-\tilde{f}u\right)=-\frac{\partial p}{\partial z}+\frac{\partial R_{zx}}{\partial x}+\frac{\partial R_{zy}}{\partial y}+\frac{\partial R_{zz}}{\partial z}-\rho\,g\,; \tag{77}$$

- Balance of energy

$$\begin{aligned}\rho c_v\left(\frac{\partial T}{\partial t}+u\,\frac{\partial T}{\partial x}+v\,\frac{\partial T}{\partial y}+w\frac{\partial T}{\partial z}\right)&=-p\left(\frac{\partial u}{\partial x}+\frac{\partial v}{\partial y}+\frac{\partial w}{\partial z}\right)\\&\quad-\left(\frac{\partial Q^\epsilon_x}{\partial x}+\frac{\partial Q^\epsilon_y}{\partial y}+\frac{\partial Q^\epsilon_z}{\partial z}\right)+\phi^{(T)}\,;\end{aligned} \tag{78}$$

$$\begin{aligned}&\rho c_p\left(\frac{\partial T}{\partial t}+u\,\frac{\partial T}{\partial x}+v\,\frac{\partial T}{\partial y}+w\frac{\partial T}{\partial z}\right)-\frac{\mathrm{d}\,p}{\mathrm{d}\,t}\\&\quad=-\left(\frac{\partial Q^h_x}{\partial x}+\frac{\partial Q^h_y}{\partial y}+\frac{\partial Q^h_z}{\partial z}\right)+\left(\frac{\partial \mathcal{P}_x}{\partial x}+\frac{\partial \mathcal{P}_y}{\partial y}+\frac{\partial \mathcal{P}_z}{\partial z}\right)+\phi^{(T)}\,;\end{aligned} \tag{79}$$

- Balance of species mass[19]

$$\begin{aligned}\rho\left(\frac{\partial c_\alpha}{\partial t}+u\,\frac{\partial c_\alpha}{\partial x}+v\,\frac{\partial c_\alpha}{\partial y}+w\,\frac{\partial c_\alpha}{\partial z}\right)&=-\frac{\partial J_{\alpha x}}{\partial x}-\frac{\partial J_{\alpha y}}{\partial y}-\frac{\partial J_{\alpha z}}{\partial z}+\\&\quad\frac{\partial}{\partial z}(\rho\,c_\alpha w^s_\alpha)+\phi^{(c_\alpha)}\,,\quad \alpha=1,\dots,N\,.\end{aligned} \tag{80}$$

In these equations u, v, w are the Cartesian velocity components in the x, y, z directions, $Q_x^{\epsilon,h}, Q_y^{\epsilon,h}, Q_z^{\epsilon,h}$ are the Cartesian components of the heat flux vectors in the internal energy and enthalpy formulations, respectively; moreover, $J_{\alpha x}, J_{\alpha y}, J_{\alpha z}$ are the Cartesian components of $\boldsymbol{J}_\alpha$, and f, $\tilde{f}$ are the first and second CORIOLIS parameters,

$$f=2\Omega\,\sin\varphi,\quad \tilde{f}=2\Omega\,\cos\varphi, \tag{81}$$

in which $\Omega\equiv\|\boldsymbol{\Omega}\|$ is the angular velocity of the Earth ($\Omega=7.272\times10^{-5}$ [s^{-1}]) and φ is the latitude angle. Writing (76)–(80) one has made use of the closure assumptions (10), (44).

[19]This equation holds with $\boldsymbol{w}^s_\alpha=w^s_\alpha\boldsymbol{e}_z$. If $\boldsymbol{w}^s_\alpha$ is parameterized as in equation (11), then

$$\frac{\partial}{\partial x}(\rho\,c_\alpha w^s_\alpha\tan\theta\cos\xi)+\frac{\partial}{\partial y}(\rho\,c_\alpha w^s_\alpha\tan\theta\sin\xi)$$

must be added to the right-hand side of equation (80). Here, ξ is the angle between the x-axis and $\boldsymbol{v}_H$.

It is now assumed that the typical processes have large horizontal but small vertical scales. For instance, typical horizontal scales of water disturbances are often many kilometers, while the corresponding depth variations are generally tens of meters and less; similarly, horizontal velocity components are generally large, while corresponding vertical velocity components are a factor of 10^{-3} smaller. This suggests to introduce the aspect ratios [20]

$$\mathcal{A}_L \equiv \frac{\text{typical vertical length scale}}{\text{typical horizontal length scale}} = \frac{[H]}{[L]},$$
$$\mathcal{A}_V \equiv \frac{\text{typical vertical velocity scale}}{\text{typical horizontal velocity scale}} = \frac{[W]}{[V]},$$

to substitute these into the governing field equations, to suppose that

$$0 < \mathcal{A}_L = \mathcal{A}_V \equiv \mathcal{A} \ll 1,$$

and to look at the governing equations in the limit as $\mathcal{A} \to 0$.

To compare the various terms arising in the governing equations, each quantity, say Ψ, is written in the form $\Psi = [\Psi]\overline{\Psi}$, where $[\Psi]$ is the scale for Ψ (and has the physical units of Ψ) and $\overline{\Psi}$ is dimensionless and of the order of unity if the value for $[\Psi]$ is correctly selected. The procedure is well known and is e.g. demonstrated in [18], p. 150–154. We shall select the scales according to

$$\begin{aligned}
(x, y, z) &= ([L]\,\overline{x},\ [L]\,\overline{y},\ [H]\,\overline{z}), \quad (t, f, \tilde{f}) = \left(\frac{1}{[f]}\,\overline{t},\ [f]\overline{f},\ [f]\overline{\tilde{f}}\right), \\
(u, v, w, w^s_\alpha) &= \left([V]\,\bar{u},\ [V]\,\overline{v},\ \frac{[H]}{[L]}[V]\,\overline{w},\ \frac{[H]}{[L]}[V]\,\overline{w^s_\alpha}\right), \\
\rho &= \rho^*\,(1 + [\sigma]\,\overline{\sigma}\,), \quad p = -\rho^* g z + \rho^*[f][V][L]\,\overline{p}, \\
T &= T_0 + [\Delta T]\,\overline{T}, \quad c_\alpha = [c_\alpha]\,\overline{c_\alpha}, \quad c_v = [c_v]\,\overline{c_v}, \quad c_p = [c_p]\,\overline{c_p}, \\
\phi^{(T)} &= [\phi^{(T)}]\overline{\phi^{(T)}}, \qquad \phi^{(c_\alpha)} = [\phi^{(c_\alpha)}]\overline{\phi^{(c_\alpha)}}, \quad \boldsymbol{\mathcal{P}} = \rho^*[c_p][f][H][\Delta T]\,\overline{\boldsymbol{\mathcal{P}}}.
\end{aligned} \tag{82}$$

Moreover, we introduce the kinematic turbulent viscosity, $\mathcal{N}$, heat diffusivity, $\mathcal{D}^{(T)}$, and species mass diffusivity, $\mathcal{D}^{(c_\alpha)}$, by

$$\nu_t = [f][H^2]\mathcal{N}, \quad D^{(T)} = [f][H^2]\mathcal{D}^{(T)}, \quad D^{(c_\alpha)} = [f][H^2]\mathcal{D}^{(c_\alpha)}. \tag{83}$$

After some lengthy but straightforward calculations and with the assumption $\boldsymbol{R} = 2\rho\,\nu_t\,\boldsymbol{D}$ for the turbulent REYNOLDS stress[21], the field equations (76)–(80) take the following forms (the overbars characterizing dimensionless quantities are omitted):

[20] The symbol $[f]$ denotes an order of magnitude for the quantity f within the range of values which f may assume (in the physical dimensions in which it is expressed) in the processes under consideration.

[21] We neglect the contribution of the turbulent kinetic energy in $(52)_1$.

Table 3: Physical parameters and typical orders of magnitude for the scales in (82)

Parameter	*Order of magnitude*	*Nomenclature*
ρ^*	10^3 kg m^{-3}	Reference density at 4°C
$[\sigma]$	$\approx 10^{-3}$	Density anomaly
$[L]$	$\approx 10^4 - 10^6$ m	Horizontal length scale
$[H]$	$\approx 10^1 - 10^3$ m	Vertical length scale
$[V]$	$\approx 10^{-2} - 10^1$ m s^{-1}	Horizontal velocity scale
$[f]$	$\approx 10^{-4}$ s^{-1}	CORIOLIS parameter
T_0	$\approx 10°$ C	Reference temperature
$[\Delta T]$	$\approx 10°$ C	Temperature range
$[c_v]$	≈ 4200 m^2 s^{-2} K^{-1}	Specific heat at constant volume
$[c_p]$	≈ 4200 m^2 s^{-2} K^{-1}	Specific heat at constant pressure
$[c_\alpha]$	$\approx 10^{-3} - 10^{-1}$	Scale for mass fraction of tracer α
$[\phi^{(T)}]$		Scale for energy production
$[\phi^{(c_\alpha)}]$		Scale for production of tracer α

- Balance of mass

$$\frac{[\sigma]}{\mathcal{R}o}\frac{\partial \sigma}{\partial t} + \operatorname{div}\boldsymbol{v} + [\sigma]\operatorname{div}(\sigma\boldsymbol{v}) = 0\,; \tag{84}$$

- Balance of momentum

$$\begin{aligned}(1+[\sigma]\sigma)\left\{\frac{\partial u}{\partial t} + \mathcal{R}o\,(\operatorname{grad}\,u)\cdot\boldsymbol{v} + \mathcal{A}\tilde{f}w - fv\right\} = -\frac{\partial p}{\partial x} + \\ \mathcal{A}^2\left\{2\frac{\partial}{\partial x}\left[(1+[\sigma]\sigma)\mathcal{N}\frac{\partial u}{\partial x}\right] + \frac{\partial}{\partial y}\left[(1+[\sigma]\sigma)\mathcal{N}\left(\frac{\partial u}{\partial y} + \frac{\partial v}{\partial x}\right)\right]\right\} + \\ \frac{\partial}{\partial z}\left[(1+[\sigma]\sigma)\mathcal{N}\left(\frac{\partial u}{\partial z} + \mathcal{A}^2\frac{\partial w}{\partial x}\right)\right],\end{aligned} \tag{85}$$

$$
\begin{aligned}
(1+[\sigma]\sigma)\left\{\frac{\partial v}{\partial t}+\mathcal{R}o\,(\operatorname{grad}\,v)\cdot\boldsymbol{v}+fu\right\} &= -\frac{\partial p}{\partial y}+ \\
\mathcal{A}^2\left\{\frac{\partial}{\partial x}\left[(1+[\sigma]\sigma)\mathcal{N}\left(\frac{\partial u}{\partial y}+\frac{\partial v}{\partial x}\right)\right]+2\frac{\partial}{\partial y}\left[(1+[\sigma]\sigma)\mathcal{N}\frac{\partial v}{\partial y}\right]\right\} &+ \\
\frac{\partial}{\partial z}\left[(1+[\sigma]\sigma)\mathcal{N}\left(\frac{\partial v}{\partial z}+\mathcal{A}^2\frac{\partial w}{\partial y}\right)\right] &,
\end{aligned}
\tag{86}
$$

$$
\begin{aligned}
(1+[\sigma]\sigma)\left\{\mathcal{A}^2\left[\frac{\partial w}{\partial t}+\mathcal{R}o\,(\operatorname{grad}\,w)\cdot\boldsymbol{v}\right]-\mathcal{A}\tilde{f}u\right\} &= -\frac{\partial p}{\partial z}+ \\
\mathcal{A}^2\frac{\partial}{\partial x}\left[(1+[\sigma]\sigma)\mathcal{N}\left(\frac{\partial u}{\partial z}+\mathcal{A}^2\frac{\partial w}{\partial x}\right)\right] &+ \\
\mathcal{A}^2\frac{\partial}{\partial y}\left[(1+[\sigma]\sigma)\mathcal{N}\left(\frac{\partial v}{\partial z}+\mathcal{A}^2\frac{\partial w}{\partial y}\right)\right]+2\mathcal{A}^2\frac{\partial}{\partial z}\left[(1+[\sigma]\sigma)\mathcal{N}\frac{\partial w}{\partial z}\right] &- \mathcal{B}\sigma\,;
\end{aligned}
\tag{87}
$$

- Balance of energy

$$
\begin{aligned}
c_v(1+[\sigma]\sigma)\left\{\frac{\partial T}{\partial t}+\mathcal{R}o\,(\operatorname{grad}T)\cdot\boldsymbol{v}\right\} &= -\mathcal{F}\left(-\frac{\mathcal{B}}{[\sigma]}z+p\right)\operatorname{div}\boldsymbol{v}+ \\
\mathcal{A}^2\left[\frac{\partial}{\partial x}\left(\mathcal{D}^{(T)}\frac{\partial T}{\partial x}\right)+\frac{\partial}{\partial y}\left(\mathcal{D}^{(T)}\frac{\partial T}{\partial y}\right)\right] &+ \frac{\partial}{\partial z}\left(\mathcal{D}^{(T)}\frac{\partial T}{\partial z}\right)+\mathcal{P}_\epsilon^{(T)}\phi^{(T)}\,,
\end{aligned}
\tag{88}
$$

$$
\begin{aligned}
c_p(1+[\sigma]\sigma)\left\{\frac{\partial T}{\partial t}+\mathcal{R}o(\operatorname{grad}\,T)\cdot\boldsymbol{v}\right\}-\Pi\left\{\frac{\partial p}{\partial t}+\mathcal{R}o(\operatorname{grad}\,p)\cdot\boldsymbol{v}-\mathcal{G}w\right\} & \\
=\mathcal{A}^2\left[\frac{\partial}{\partial x}\left(\mathcal{D}^{(T)}\frac{\partial T}{\partial x}\right)+\frac{\partial}{\partial y}\left(\mathcal{D}^{(T)}\frac{\partial T}{\partial y}\right)\right]+\frac{\partial}{\partial z}\left(\mathcal{D}^{(T)}\frac{\partial T}{\partial z}\right) & \\
+\mathcal{A}\left[\frac{\partial \mathcal{P}_x}{\partial x}+\frac{\partial \mathcal{P}_y}{\partial y}\right]+\frac{\partial \mathcal{P}_z}{\partial z}+\mathcal{P}_h^{(T)}\phi^{(T)}\,; &
\end{aligned}
\tag{89}
$$

- Balance of tracer mass

$$
\begin{aligned}
(1+[\sigma]\sigma)\left\{\frac{\partial c_\alpha}{\partial t}+\mathcal{R}o\,(\operatorname{grad}c_\alpha)\cdot\boldsymbol{v}\right\} &= \mathcal{A}^2\left[\frac{\partial}{\partial x}\left(\mathcal{D}^{(c_\alpha)}\frac{\partial c_\alpha}{\partial x}\right)+\frac{\partial}{\partial y}\left(\mathcal{D}^{(c_\alpha)}\frac{\partial c_\alpha}{\partial y}\right)\right] \\
&+\frac{\partial}{\partial z}\left(\mathcal{D}^{(c_\alpha)}\frac{\partial c_\alpha}{\partial z}\right)+\mathcal{R}o\frac{\partial}{\partial z}\left\{(1+[\sigma]\sigma)\,c_\alpha w_\alpha^s\right\}+\mathcal{P}^{(c_\alpha)}\phi^{(c_\alpha)}\,.
\end{aligned}
\tag{90}
$$

In these equations all variables, including the operators, are dimensionless. The dimensionless parameters arising in equations (84)–(90) are listed in Table 4 together with their nomenclature and (some) together with their orders of magnitude as obtained with the scales of Table 3. Note that the buoyancy parameter may also be written as

$$
\mathcal{B}=\frac{\mathcal{A}[\sigma]g}{[f][V]}\,,
$$

Table 4: Dimensionless parameters

Parameter	*Order of magnitude*	*Name*
$\mathcal{A} = \dfrac{[H]}{[L]}$	$10^{-5} - 10^{-2}$	Aspect ratio
$\mathcal{B} = \dfrac{g[\sigma][H]}{[f][L][V]}$	$10^{-2} - 10^{2}$	Buoyancy parameter
$\mathcal{D}^{(T)} = \dfrac{D^{(T)}}{[f][H^2]}$	$10^{-4} - 10^{0}$	Heat diffusivity
$\mathcal{D}^{(c_\alpha)} = \dfrac{D^{(c_\alpha)}}{[f][H^2]}$	$10^{-4} - 10^{0}$	Species mass diffusivity
$\mathcal{F} = \dfrac{[V^2]}{[c_v][\Delta T]}$	$10^{-7} - 10^{-1}$	Pressure work parameter
$\mathcal{G} = \dfrac{g[H]}{[f^2][L^2]}$	$10^{0} - 10^{3}$	Squared velocity ratio
$\mathcal{N} = \dfrac{\nu_t}{[f][H^2]}$	$10^{-6} - 10^{1}$	Dimensionless kinematic turbulent viscosity
$\Pi = \dfrac{[f][L][V]}{[c_p][\Delta T]}$	$10^{-7} - 10^{-2}$	Pressure work parameter
$\mathcal{P}_{\epsilon}^{(T)} = \dfrac{[\phi^{(T)}]}{\rho^*[f][c_v][\Delta T]}$		Power working parameter
$\mathcal{P}_{h}^{(T)} = \dfrac{[\phi^{(T)}]}{\rho^*[f][c_p][\Delta T]}$		Power working parameter
$\mathcal{P}^{(c_\alpha)} = \dfrac{[\phi^{(c_\alpha)}]}{\rho^*[f][c_\alpha]}$		Constituent mass production parameter
$\mathcal{R}o = \dfrac{[V]}{[f][L]}$	$10^{-4} - 10^{0}$	ROSSBY number

and thus depends linearly on the aspect ratio $\mathcal{A}$, but it is not thought to take the limit value 0 as $\mathcal{A} \to 0$. It is rather assumed that $\mathcal{B}$ assumes a finite value as $\mathcal{A}$ becomes vanishingly small. This is indeed the only correct limit as long as gravity is acting as one of the driving mechanism. This is also the reason why $\mathcal{A}$ has not been put in evidence in the expression of $\mathcal{B}$ in Table 4. Special attention should also be devoted to certain combinations of the dimensionless quantities of Table 3 as they occur in the energy equations (88) and (89). One of these is

$$\frac{\mathcal{B}\mathcal{F}}{[\sigma]} = \frac{g\mathcal{A}[V]}{[f][c_v][\Delta T]} \approx 0.25(10^3 - 10^5)\,. \tag{91}$$

Note that, while $\mathcal{B}$ arises together with $[\sigma]$, the combination $\mathcal{B}\mathcal{F}/[\sigma]$ is free of $[\sigma]$. On the other hand, $\mathcal{F}$ by itself is much smaller than (91). This shows (see the term multiplied with $\operatorname{div}\boldsymbol{v}$ on the right-hand side of (88)) that the power of working due to the dynamic pressure is much smaller than the corresponding power due to the hydrostatic pressure. An analogous inference also follows from the corresponding term in (89). Here, it can be shown that $\Pi = \mathcal{O}(10^{-7} - 10^{-2})$, while $\mathcal{G}\Pi = \mathcal{O}(10^{-7} - 10^{-1})$ is generally somewhat larger, but it is not so clear whether the dynamic or the static pressure or both or none ought to be kept in the equation.

In the present context, our interest is in orders of magnitude of numerical values for the parameters $[\sigma]$ and $\mathcal{A}$. This information suggests derivation of approximate models:

Boussinesq approximation The Boussinesq approximation obtains if the limiting equations are used for which $[\sigma] \to 0$. Inspection of (84)–(90) shows that in this case the variable density is set equal to a constant except in the gravity term. The only term of concern is the combination (91) which shows that the limit $[\sigma] \to 0$ does not affect the values for $\mathcal{B}\mathcal{F}/[\sigma]$. Nevertheless the value for (91) is generally large, a fact which explicitly indicates that the power of working due to the hydrostatic pressure may not be negligible at large depths, whereas the corresponding dynamic contribution may be negligible. In any case, these terms can only contribute when the velocity field is not solenoidal, i. e., when

$$\lim_{[\sigma]\to 0} \frac{[\sigma]}{\mathcal{R}o} = \mathcal{O}(1)\,,$$

for which the first term of (84) survives. Except for these cases the mass balance equation reduces to $\operatorname{div}\boldsymbol{v} = 0$, which agrees with the continuity equation of a density preserving fluid even though density variations are accounted for.

Shallow water approximation The shallow water approximation is obtained if equations (84)–(90) are applied in the limit as $\mathcal{A} \to 0$. Inspection of (84)–(90) then implies the following inferences:

- The second Coriolis parameter drops out of the equations. It enters the equations only when $\mathcal{O}(\mathcal{A})$-terms are kept.

- The vertical momentum balance reduces to a force balance between the vertical pressure gradient and the gravity force (in dimensionless formulation):

$$\frac{\partial p}{\partial z} + \mathcal{B}\sigma = 0\,, \tag{92}$$

or, in dimensional coordinates,

$$\frac{\partial p}{\partial z} + \rho\, g = 0\,, \tag{93}$$

equivalent to the hydrostatic pressure assumption. This equation is violated provided $\mathcal{O}(\mathcal{A})$ or higher order terms are accounted for.

- In the balance equations of momentum, energy and species masses, only the vertical gradients of the flux terms survive. This means:

$$\begin{aligned}
\frac{\partial}{\partial z}\left[(1+[\sigma]\sigma)\,\mathcal{N}\frac{\partial u}{\partial z}\right] \quad &\longleftrightarrow \quad \frac{\partial R_{xz}}{\partial z}\,,\\
\frac{\partial}{\partial z}\left[(1+[\sigma]\sigma)\,\mathcal{N}\frac{\partial v}{\partial z}\right] \quad &\longleftrightarrow \quad \frac{\partial R_{yz}}{\partial z}\,,\\
\frac{\partial}{\partial z}\left(\mathcal{D}^{(T)}\frac{\partial T}{\partial z}\right) \quad &\longleftrightarrow \quad \frac{\partial Q_z^{\varepsilon}}{\partial z}\\
\frac{\partial}{\partial z}\left(\mathcal{D}^{(c_\alpha)}\frac{\partial c_\alpha}{\partial z}\right) + \mathcal{R}o\frac{\partial}{\partial z}\left\{(1+[\sigma]\sigma)\,c_\alpha w_\alpha^s\right\} \quad &\longleftrightarrow \quad \frac{\partial}{\partial z}\left(-J_{\alpha z} + \rho c_\alpha w_\alpha^s\right)\,,
\end{aligned}$$

are the only flux terms which contribute in the shallow water approximation to the field equations. This is a well-established result in Geophysical Fluid Mechanics.

Boussinesq **and shallow water approximation** The governing equations in both the Boussinesq assumption, $[\sigma] \to 0$, and the shallow water assumption, $\mathcal{A} \to 0$, are obtained from (84) – (90) and have the following forms in dimensional notation:

- Balance of mass (continuity equation)

$$\operatorname{div} \boldsymbol{v} = 0\,; \tag{94}$$

- Balance of momentum

$$\begin{aligned}
\frac{\partial u}{\partial t} + (\operatorname{grad} u)\cdot\boldsymbol{v} - f v \quad &= \quad -\frac{1}{\rho^*}\frac{\partial p}{\partial x} + \frac{\partial}{\partial z}\left(\nu_t \frac{\partial u}{\partial z}\right),\\
\frac{\partial v}{\partial t} + (\operatorname{grad} v)\cdot\boldsymbol{v} + f u \quad &= \quad -\frac{1}{\rho^*}\frac{\partial p}{\partial y} + \frac{\partial}{\partial z}\left(\nu_t \frac{\partial v}{\partial z}\right),\\
0 \quad &= \quad \frac{1}{\rho^*}\frac{\partial p}{\partial z} + g\,;
\end{aligned} \tag{95}$$

- Balance of energy (heat conduction equation)

$$\rho^* c_v \left\{ \frac{\partial T}{\partial t} + (\text{grad } T) \cdot \boldsymbol{v} \right\} = \rho^* [c_v] \frac{\partial}{\partial z} \left(D^{(T)} \frac{\partial T}{\partial z} \right) + \phi^{(T)} , \tag{96}$$

$$\begin{aligned} \rho^* c_p \left\{ \frac{\partial T}{\partial t} + (\text{grad } T) \cdot \boldsymbol{v} \right\} &= - \left\{ \frac{\partial p}{\partial t} + \text{grad } p \cdot \boldsymbol{v} \right\} + \\ & \rho^* [c_p] \frac{\partial}{\partial z} \left(D^{(T)} \frac{\partial T}{\partial z} \right) + \frac{\partial \mathcal{P}_z}{\partial z} + \phi^{(T)} ; \end{aligned} \tag{97}$$

- Balance of tracer mass

$$\begin{aligned} \rho^* \left\{ \frac{\partial c_\alpha}{\partial t} + (\text{grad } c_\alpha) \cdot \boldsymbol{v} \right\} = \rho^* \frac{\partial}{\partial z} \left(D^{(c_\alpha)} \frac{\partial c_\alpha}{\partial z} \right) + \rho^* \frac{\partial}{\partial z} (c_\alpha w_\alpha^s) + \phi^{(c_\alpha)} , \\ \alpha = 1, \ldots, N . \end{aligned} \tag{98}$$

In the above equations, ν_t stands for the sum of the laminar plus turbulent viscosities, the former can in general be ignored in comparison to the latter, but is better included when the turbulent viscosity should become small; c_v is the heat capacity of water at constant volume and c_p is the heat capacity of water at constant pressure, while $D^{(c_\alpha)}$ is the mass diffusivity of the suspended particles of the size range α. Moreover, $\phi^{(T)}$ is the dissipative work power and $\phi^{(c_\alpha)}$ the mass production rate of the particles of size range α. Both are generally ignored in sedimentation processes in lakes.[22]

2.4 Boussinesq and hydrostatic pressure assumption in Model 2

In a comparison with (84)–(90) equations (94)–(98) show that in the shallow water approximation the horizontal diffusive flux terms are all dropped in a zeroth order shallowness approximation ($\mathcal{A} \to 0$). Inspection of (84)–(90) further shows that these terms are $\mathcal{O}(\mathcal{A}^2)$. Resurrection of the horizontal flux terms in the balance laws of momentum, energy and constituent masses therefore strictly means that the full equations (84)–(90) must be kept and only be reduced by the Boussinesq approximation $[\sigma] \to 0$. However, as shown by (87), the hydrostatic pressure assumption can not be maintained if the $\mathcal{O}(\mathcal{A}^2)$-terms are kept in the remaining field equations. Moreover, since the Coriolis terms in (85)–(87) are of $\mathcal{O}(\mathcal{A})$, these terms should also be kept (the $\tilde{f}$ term in (85) and (87)!). Nevertheless, in the literature equations are used in which the Boussinesq approximation is combined with the hydrostatic pressure assumption. A derivation from a systematic scaling analysis is not known to us, but the following suppositions lead to the very popular system of field equations in the Boussinesq and hydrostatic pressure approximations:

Hydrostatic pressure assumption: Ignore in the vertical momentum equation (87) all acceleration and diffusive terms and keep only those of zeroth order in $\mathcal{A}$.

[22] $\phi^{(c_\alpha)}$ could consist of fragmentation and abrasion of suspended particles, which, however, are unlikely processes.

This hypothesis reduces (87) to (92) or, in dimensional form, to equation (93). Writing the latter as

$$\frac{\partial p}{\partial z} = -\rho^{**}g + g(\rho^{**} - \rho) = -\rho^{**}g - \rho^{**}g\sigma(x,y,z,t)\,, \quad \sigma(x,y,z,t) \equiv \frac{\rho(x,y,z,t)}{\rho^{**}} - 1\,, \tag{99}$$

after integration we obtain

$$p(x,y,z,t) = \underbrace{\rho^{**}g\,(\zeta(x,y,t) - z) + p^{\text{atm}}(x,y,t)}_{p^{\text{ext}}} + \underbrace{\rho^{**}g\int_z^{\zeta(x,y,t)} \sigma(\cdot,\bar{z})\,d\bar{z}}_{p^{\text{int}}}\,. \tag{100}$$

Here, ρ^{**} is a constant density (smaller than any density in the lake, e.g., $\rho^{**} = \rho(30°\text{C})$, so that $\sigma > 0$), $z = \zeta(x,y,t)$ defines the deformed free surface, and p^{atm} is the atmospheric pressure. In lake applications one usually assumes that p^{atm} is spatially constant. The derivatives of (100),

$$\begin{aligned}
\frac{\partial p}{\partial x} &= \rho^{**}g\frac{\partial \zeta}{\partial x} + \frac{\partial p^{\text{atm}}}{\partial x} + \rho^{**}g\frac{\partial}{\partial x}\int_z^{\zeta(x,y,t)} \sigma(x,y,\bar{z},t)\,d\bar{z}\,,\\
\frac{\partial p}{\partial y} &= \rho^{**}g\frac{\partial \zeta}{\partial y} + \frac{\partial p^{\text{atm}}}{\partial y} + \rho^{**}g\frac{\partial}{\partial y}\int_z^{\zeta(x,y,t)} \sigma(x,y,\bar{z},t)\,d\bar{z}\,,
\end{aligned} \tag{101}$$

may then be substituted into (85), (86) to eliminate the pressure formally as a variable from the horizontal momentum equations.

In oceanography the hydrostatic pressure assumption is often combined with other ad hoc assumptions, which can not be motivated by the shallow water assumption. These assumptions are the following:

- Assume the horizontal diffusivities in the horizontal momentum equations to be large of $\mathcal{O}(\mathcal{A}^{-2})$ and *constant*, and the vertical diffusivities to be variable and of $\mathcal{O}(1)$:
  - horizontal momentum diffusivities: $\mathcal{N} \to \mathcal{N}_{\text{hor}}/\mathcal{A}^2$ and constant;
  - vertical momentum diffusivities: $\mathcal{N} \to \mathcal{N}_{\text{vert}}(x,y,z,t)$.
- Assume in the energy and constituent mass balances the horizontal diffusivities to be large of $\mathcal{O}(\mathcal{A}^{-2})$:
  - horizontal energy diffusivities: $\mathcal{D}^{(T)} \to \mathcal{D}^{(T)}_{\text{hor}}/\mathcal{A}^2$;
  - vertical energy diffusivities: $\mathcal{D}^{(T)} \to \mathcal{D}^{(T)}_{\text{vert}}$;
  - horizontal constituent mass diffusivities: $\mathcal{D}^{(c_\alpha)} \to \mathcal{D}^{(c_\alpha)}_{\text{hor}}/\mathcal{A}^2$;
  - vertical constituent mass diffusivities: $\mathcal{D}^{(c_\alpha)} \to \mathcal{D}^{(c_\alpha)}_{\text{vert}}$.

If these assumptions are substituted into (84)–(90) and the limits $\mathcal{A} \to 0$ and $[\sigma] \to 0$ are taken, the following system of equations (in physical dimensions) emerges:

- Balance of mass:

$$\operatorname{div} \boldsymbol{v} = 0\,; \tag{102}$$

- Balance of momentum:

$$\begin{aligned} \frac{\partial u}{\partial t} + (\operatorname{grad} u) \cdot \boldsymbol{v} - f u = -\frac{1}{\rho_*}\frac{\partial p}{\partial x} + \\ \nu_{\text{hor}} \left[\left(\frac{\partial^2 u}{\partial x^2} + \frac{\partial^2 u}{\partial y^2} \right) + \underbrace{\frac{\partial}{\partial x}\left(\frac{\partial u}{\partial x} + \frac{\partial u}{\partial y} \right)} \right] + \frac{\partial}{\partial z}\left(\nu_{\text{vert}} \frac{\partial u}{\partial z} \right), \end{aligned} \tag{103}$$

$$\begin{aligned} \frac{\partial v}{\partial t} + (\operatorname{grad} v) \cdot \boldsymbol{v} - f v = -\frac{1}{\rho_*}\frac{\partial p}{\partial y} + \\ \nu_{\text{hor}} \left[\left(\frac{\partial^2 v}{\partial x^2} + \frac{\partial^2 v}{\partial y^2} \right) + \underbrace{\frac{\partial}{\partial y}\left(\frac{\partial v}{\partial x} + \frac{\partial v}{\partial y} \right)} \right] + \frac{\partial}{\partial z}\left(\nu_{\text{vert}} \frac{\partial v}{\partial z} \right); \end{aligned} \tag{104}$$

- Balance of energy:

$$\begin{aligned} \rho^\star c_v \left(\frac{\partial T}{\partial t} + (\operatorname{grad} T) \cdot \boldsymbol{v} \right) = \\ \rho^\star [c_v] D^{(T)}_{\text{hor}} \left(\frac{\partial^2 T}{\partial x^2} + \frac{\partial^2 T}{\partial y^2} \right) + \rho^\star [c_v] \frac{\partial}{\partial z}\left(D^{(T)}_{\text{vert}} \frac{\partial T}{\partial z} \right) + \phi^{(T)}, \end{aligned} \tag{105}$$

$$\begin{aligned} \rho^\star c_p \left(\frac{\partial T}{\partial t} + (\operatorname{grad} T) \cdot \boldsymbol{v} \right) = -\left(\frac{\partial p}{\partial t} + (\operatorname{grad} p) \cdot \boldsymbol{v} \right) + \\ \rho^\star [c_p] D^{(T)}_{\text{hor}} \left(\frac{\partial^2 T}{\partial x^2} + \frac{\partial^2 T}{\partial y^2} \right) + \rho^\star [c_p] \frac{\partial}{\partial z}\left(D^{(T)}_{\text{vert}} \frac{\partial T}{\partial z} \right) + \phi^{(T)}; \end{aligned} \tag{106}$$

- Balance of tracer mass:

$$\begin{aligned} \rho^\star \left(\frac{\partial c_\alpha}{\partial t} + (\operatorname{grad} c_\alpha) \cdot \boldsymbol{v} \right) = \rho^\star D^{(c_\alpha)}_{\text{hor}} \left(\frac{\partial^2 c_\alpha}{\partial x^2} + \frac{\partial^2 c_\alpha}{\partial y^2} \right) + \\ \rho^\star \frac{\partial}{\partial z}\left(D^{(c_\alpha)}_{\text{vert}} \frac{\partial c_\alpha}{\partial z} \right) + \rho^\star \frac{\partial}{\partial z}(c_\alpha w - \alpha^s) + \phi^{(c_\alpha)}. \end{aligned} \tag{107}$$

These equations are to be complemented by the pressure equation (100). We further remark, that physical values for ν_{hor} are $1\,\text{m}^2\text{s}^{-1}$, while those for ν_{vert} are $10^{-4} - 10^{-2}\,\text{m}^2\text{s}^{-1}$. Similar order of magnitude differences also exist for the horizontal and vertical diffusivities $D^{(T)}_{\text{hor}}$, $D^{(T)}_{\text{vert}}$, $D^{(c_\alpha)}_{\text{hor}}$, and $D^{(c_\alpha)}_{\text{vert}}$.

However, the underbraced terms are omitted in the oceanographic and limnological literature. In that reduced form the momentum equations were first presented by Munk in

1950 [31]. We also note that there is no rational justification of the above laws which would be based on continuum mechanical principles of an anisotropic viscous stress-stretching relation. Wang (1996) [50], however, presents in his dissertation a derivation based on such principles and delimits the conditions under which equations (102)–(107) hold true. This derivation is also given in Hutter et al. (2011) [18].

3 A primer on boundary and transition conditions

The free surface, the transition surface between regions I and II (Fig. 3) and the lower boundary separating the detritus region from the immobile rigid bed are *singular surfaces*; these are so called, since physical quantities may suffer a jump discontinuity from values on one side to the other side when the surface is crossed. For instance, from region I in Fig. 3, to the atmosphere, the density changes by a factor of 10^{-3}; likewise the velocity changes from that of the lake water to that of the air. Depending on specific conditions such surfaces may be occupied by the same material particles for all times, or may be simply discontinuity surfaces for some fields; they are then called *material* and *non-material* surfaces, respectively. Two kinds of mathematical statements can be derived for such surfaces: (i) those of geometric-kinematic nature and (ii) those of dynamic meaning. They are used to formulate boundary conditions for the equations in the bulk adjacent bodies. Our derivation will be brief and partly incomplete. The reader is directed to the specialized literature e.g. Müller (1985) [30], Hutter (1992) [15], Slattery et al. (2007) [40]. In order to present these conditions we need some basics from the geometry and kinematics of a moving surface.

First, we consider *geometric* properties of a (stagnant) surface $\mathcal{S}$, given parametrically in a Cartesian reference system $Ox^1x^2x^3$ by

$$\boldsymbol{r} = \boldsymbol{x}(\xi^1, \xi^2) = x^k(\xi^1, \xi^2)\, \boldsymbol{e}_k\,, \quad (\xi^1, \xi^2) \in \Delta_0\,, \tag{108}$$

where $\{\boldsymbol{e}_1, \boldsymbol{e}_2, \boldsymbol{e}_3\}$ is the Cartesian basis. It is supposed that the function $\boldsymbol{r}$ is such that the vectors

$$\boldsymbol{\tau}_{\mathfrak{a}} \equiv \frac{\partial \boldsymbol{r}}{\partial \xi^{\mathfrak{a}}} = \frac{\partial x^k}{\partial \xi^{\mathfrak{a}}}\, \boldsymbol{e}_k\,, \quad \mathfrak{a} = 1,\, 2\,, \tag{109}$$

satisfy the condition

$$\boldsymbol{\tau}_1 \times \boldsymbol{\tau}_2 \neq \boldsymbol{0}\,, \quad \forall\ (\xi^1, \xi^2) \in \Delta_0\,,$$

implying, in particular, that $\boldsymbol{\tau}_1$, $\boldsymbol{\tau}_2$ are not zero. At $\boldsymbol{r}(\xi^1, \xi^2)$ the vectors $\boldsymbol{\tau}_1$ and $\boldsymbol{\tau}_2$ are tangent vectors (generally not perpendicular to one another and neither necessarily of unit length) to the coordinate lines ξ^2 = constant and ξ^1 = constant, respectively. Their span defines the tangent space to $\mathcal{S}$ at $\boldsymbol{r}(\xi^1, \xi^2)$, and

$$\boldsymbol{n} \equiv \frac{\boldsymbol{\tau}_1 \times \boldsymbol{\tau}_2}{\|\boldsymbol{\tau}_1 \times \boldsymbol{\tau}_2\|} \tag{110}$$

is a unit vector normal to this tangent space. This way one obtains a basis, $\{\boldsymbol{\tau}_1, \boldsymbol{\tau}_2, \boldsymbol{n}\}$, for the space of three-dimensional vectors, and hence we may write[23]

$$\frac{\partial \boldsymbol{\tau}_{\mathfrak{a}}}{\partial \xi^{\mathfrak{b}}} = \Gamma^{\mathfrak{c}}_{\mathfrak{a}\mathfrak{b}}\, \boldsymbol{\tau}_{\mathfrak{c}} + b_{\mathfrak{a}\mathfrak{b}}\, \boldsymbol{n}\,,$$

which is the representation of $\partial \boldsymbol{\tau}_{\mathfrak{a}}/\partial \xi^{\mathfrak{b}}$ with respect to this basis. The coefficients $\Gamma^{\mathfrak{c}}_{\mathfrak{a}\mathfrak{b}}$ are called CHRISTOFFEL symbols and are proved to be given by

$$\Gamma^{\mathfrak{c}}_{\mathfrak{a}\mathfrak{b}} = \tfrac{1}{2} g^{\mathfrak{c}\mathfrak{d}} \left(\frac{\partial g_{\mathfrak{d}\mathfrak{a}}}{\partial \xi^{\mathfrak{b}}} + \frac{\partial g_{\mathfrak{d}\mathfrak{b}}}{\partial \xi^{\mathfrak{a}}} - \frac{\partial g_{\mathfrak{a}\mathfrak{b}}}{\partial \xi^{\mathfrak{d}}} \right), \tag{111}$$

where $g_{\mathfrak{a}\mathfrak{b}}$ are the *coefficients of the first fundamental form* of $\mathcal{S}$,

$$g_{\mathfrak{a}\mathfrak{b}} \equiv \boldsymbol{\tau}_{\mathfrak{a}} \cdot \boldsymbol{\tau}_{\mathfrak{b}}\,,$$

and $g^{\mathfrak{a}\mathfrak{b}}$ are defined as

$$g^{\mathfrak{a}\mathfrak{b}} \equiv \boldsymbol{\tau}^{\mathfrak{a}} \cdot \boldsymbol{\tau}^{\mathfrak{b}}\,,$$

with $\{\boldsymbol{\tau}^1, \boldsymbol{\tau}^2\}$ the reciprocal basis of the *natural basis* $\{\boldsymbol{\tau}_1, \boldsymbol{\tau}_2\}$ of the tangent space, i.e.,

$$\boldsymbol{\tau}^{\mathfrak{a}} \cdot \boldsymbol{\tau}_{\mathfrak{b}} = \delta^{\mathfrak{a}}{}_{\mathfrak{b}}\,,$$

where $\delta^{\mathfrak{a}}{}_{\mathfrak{b}}$ is the KRONECKER delta; the matrix $(g^{\mathfrak{a}\mathfrak{b}})$ is the matrix inverse of $(g_{\mathfrak{a}\mathfrak{b}})$: $(g^{\mathfrak{a}\mathfrak{b}}) = (g_{\mathfrak{a}\mathfrak{b}})^{-1}$. On the other hand, $b_{\mathfrak{a}\mathfrak{b}}$ are the so-called *coefficients of the second fundamental form* of $\mathcal{S}$, and they can be calculated as

$$b_{\mathfrak{a}\mathfrak{b}} = \frac{\partial \boldsymbol{\tau}_{\mathfrak{a}}}{\partial \xi^{\mathfrak{b}}} \cdot \boldsymbol{n} = -\boldsymbol{\tau}_{\mathfrak{a}} \cdot \frac{\partial \boldsymbol{n}}{\partial \xi^{\mathfrak{b}}} = b_{\mathfrak{b}\mathfrak{a}}\,, \tag{112}$$

once the functions $x^k(\xi^1, \xi^2)$, $k = 1, 2, 3$ (see (108)) are known. Since

$$\frac{\partial \boldsymbol{n}}{\partial \xi^{\mathfrak{b}}} = -b_{\mathfrak{a}\mathfrak{b}}\, \boldsymbol{\tau}^{\mathfrak{a}}\,, \quad \mathfrak{b} = 1, 2\,,$$

it is clear that the scalars $b_{\mathfrak{a}\mathfrak{b}}$ give an insight on how much the surface is 'curved'. An intrinsic (i.e., independent of the parameterization (108) for $\mathcal{S}$) quantity measuring the curvature of $\mathcal{S}$ is the *mean curvature*

$$K \equiv \tfrac{1}{2}\, g^{\mathfrak{a}\mathfrak{b}}\, b_{\mathfrak{a}\mathfrak{b}}\,. \tag{113}$$

Now, we refer to the *kinematic* properties of a moving surface $\mathcal{S}$. Thus, now $\mathcal{S}$ denotes a one-parameter family $\{\mathcal{S}_t\}_{t\in I}$, with $I \subset \mathbb{R}$ an open (time) interval, of surfaces $\mathcal{S}_t$ given by

$$\boldsymbol{x} = \boldsymbol{r}(\xi^1, \xi^2, t) = x^k(\xi^1, \xi^2, t)\, \boldsymbol{e}_k\,, \quad (\xi^1, \xi^2) \in \Delta_0\,, \quad t \in I\,. \tag{114}$$

[23]We employ the summation convention from 1 to 2 over doubly repeated coefficients of contra and covariant tensor components: $A^{\mathfrak{c}}_{\mathfrak{a}\mathfrak{b}} v_{\mathfrak{c}}$ or $A^{\mathfrak{a}\mathfrak{b}}_{\mathfrak{c}} v^{\mathfrak{c}}$, etc.

The vector
$$\boldsymbol{w} \equiv \frac{\partial \boldsymbol{r}}{\partial t} \tag{115}$$
is the *velocity of the surface point* (ξ^1, ξ^2) at the moment t. With respect to the basis $\{\boldsymbol{\tau}_1, \boldsymbol{\tau}_2, \boldsymbol{n}\}$ it has the representation
$$\boldsymbol{w} = w^{\mathfrak{a}} \boldsymbol{\tau}_{\mathfrak{a}} + \mathcal{U}\boldsymbol{n}\,. \tag{116}$$
The normal component $\mathcal{U}$ of $\boldsymbol{w}$ is independent of the choice of the parametric representation (114), and is called the speed of displacement of that point on $\mathcal{S}_t$ for which the position vector is $\boldsymbol{r}(\xi^1, \xi^2, t)$, or simply, the *speed of displacement of* $\mathcal{S}$.

3.1 Kinematic surface condition

The moving surface $\mathcal{S}$ may be given implicitly, that is, by an equation of the form
$$F(\boldsymbol{x}, t) = 0\,. \tag{117}$$
Choosing a local parameterization for $\mathcal{S}$, say in the form (114), we have
$$F(\boldsymbol{r}(\xi^1, \xi^2, t), t) = 0$$
for all $(\xi^1, \xi^2) \in \Delta_0$ and for all $t \in I$. Differentiating this relation with respect to t and recalling definition (115) of $\boldsymbol{w}$, we obtain
$$\frac{\partial F}{\partial t} + \operatorname{grad} F \cdot \boldsymbol{w} = 0\,, \tag{118}$$
which is called the *kinematic condition* for F. Now, if the surface parameters are conveniently ordered, the unit normal vector (110) is $\boldsymbol{n} = \operatorname{grad} F / \|\operatorname{grad} F\|$, and so with (116) we rewrite (118) in the form
$$\frac{\partial F/\partial t}{\|\operatorname{grad} F\|} + \underbrace{\underbrace{\frac{\operatorname{grad} F}{\|\operatorname{grad} F\|}}_{=\boldsymbol{n}} \cdot \boldsymbol{w}}_{=\mathcal{U}} = 0 \iff \mathcal{U} = -\frac{\partial F/\partial t}{\|\operatorname{grad} F\|}\,, \tag{119}$$
which serves to calculate the speed of displacement $\mathcal{U}$ if the function F is known, or stands as a partial differential equation for F if the normal velocity $\mathcal{U}$ is known. It is customary to denote the semi-space to which $\boldsymbol{n}$ is directed the positive side of the surface and the other semi-space the negative side of it, see Fig. 6. Altering the orientation from (+) to (−) is possible by replacing F with $-F$.

It may happen that the surface $\mathcal{S}$ is a material surface, that is, it is always occupied by the same bodily particles identified with their position vectors $\boldsymbol{X}$ in a reference configuration and having their own motion on $\mathcal{S}$. Thus, if
$$\boldsymbol{x} = \boldsymbol{\chi}(\boldsymbol{X}, t)$$

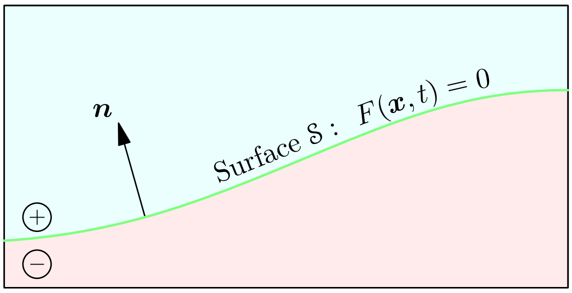

Figure 6: A surface $\mathcal{S}$, given by the equation $F = 0$, separates the three-dimensional space into the semi-spaces on the (+)- and (−)-sides of $\mathcal{S}$. The (+)-side is on that side into which the unit normal vector points.

represents the motion of the particle $\boldsymbol{X}$, since for all times t the particle lies on $\mathcal{S}$, we have

$$F(\boldsymbol{\chi}(\boldsymbol{X}, t), t) = 0\,.$$

Differentiating this relation with respect to t and defining the velocity $\boldsymbol{v}_{\mathcal{S}}$ of the surface particle $\boldsymbol{X}$ as

$$\boldsymbol{v}_{\mathcal{S}} \equiv \frac{\partial \boldsymbol{\chi}}{\partial t}\,, \tag{120}$$

we obtain the *kinematic condition for the material surface* $\mathcal{S}$:

$$\frac{\partial F}{\partial t} + \operatorname{grad} F \cdot \boldsymbol{v}_{\mathcal{S}} = 0\,. \tag{121}$$

This gives

$$\boldsymbol{v}_{\mathcal{S}} \cdot \boldsymbol{n} = -\frac{\partial F}{\partial t} / \|\operatorname{grad} F\|\,,$$

which, when comparing with (119), shows that for material surfaces equality $\boldsymbol{v}_{\mathcal{S}} \cdot \boldsymbol{n} = \mathcal{U}$ holds (for details see Fig. 9). If $\mathcal{S}$ consists of particles of a three-dimensional continuum body $\mathcal{B}$, then $\boldsymbol{v}_{\mathcal{S}} = \boldsymbol{v}$, where $\boldsymbol{v}$ is the velocity field corresponding to $\mathcal{B}$, and (121) takes the form

$$\frac{\partial F}{\partial t} + \operatorname{grad} F \cdot \boldsymbol{v} = 0\,. \tag{122}$$

3.2 Dynamic surface jump conditions

Consider a bodily region, in which the physical fields are continuously differentiable (smooth), except for singular surface(s) $\mathcal{S}$ across which some fields may suffer jump discontinuities; $\mathcal{S}$ is supposed to not have its own physical properties. Figure 7 and its caption explain the situation. Applying the balance law

$$\frac{d}{dt}\int_{\mathcal{B}=\mathcal{B}^+\cup\mathcal{B}^-} f\,dv = -\int_{\partial\mathcal{B}=\partial\mathcal{B}^+\cup\partial\mathcal{B}^-} \boldsymbol{\phi}^f \cdot \boldsymbol{n}\,da + \int_{\mathcal{B}^+\cup\mathcal{B}^-} (s^f + \pi^f)\,dv \tag{123}$$

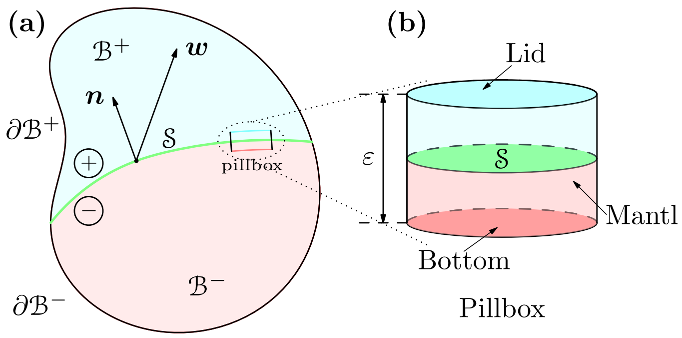

Figure 7: (a) Body $\mathcal{B} = \mathcal{B}^+ \cup \mathcal{B}^-$ whose physical fields may suffer jump discontinuities across $\mathcal{S}$, but are smooth tangential to $\mathcal{S}$. **(b)** Pillbox, zoomed from panel (a). Its total surface consists of the lid on the (+)-side of $\mathcal{S}$ and the bottom on the (–)-side; its mantle surface has thickness ε. Balance laws (124) for this bodily surface will be formulated in the limit as $\varepsilon \to 0$. The unit normal vector to $\mathcal{S}$ points into $\mathcal{B}^+$ and $\boldsymbol{w}$ is the velocity of surface coordinates on $\mathcal{S}$, but only $\mathcal{U} = \boldsymbol{w}\cdot\boldsymbol{n}$ is kinematically relevant for $\mathcal{S}$.

to the pillbox volume $\mathcal{B}$ (Fig. 7 b) and performing the limit $\varepsilon \to 0$ in the emerging statement such that $\mathcal{S}$ stays between lid and bottom, leads to the expression

$$[\![f\,(\boldsymbol{v} - \boldsymbol{w}) \cdot \boldsymbol{n}]\!] + [\![\boldsymbol{\phi}^f \cdot \boldsymbol{n}]\!] = 0\,. \tag{124}$$

In the above equations, f, $\boldsymbol{\phi}^f$, s^f and π^f denote the physical quantity inside $\mathcal{B} = \mathcal{B}^+ \cup \mathcal{B}^-$, its flux across the outer surface $\partial\mathcal{B} = \partial\mathcal{B}^+ \cup \partial\mathcal{B}^-$, the supply and the production rates within $\mathcal{B} = \mathcal{B}^+ \cup \mathcal{B}^-$, respectively. Moreover, with $\psi^\pm$ the values of a quantity ψ immediately on the (+)- and (–)-side of $\mathcal{S}$, respectively, $[\![\, \psi \,]\!] \equiv \psi^+ - \psi^-$ is the jump of ψ across $\mathcal{S}$. The derivation of (124) from (123) is given in books on continuum mechanics, e.g. Hutter and Jöhnk (2004) [17].

In the balance statement (123) it is assumed that the integral $\int_{\mathcal{B}} (s^f + \pi^f)\,dv$ vanishes as $\varepsilon \to 0$, so that s^f and π^f do not arise in (124). Similarly, it is also assumed that $\int_{\mathcal{B}} f\,dv$ vanishes as $\varepsilon \to 0$. The relevant quantities f and $\boldsymbol{\phi}^f$ are collectively summarized in Table 5 for the physical laws (76)–(80).

For instance, when referred to the physical laws (76)–(80), to which the entries of Table 5 correspond, the jump condition (124) takes the forms

$$\begin{gathered}
[\![\rho(\boldsymbol{v} - \boldsymbol{w}) \cdot \boldsymbol{n}]\!] = 0\,, \\
[\![\rho\, c_\alpha (\boldsymbol{v} - \boldsymbol{w}) \cdot \boldsymbol{n}]\!] + [\![\boldsymbol{J}_\alpha - \rho c_\alpha \boldsymbol{w}_s^\alpha]\!] \cdot \boldsymbol{n} = 0\,, \quad \alpha = 1, \dots, N\,, \\
[\![\rho((\boldsymbol{v} - \boldsymbol{w})\cdot\boldsymbol{n})\boldsymbol{v}]\!] - [\![-p\boldsymbol{I} + \boldsymbol{R}]\!]\boldsymbol{n} = \boldsymbol{0}\,, \\
[\![\rho(\epsilon + \tfrac{1}{2}\boldsymbol{v}\cdot\boldsymbol{v})(\boldsymbol{v} - \boldsymbol{w})\cdot\boldsymbol{n}]\!] + [\![\boldsymbol{Q}_\epsilon + (p\boldsymbol{I} - \boldsymbol{R})\boldsymbol{v}]\!] \cdot \boldsymbol{n} = 0\,, \\
[\![\rho(h + \tfrac{1}{2}\boldsymbol{v}\cdot\boldsymbol{v})(\boldsymbol{v} - \boldsymbol{w})\cdot\boldsymbol{n}]\!] + [\![\boldsymbol{Q}_h + (p\boldsymbol{I} - \boldsymbol{R})\boldsymbol{v}]\!] \cdot \boldsymbol{n} = 0\,.
\end{gathered} \tag{125}$$

Table 5: Expressions for the quantity f and its flux $\boldsymbol{\phi}^f$ in the physical balance laws[a]

Quantity f	f	$\boldsymbol{\phi}^f$
Mixture mass balance	ρ	$\boldsymbol{0}$
Constituent mass balance	ρc_α	$\boldsymbol{J}_\alpha - \rho c_\alpha \boldsymbol{w}_s^\alpha$
Mixture momentum balance	$\rho\,\boldsymbol{v}$	$p\boldsymbol{I} - \boldsymbol{R}$
Mixture energy balance	$\rho(\epsilon + \frac{1}{2}\boldsymbol{v}\cdot\boldsymbol{v})$	$\boldsymbol{Q}_\epsilon + (p\boldsymbol{I} - \boldsymbol{R})\boldsymbol{v}$
Mixture energy balance	$\rho(h + \frac{1}{2}\boldsymbol{v}\cdot\boldsymbol{v})$	$\boldsymbol{Q}_h + (p\boldsymbol{I} - \boldsymbol{R})\boldsymbol{v}$

[a] ρ is the mixture density, c_α – the mass fraction of tracer α, $\boldsymbol{J}_\alpha$ – the constituent laminar and turbulent mass flux vector, $\boldsymbol{w}_s^\alpha$ – the settling velocity of constituent α, $\boldsymbol{v}$ – the barycentric velocity, p – the mixture pressure, $\boldsymbol{R}$ – the turbulent Reynolds stress tensor, ϵ – the internal energy, h – the enthalpy, $\boldsymbol{Q}_\epsilon$, $\boldsymbol{Q}_h$ – turbulent heat flux vectors.

These describe the jump conditions of the mass of the mixture as a whole and of the tracer masses, of the mixture momentum and mixture energy balances. All are written by using the mass fraction c_α and the barycentric velocity as basic fields. In the Boussinesq approximation ρ may be replaced by ρ^*. Of special interest is the situation when $\boldsymbol{w}\cdot\boldsymbol{n} = \boldsymbol{v}\cdot\boldsymbol{n}$. In this case only the second terms on the left-hand sides of (125) survive. Even though this does not exactly define the physical jump conditions for a *material* surface, it is customary to call such surfaces material. The better denotation is to say that such *surfaces follow the barycentric motion.*

Note that, due to the jump condition $(125)_1$, explicitly

$$\underbrace{\rho^+(\boldsymbol{v}^+ - \boldsymbol{w})\cdot\boldsymbol{n}}_{\equiv\,\mathcal{M}^+} = \underbrace{\rho^-(\boldsymbol{v}^- - \boldsymbol{w})\cdot\boldsymbol{n}}_{\equiv\,\mathcal{M}^-}\,, \tag{126}$$

in fluid mechanical applications the kinematic surface relation (118) is often written as

$$\frac{\partial F/\partial t}{\|\mathrm{grad}\,F\|} + \boldsymbol{v}^\pm\cdot\boldsymbol{n} = \frac{\mathcal{M}}{\rho^\pm}\,, \tag{127}$$

where $\mathcal{M} \equiv \mathcal{M}^+ = \mathcal{M}^-$. We emphasize that (118) is a pure kinematic statement, while (127) is a mixed kinematic-dynamic statement.

3.3 Surface balance laws

The above jump conditions are obtained on the assumption that the singular surface $\mathcal{S}$ does not possess its own physical properties. We shall now relax this assumption and request that $\mathcal{S}$ contributes to the balance law of the pillbox with a surface density $f_\mathcal{S}$,

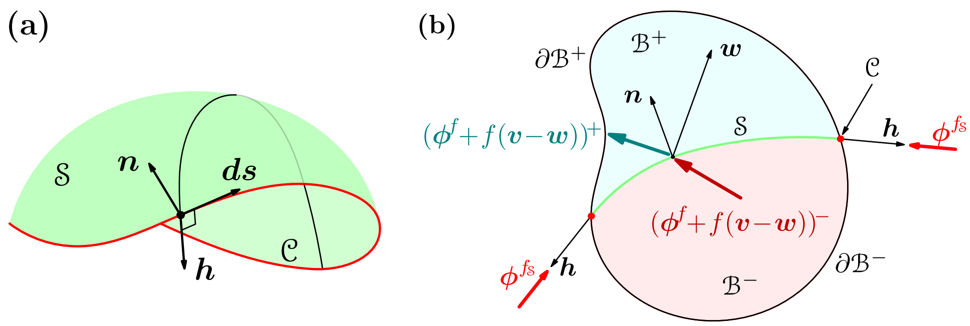

Figure 8: (a) Surface $\mathcal{S}$ spanned over a simple double-point free closed loop $\mathcal{C}$; $\boldsymbol{n}$ is the unit normal vector on $\mathcal{S}$ at a point on $\mathcal{C}$; $\boldsymbol{ds}$ is the incremental tangent vector to the curve $\mathcal{C}$; $\boldsymbol{h}$ is the unit vector normal to $\mathcal{C}$ and tangential to $\mathcal{S}$; $\boldsymbol{h}$, $\boldsymbol{ds}$, and $\boldsymbol{n}$ form a right-handed orthogonal triad. **(b)** Two-dimensional sketch of the singular surface $\mathcal{S}$ with unit normal vector $\boldsymbol{n}$ and spanned by the closed loop $\mathcal{C}$. The panel shows positive ($\mathcal{B}^+$) and negative ($\mathcal{B}^-$) regions separated by $\mathcal{S}$, the surface flux $\boldsymbol{\phi}^{f_\mathcal{S}}$ into $\mathcal{S}$ along $\mathcal{C}$, the vector $\boldsymbol{h}$ (compare panel (a)) and the conductive and convective fluxes from the bulk region.

having a production $\pi^{f_\mathcal{S}}$ and a supply $s^{f_\mathcal{S}}$ per unit area of $\mathcal{S}$, and a flux $\boldsymbol{\phi}^{f_\mathcal{S}}$ per unit length and tangential to $\mathcal{S}$ through the boundary $\mathcal{C}$ of $\mathcal{S}$ (see Fig. 8):

$$
\begin{aligned}
\frac{d}{dt}\left\{\int_{\mathcal{B}=\mathcal{B}^+\cup\mathcal{B}^-} f\,dv + \int_{\mathcal{S}} f_\mathcal{S}\,da\right\} = -\int_{\partial\mathcal{B}=\partial\mathcal{B}^+\cup\partial\mathcal{B}^-} \boldsymbol{\phi}^f\cdot\boldsymbol{n}\,da - \int_{\mathcal{C}=\partial\mathcal{S}} \boldsymbol{\phi}^{f_\mathcal{S}}\cdot\boldsymbol{h}\,ds\, + \\
\int_{\mathcal{B}^+\cup\mathcal{B}^-} (\pi^f + s^f)\,dv + \int_{\mathcal{S}} (\pi^{f_\mathcal{S}} + s^{f_\mathcal{S}})\,da\,.
\end{aligned}
\tag{128}
$$

Here, ds is the line element along the closed loop $\mathcal{C}$ (without double point), generated by the intersection of $\mathcal{S}$ with the mantle surface of the pillbox; $\boldsymbol{h}$ is the unit tangent vector to $\mathcal{S}$, exterior to the pillbox mantle and normal to $\mathcal{C}$ (thus, $\boldsymbol{h}$ together with the positive direction of $\mathcal{C}$ and the orientation of the unit normal vector $\boldsymbol{n}$ of $\mathcal{S}$ form a counterclockwise skrew, Fig. 8 a.

The derivation from the global balance law (128) of the local balance law valid on $\mathcal{S}$ can be found, e.g., in the book by Slattery et al. [40] (2007). Here we sketch the proof. Thus, letting the thickness of the pillbox approaching zero ($\varepsilon \to 0$ as in Fig. 7b) turns (128) into

$$
\begin{aligned}
&\frac{d}{dt}\int_{\mathcal{S}} f_\mathcal{S}\,da = \\
&\qquad \underbrace{-\int_{\mathcal{C}} \boldsymbol{\phi}^{f_\mathcal{S}}\cdot\boldsymbol{h}\,ds}_{(1)} + \underbrace{\int_{\mathcal{S}} \left(\pi^{f_\mathcal{S}} + s^{f_\mathcal{S}}\right)\,da}_{(2)} \underbrace{-\int_{\mathcal{S}} [\![\boldsymbol{\phi}^f + f(\boldsymbol{v}-\boldsymbol{w})]\!]\cdot\boldsymbol{n}\,da}_{(3)}\,.
\end{aligned}
\tag{129}
$$

The three underlined terms represent

(1) the flux of $f_{\mathcal{S}}$ out of $\mathcal{S}$ and tangential to $\mathcal{S}$ along the loop $\mathcal{C}$,
(2) the production and supply of $f_{\mathcal{S}}$ on $\mathcal{S}$,
(3) the conductive plus convective flow of the bulk quantity f through $\mathcal{S}$.

The term on the left-hand side of (129) will be transformed with the aid of the transport theorem for a material surface (see Fig. 9),

$$\begin{aligned}\frac{d}{dt}\int_{\Sigma_t} f_{\mathcal{S}}(\boldsymbol{x},t)\,da = \int_{\Sigma_t}\left\{\frac{\partial f_{\mathcal{S}}}{\partial t} + \frac{\partial f_{\mathcal{S}}}{\partial \xi^{\mathfrak{a}}}\,\dot{\xi}^{\mathfrak{a}} + f_{\mathcal{S}}\left(v^{\mathfrak{a}}_{\mathcal{S};\mathfrak{a}} - 2\mathcal{U}K\right)\right\} da = \\ \int_{\Sigma_t}\left\{\frac{\partial f_{\mathcal{S}}}{\partial t} + \mathrm{Div}(f_{\mathcal{S}}\boldsymbol{v}_{\mathcal{S}}) - \frac{\partial f_{\mathcal{S}}}{\partial \xi^{\mathfrak{a}}}\,w^{\mathfrak{a}}\right\} da\,.\end{aligned} \tag{130}$$

Here $\dot{\xi}^{\mathfrak{a}}$ is explained in Fig. 9, $\boldsymbol{v}_{\mathcal{S}}$ is the velocity of a surface material point (see (120)), $w^{\mathfrak{a}}$ and $\mathcal{U}$ are the components of the surface velocity, see (116), $\psi^{\mathfrak{a}}{}_{;\,\mathfrak{b}}$ denotes the covariant derivative of a tangent surface vector field $\boldsymbol{\psi} = \psi^{\mathfrak{a}}\boldsymbol{\tau}_{\mathfrak{a}}$,

$$\psi^{\mathfrak{a}}{}_{;\,\mathfrak{b}} \equiv \frac{\partial \psi^{\mathfrak{a}}}{\partial \xi^{\mathfrak{b}}} + \Gamma^{\mathfrak{a}}_{\mathfrak{cb}}\,\psi^{\mathfrak{c}}$$

(see (111) for the definition of CHRISTOFFEL symbols $\Gamma^{\mathfrak{a}}_{\mathfrak{cb}}$), K is the mean curvature, and $\partial f_{\mathcal{S}}/\partial t$ and the surface divergence operator Div are defined by

$$\frac{\partial f_{\mathcal{S}}}{\partial t} \equiv \frac{\partial}{\partial t}\,f_{\mathcal{S}}(\xi^1,\xi^2,t)\,, \quad \mathrm{Div}\,(f_{\mathcal{S}}\boldsymbol{v}_{\mathcal{S}}) \equiv \frac{\partial f_{\mathcal{S}}\boldsymbol{v}_{\mathcal{S}}}{\partial \xi^{\mathfrak{a}}}\,\boldsymbol{\tau}^{\mathfrak{a}}\,. \tag{131}$$

For the term (1) on the right-hand side of (129) the GAUSS' law will be used. This process yields the local, point form of the *surface balance law* as

$$\frac{\partial f_{\mathcal{S}}}{\partial t} + \mathrm{Div}(f_{\mathcal{S}}\boldsymbol{v}_{\mathcal{S}} + \boldsymbol{\phi}^{f_{\mathcal{S}}}) - \frac{\partial f_{\mathcal{S}}}{\partial \xi^{\mathfrak{a}}}\,w^{\mathfrak{a}} = -[\![\boldsymbol{\phi}^f + f(\boldsymbol{v}-\boldsymbol{w})]\!]\cdot\boldsymbol{n} + (\pi^{f_{\mathcal{S}}} + s^{f_{\mathcal{S}}})\,. \tag{132}$$

Apparently, due to the tangential components $w^{\mathfrak{a}}$ of the surface velocity $\boldsymbol{w}$, relation (132) would depend on the parameterization of $\mathcal{S}$. However, this is not so, since the combination $\partial f_{\mathcal{S}}/\partial t - w^{\mathfrak{a}}\partial f_{\mathcal{S}}/\partial \xi^{\mathfrak{a}}$, representing the delta-time derivative (THOMAS [44] (1961)), is independent of the parameterization of $\mathcal{S}$. Relation (132) is the extension of the classical jump condition (124) if smooth surface fields $f_{\mathcal{S}}$, $\boldsymbol{\phi}^{f_{\mathcal{S}}}$, $\pi^{f_{\mathcal{S}}}$, $s^{f_{\mathcal{S}}}$ are occupying the singular surface $\mathcal{S}$; (132) reduces to (124) if all surface fields vanish.

If $f_{\mathcal{S}}$ is a scalar field, the balance law (132) reads

$$\frac{\partial f_{\mathcal{S}}}{\partial t} + \left(f_{\mathcal{S}}\boldsymbol{v}_{\mathcal{S}} + \boldsymbol{\phi}^{f_{\mathcal{S}}}\right)^{\mathfrak{a}}_{;\mathfrak{a}} - \frac{\partial f_{\mathcal{S}}}{\partial \xi^{\mathfrak{a}}}\,w^{\mathfrak{a}} - 2f_{\mathcal{S}}\mathcal{U}K = -[\![\boldsymbol{\phi}^f + f(\boldsymbol{v}-\boldsymbol{w})]\!]\cdot\boldsymbol{n} + (\pi^{f_{\mathcal{S}}} + s^{f_{\mathcal{S}}})\,. \tag{133}$$

Let us discuss special cases:

(a) *No curvature effects.* The curvature effects are contained explicitly in K, the mean curvature, in the last term on the left-hand side of (133). When such effects are negligible and the coordinate cover is Cartesian, we have

$$\frac{\partial \boldsymbol{\tau}_{\mathfrak{a}}}{\partial \xi^{\mathfrak{b}}} = \boldsymbol{0} \Longrightarrow \Gamma^{\mathfrak{c}}_{\mathfrak{ab}} = 0\,, \quad K = 0\,, \quad (\cdot)_; = (\cdot)_,\,,$$

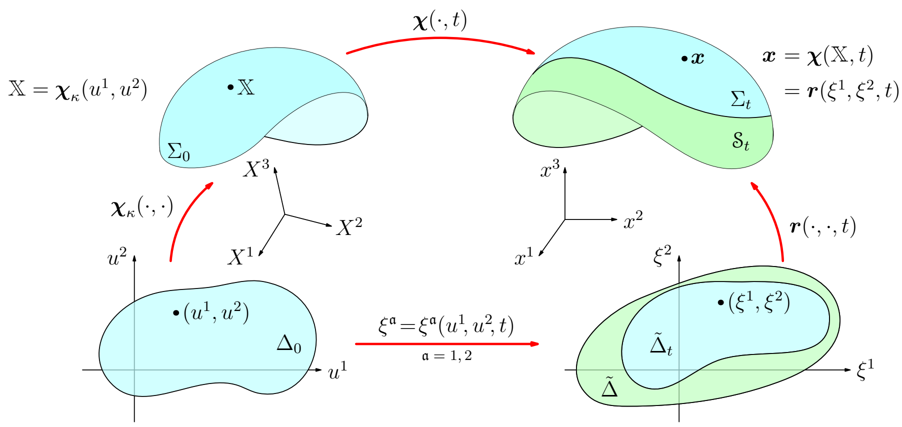

Figure 9: $\mathcal{S}\equiv\{\mathcal{S}_t\}$ is a moving ('geometric') surface; it is given parameterically by $\boldsymbol{x}=\boldsymbol{r}(\xi^1,\xi^2,t)$, $(\xi^1,\xi^2)\in\tilde{\Delta}$ and moves with the velocity $\boldsymbol{w}\equiv\partial\boldsymbol{r}(\xi^1,\xi^2,t)/\partial t$. $\Sigma\equiv\{\Sigma_t\}$ is a moving material surface: $\Sigma_t=\boldsymbol{\chi}(\Sigma_0,t)$, where Σ_0 is the material surface in a reference configuration. The velocity $\boldsymbol{v}_\mathcal{S}$ of $\mathbb{X}\in\Sigma_0$ is $\boldsymbol{v}_\mathcal{S}\equiv\partial\boldsymbol{\chi}(\mathbb{X},t)/\partial t$. Σ is so moving that $\Sigma_t\subset\mathcal{S}_t$ at each instant t. Therefore, $\Sigma_t=\boldsymbol{r}(\tilde{\Delta}_t,t)$, for a some $\tilde{\Delta}_t\subset\tilde{\Delta}$, and for $\boldsymbol{x}\in\Sigma_t$, $\boldsymbol{x}=\boldsymbol{\chi}(\mathbb{X},t)=\boldsymbol{r}(\xi^1,\xi^2,t)$, which can be written as $\boldsymbol{x}=\boldsymbol{\chi}(\boldsymbol{\chi}_\kappa(u^1,u^2),t)=\boldsymbol{r}(\xi^1(u^1,u^2,t),\xi^2(u^1,u^2,t),t)$. Differentiation of this relation with respect to t yields $\boldsymbol{v}_\mathcal{S}=\dot{\xi}^\mathfrak{a}\boldsymbol{\tau}_\mathfrak{a}+\boldsymbol{w}$, where $\dot{\xi}^\mathfrak{a}\equiv\partial\xi^\mathfrak{a}(u^1,u^2,t)/\partial t$, showing, in particular, that $\boldsymbol{v}_\mathcal{S}\cdot\boldsymbol{n}=\boldsymbol{w}\cdot\boldsymbol{n}\equiv\mathcal{U}$.

so that the balance law (133) takes the form

$$\frac{\partial f_\mathcal{S}}{\partial t}+\Big(f_\mathcal{S}\boldsymbol{v}_\mathcal{S}+\boldsymbol{\phi}^{f_\mathcal{S}}\Big)^\mathfrak{a}_{,\mathfrak{a}}-\frac{\partial f_\mathcal{S}}{\partial\xi^\mathfrak{a}}w^\mathfrak{a}=-[\![\boldsymbol{\phi}^f+f(\boldsymbol{v}-\boldsymbol{w})]\!]\cdot\boldsymbol{n}+(\pi^{f_\mathcal{S}}+s^{f_\mathcal{S}})\,. \tag{134}$$

Still further simplified versions of surface jump conditions are possible by ignoring some of the surface terms $f_\mathcal{S}$, $\boldsymbol{\phi}^{f_\mathcal{S}}$, $\pi^{f_\mathcal{S}}$, $s^{f_\mathcal{S}}$.

(b) *Surface following the bulk motion.* If $\boldsymbol{w}\cdot\boldsymbol{n}=\boldsymbol{v}\cdot\boldsymbol{n}$, the jump term in (133) reduces to the jump in volume flux, $[\![\boldsymbol{\phi}^f]\!]\cdot\boldsymbol{n}$. For mass balance this term is absent and only surface mass fields interact with one another in this case.

(c) *Reduced surface balance law.* Some of the surface fields in (133) may be small in comparison to others. When $f_\mathcal{S}=0$, (133) reduces to

$$(\boldsymbol{\phi}^{f_\mathcal{S}})^\mathfrak{a}_{\,;\,\mathfrak{a}}=-[\![\boldsymbol{\phi}^f+f(\boldsymbol{v}-\boldsymbol{w})]\!]\cdot\boldsymbol{n}+(\pi^{f_\mathcal{S}}+s^{f_\mathcal{S}})\,. \tag{135}$$

This variant (usually with $s^{f_\mathcal{S}}=0$) accounts for surface tension effects if (135) is a reduced momentum balance.

4 Boundary conditions; a simple model of detritus layer

The simplest model for the detritus transport (thin layer II in Fig. 3) is obtained if the layer concept for the detritus transport is collapsed to zero thickness, see Fig. 4. Thus, the field equations presented in Sect. 2 must be complemented by boundary conditions at the free surface $\mathcal{S}_s$ and at the basal surface $\mathcal{S}_b$. At this level two procedures are principally possible: (i) One may assume the basal surface $\mathcal{S}_b$ to be equipped with surface masses and surface momenta for all constituents α, but treat these as a mixture of class I. This then means that mass balance laws must be formulated for the solid constituents and the mixture as a whole and momentum balance is only formulated for the mixture as a whole. (ii) A full mixture formulation of class II is formulated for all constituent mass and momentum balances. In this process the interaction of the bulk fields with the surface fields from the (+)- and (−)-sides of the singular surface must be accounted for. We adopt the simpler case (i). Moreover, the time evolution of the basal surface is governed by the kinematic equation (119) and the erosion and sedimentation rates are incorporated in the surface mass balances for the N sediment classes.

4.1 Boundary conditions at the free surface

We shall treat the free surface as a surface following the barycentric motion, with

$$F(\boldsymbol{x}, t) \equiv z - s(x, y, t) = 0\,, \tag{136}$$

where $s(x, y, t)$ describes its z-position. With u, v, w the mixture 'material' velocity components in the x, y and z directions of the Cartesian coordinate system, the kinematic surface condition (122) takes the form[24]

$$\frac{\partial s}{\partial t} + \frac{\partial s}{\partial x}u + \frac{\partial s}{\partial y}v - w = 0\,, \quad \text{at} \quad z = s(x, y, t)\,. \tag{137}$$

Now we refer to the dynamic jump conditions (125), in which $\boldsymbol{v}\cdot\boldsymbol{n} = \boldsymbol{w}\cdot\boldsymbol{n}$:

(i) Condition $(125)_1$ is identically satisfied.

(ii) The *stress boundary condition* $(125)_3$ emerges as $[\![-p\boldsymbol{I} + \boldsymbol{R}]\!]\boldsymbol{n} = \boldsymbol{0}$, or, explicitly,

$$(-p\boldsymbol{I} + \boldsymbol{R})\boldsymbol{n}_s = \boldsymbol{\sigma}^{\text{atm}}\boldsymbol{n}_s \quad \text{at} \quad z = s(x, y, t)\,.$$

Projections of this equation perpendicular and tangential to $\mathcal{S}_s$ reveal the following statements at $z = s(x, y, t)$:

$$\begin{aligned} &\text{normal to } \mathcal{S}_s: && -p + \boldsymbol{n}_s\cdot\boldsymbol{R}\boldsymbol{n}_s = -p^{\,\text{atm}}\,, \\ &\text{tangential to } \mathcal{S}_s: && \boldsymbol{R}\boldsymbol{n}_s - (\boldsymbol{n}_s\cdot\mathbf{R}\boldsymbol{n}_s)\boldsymbol{n}_s = \boldsymbol{\tau}^{\text{wind}}\,, \end{aligned} \tag{138}$$

where

$$p^{\,\text{atm}} \equiv -\boldsymbol{\sigma}^{\text{atm}}\boldsymbol{n}_s\cdot\boldsymbol{n}_s\,, \quad \boldsymbol{\tau}^{\text{wind}} \equiv \boldsymbol{\sigma}^{\text{atm}}\boldsymbol{n}_s + p^{\,\text{atm}}\boldsymbol{n}_s\,.$$

In the shallow water approximation formulae (138) can easily be shown to reduce to

[24] If barotropic surface waves are ignored, i.e., the *rigid lid* approximation is imposed, then (137) is replaced by $z = 0$, where the origin of the coordinate system is at the undeformed free surface and the x and y axes are horizontal.

$$
\begin{aligned}
&\text{normal to } \mathcal{S}_s: \qquad && p = p^{\,\mathrm{atm}}\,, \\
&\text{tangential to } \mathcal{S}_s: \qquad && R_{xz} = \tau_x^{\mathrm{wind}}, \quad R_{yz} = \tau_y^{\mathrm{wind}}\,,
\end{aligned}
\tag{139}
$$

at $z = s(x, y, t)$. The atmospheric input of the surface tractions $p^{\,\mathrm{atm}}$, $\boldsymbol{\tau}_H^{\mathrm{wind}} \equiv (\tau_x^{\mathrm{wind}}, \tau_y^{\mathrm{wind}})$ is generally implemented by the parameterizations[25]

$$
\begin{aligned}
p^{\,\mathrm{atm}} &= \text{constant (often} = 0)\,, \\
\boldsymbol{\tau}_H^{\mathrm{wind}} &= \rho^{\mathrm{atm}} C_d^{\mathrm{wind}}\, \|\boldsymbol{v}_H^{\mathrm{wind}}(x, y, t)\|\, \boldsymbol{v}_H^{\mathrm{wind}}(x, y, t)\,,
\end{aligned}
\tag{140}
$$

with dimensionless drag coefficient $C_d^{\mathrm{wind}} \approx 2 \times 10^{-3}$, and $\boldsymbol{v}_H^{\mathrm{wind}} \equiv (v_x^{\mathrm{wind}}, v_y^{\mathrm{wind}})$; v_x^{wind}, v_y^{wind} are the Cartesian components in the x, y directions of the wind velocity $\boldsymbol{v}^{\mathrm{wind}}$ at the free surface $\mathcal{S}_s$.

(iii) If also temperature evolutions are in focus, the heat flow from the atmosphere into the lake must be prescribed. Relation $(125)_4$ together with the stress traction continuity and the closure law $(52)_2$ then states that

$$
\rho^*[c_v] D^{(T)}\, (\operatorname{grad} T) \cdot \boldsymbol{n}_s - \underbrace{((-p\boldsymbol{I} + \boldsymbol{R})\, \boldsymbol{n}_s) \cdot [\![\boldsymbol{v}]\!]}_{\substack{\text{power of working of the} \\ \text{surface tractions}}} = Q_\perp^{\mathrm{atm}}\,.
\tag{141}
$$

Here, $Q_\perp^{\mathrm{atm}}$ is the energy input from the atmosphere into the water: $Q_\perp^{\mathrm{atm}} \equiv -\boldsymbol{Q}^{\mathrm{atm}} \cdot \boldsymbol{n}_s$, with $\boldsymbol{Q}^{\mathrm{atm}}$ the heat flux in the atmosphere. The power of working of the surface tractions is often ignored or computed by assuming that $[\![\boldsymbol{v}]\!] = \boldsymbol{v}^{\mathrm{wind}} - \boldsymbol{v}^{\mathrm{water}} \approx \boldsymbol{v}^{\mathrm{wind}}$. With this last assumption in the shallow water approximation, (141) reduces to

$$
\rho^*[c_v] D^{(T)} \frac{\partial T}{\partial z} - \boldsymbol{\tau}_H^{\mathrm{wind}} \cdot \boldsymbol{v}_H^{\mathrm{wind}} = Q_\perp^{\mathrm{atm}}\,.
\tag{142}
$$

The contributions to the energy input $Q_\perp^{\mathrm{atm}}$ are written as $Q_\perp^{\mathrm{atm}} = Q_{ir}^{\mathrm{atm}} - Q_{ir}^{\mathrm{water}} + Q_\ell + Q_s$, with

$Q_{ir}^{\mathrm{atm}} \equiv$ (black body) radiation of air,

$Q_{ir}^{\mathrm{water}} \equiv$ (black body) radiation of water,

$Q_\ell \equiv$ latent heat flow between water and air,

$Q_s \equiv$ sensible heat flow between water and air.

Parameterizations of the latent and sensible heats are given by Hutter & Jöhnk (2004) [17].

[25]The right-hand side of $(140)_2$ should involve the difference $(\boldsymbol{v}_H^{\mathrm{wind}} - \boldsymbol{v}_H^{\mathrm{water}})_{\mathcal{S}}$, but the water velocity is very much smaller than the wind velocity, which justifies the approximation.

(iv) The free surface is not only assumed to follow the barycentric motion, it is here simultaneously supposed to be *impermeable to the suspended sediments* of all fractions. This implies that $(125)_2$ reduces to

$$(\boldsymbol{J}_\alpha - \rho c_\alpha \boldsymbol{w}_\alpha^s) \cdot \boldsymbol{n}_s = 0 \quad \text{at} \quad z = s(x,y,t)\,, \quad \alpha = 1,\ldots,N\,, \tag{143}$$

expressing vanishing mass flow of tracer α through the free surface. With gradient-type closures (see (52), (51)), (143) takes the form

$$\rho^* D^{(c_\alpha)} \frac{\partial\, c_\alpha}{\partial \boldsymbol{n}_s} + \rho\, c_\alpha \boldsymbol{w}_\alpha^s \cdot \boldsymbol{n}_s = 0 \quad \text{at} \quad z = s(x,y,t)\,, \quad \alpha = 1,\ldots,N\,, \tag{144}$$

or, in the shallow water and Boussinesq approximations,

$$D^{(c_\alpha)} \frac{\partial\, c_\alpha}{\partial\, z} + \, c_\alpha w_\alpha^s = 0, \quad \alpha = 1,\ldots,N\,, \quad \text{at} \quad z = s(x,y,t)\,. \tag{145}$$

With this the discussion of the dynamic jump conditions (125) is completed.

Remark The parameterization of w_α^s in (144) and (145) with the final free fall velocity (69) seems rather inappropriate at the free surface, where the turbulent intensity is generally large and falling distances for particles are restricted. When k is parameterized by $(53)_2$ or the $(k-\varepsilon)$ model is employed, (75) ought to be used instead.

If the $(k-\varepsilon)$ model for turbulent closure is employed, physically acceptable postulations for the boundary conditions of the turbulent kinetic energy and its dissipation are

$$\frac{\partial\, k}{\partial\, \boldsymbol{n}_s} = \boldsymbol{0}, \quad \frac{\partial\, \varepsilon}{\partial\, \boldsymbol{n}_s} = \boldsymbol{0}\,, \quad \text{at} \;\; z = s(x,y,t)\,, \tag{146}$$

or in the shallow water approximation,

$$\frac{\partial\, k}{\partial\, z} = 0, \quad \frac{\partial\, \varepsilon}{\partial\, z} = 0\,, \quad \text{at} \quad z = s(x,y,t)\,. \tag{147}$$

In this case, the rigid lid assumption, $s(x,y,t) = 0$, is often justified.

4.2 Boundary conditions at the rigid bed

The simplest description of detritus transport does not use the concept of the motion of a thin layer of sediments. The existence of this layer is negated and the lower boundary of the lake domain is directly the singular surface between the slurry layer and the rigid bed of alluvial detritus. We treat this surface as having its own physical properties in the context of a mixture of class I, and so the surface balance law (132) will be now used. Moreover, the surface moves and deforms with time owing to the removal of grains from the bed, their incorporation in the particle laden water, and the deposition of some components of the washload from the slurry above the bottom surface. Therefore, in these simple models essentially only two physically significant statements are made:

- A criterion, or more generally, some criteria are established, which define the onset of erosion of sediments of grain class α. It is expected that a characteristic variable will act as a threshold measure. Below a certain value of this variable only sediments of classes α will be lifted, for which the grain size is smaller than for class α_{thres}[26].
- For those components α which are eroded and incorporated in the slurry, the amount of eroded material per unit time for each grain class, i.e., the mass flow for each component from the rigid bed to the ambient water must be quantified.

For the ensuing developments it is perhaps advantageous, if the classical approach to sediment transport is briefly illustrated. Thus, the next two sections are devoted to this issue.

4.2.1 Erosion inception

In the words of KRAFT et al. (2011) [23], 'the erosion of sediment begins when the shear stress on the bed surface, τ_w, exceeds the critical wall shear stress of the corresponding sediment material, τ_c'. A widely used procedure for the determination of the beginning of entrainment of cohesionless particles is represented by the SHIELDS curve (1936) [39]; see also VAN RIJN (1984) [47], which is based on the results of numerous laboratory measurements with different grain sizes, densities and wall shear stresses. A critical SHIELDS parameter (the dimensionless critical shear stress) is defined by

$$\tau_c^*(=\theta_c) \equiv \frac{\tau_c}{\Delta\rho\, g\, \mathfrak{d}}\,, \qquad \Delta \equiv \frac{\rho_s}{\rho} - 1\,, \tag{148}$$

where $\mathfrak{d}$ is the mean particle diameter for class α of particles with a range of particle diameters in the interval $[d_{\alpha-1}, d_\alpha)$; we suggest to take this mean value to be $\mathfrak{d} = \frac{1}{2}(d_{\alpha-1} + d_\alpha)$. Moreover, ρ_s is the true density of the sediment and ρ is the mixture density.

A large number of laboratory experiments has been conducted (for a review, see VETSCH (2012) [49]) and identified the critical dimensionless shear stress τ_c^* or θ_c for a grain size $\mathfrak{d}$ as a function of the critical particle REYNOLDS number

$$Re_c^* \equiv \frac{u^*\mathfrak{d}}{\nu}, \quad \text{where} \quad u^* \equiv \left(\frac{g\,\nu}{\Delta}\right)^{1/3}. \tag{149}$$

Thus,

$$\tau_c^* = f(Re_c^*)\,. \tag{150}$$

Re_c^* is sometimes also called 'dimensionless particle diameter' and is then identified with

$$\mathfrak{d}^\star \equiv \mathfrak{d}\left(\frac{g}{\nu^2\Delta}\right)^{1/3} (= Re_c^*)\,, \tag{151}$$

see KRAFT et al. [23]. This formula can be motivated by dimensional analysis, see Appendix C. A great number of representations of $f(Re_c^*) = f(\mathfrak{d}^\star)$ have been proposed,

[26] If $\mathfrak{d}_\alpha$ and $\mathfrak{d}_{\alpha_{\text{thres}}}$ are the nominal grain diameters of the grain size classes α and α_{thres}, respectively, then all grains with $\mathfrak{d}_\alpha < \mathfrak{d}_{\alpha_{\text{thres}}}$ are mobilized, whilst those with $\mathfrak{d}_\alpha > \mathfrak{d}_{\alpha_{\text{thres}}}$ are still at rest.

see again VETSCH for a review; he lists, among many others, expressions by VAN RIJN (1984, 2007) [47], [48], viz.,

$$\tau_c^* = \begin{cases} 0.115(\mathfrak{d}^\star)^{-0.5}, & \text{for} \quad 1 < \mathfrak{d}^\star < 4\,, \\ 0.14(\mathfrak{d}^\star)^{-0.64}, & \text{for} \quad 4 \leqslant \mathfrak{d}^\star < 10\,, \\ 0.04(\mathfrak{d}^\star)^{-0.1}, & \text{for} \quad 10 \leqslant \mathfrak{d}^\star < 20\,, \\ 0.013(\mathfrak{d}^\star)^{0.29}, & \text{for} \quad 20 \leqslant \mathfrak{d}^\star < 150\,, \\ 0.055, & \text{for} \quad 150 \leqslant \mathfrak{d}^\star\,. \end{cases} \tag{152}$$

This automatically suggests a possible division of the grain size distribution into five regimes. Again according to VETSCH, YALIN and DA SILVA (2001) [55] approximate the VAN RIJN data by a continuous functional relation

$$\tau_c^* = 0.13(\mathfrak{d}^\star)^{-0.392}\exp(-0.015(\mathfrak{d}^\star)^2) + 0.045\left(1 - \exp\left(-0.068(\mathfrak{d}^\star)^2\right)\right)\,. \tag{153}$$

There are also a number of other formulae for the critical shear stress τ_c^*. For instance, KRAFT et al. (2011) [23] list a formula due to ZANKE (2001) [57],

$$\tau_c^* = \psi_Z \tan(\varphi) - \theta'_w\,, \tag{154}$$

in which φ is the angle of internal friction of the sediment and θ'_w is the root mean square turbulent fluctuation of the wall shear stress. For natural sediments the coefficient ψ_Z takes the value $\psi_Z = 0.7$.

This is about the appropriate place where a clarifying remark about the critical shear stress should be made. Formulae (148) to (154) are expressed in terms of a shear stress τ_c, since the stress distribution in river flow is close to *simple shearing* plus a hydrostatic pressure,

$$\boldsymbol{\sigma} = \begin{pmatrix} 0 & 0 & \tau_c \\ 0 & 0 & 0 \\ \tau_c & 0 & 0 \end{pmatrix} - p \begin{pmatrix} 1 & 0 & 0 \\ 0 & 1 & 0 \\ 0 & 0 & 1 \end{pmatrix} \Longrightarrow \boldsymbol{\sigma}_E = \begin{pmatrix} 0 & 0 & \tau_c \\ 0 & 0 & 0 \\ \tau_c & 0 & 0 \end{pmatrix}, \tag{155}$$

in which $\boldsymbol{\sigma}_E$ is the stress deviator of $\boldsymbol{\sigma}$. In a more general flow, the actual basal criterion describing the onset of sediment motion cannot so simply be described. A likely adequate definition of the onset of the sediment movement, which subsequently will systematically be used, is to identify τ_c in (148) as

$$\tau_c \equiv (II_{\boldsymbol{\sigma}_E})^{1/2}_{\text{crit}}\,, \tag{156}$$

where $II_{\boldsymbol{\sigma}_E} \equiv \frac{1}{2}\mathrm{tr}\left((\boldsymbol{\sigma}_E)^2\right)$ is the second invariant of the stress deviator $\boldsymbol{\sigma}_E$ evaluated just below the sediment bed. For simple shearing this is just the shear stress. Thus, a stress state invariant definition of θ_c or τ_c^* is[27]

$$\theta_c = \frac{(II_{\boldsymbol{\sigma}_E})^{1/2}_{\mathrm{crit}}}{\Delta\rho\, g\, \mathfrak{d}}\,. \tag{157}$$

4.2.2 Erosion amount

The second statement, which is needed, is the parameterization of the *entrainment amount*. The literature again knows a large number of formulations for determining the erosion rate. Kraft et al. (2011) [23] quote three formulae which here are briefly outlined as well:

- van Rijn (1984) [46] conducted laboratory experiments to determine the sediment erosion rate for various particle sizes and flow velocities and proposed for the pick-up rate per unit mass, area and time the function

$$\phi_p = \frac{E}{\rho_s\,(\Delta g \mathfrak{d})^{0.5}} = 0.0003(\mathfrak{d}^\star)^{0.3}\tilde{T}^{1.5}, \quad \tilde{T} \equiv \mathcal{H}\left(\left(\frac{u_{\tau_w}}{u_{\tau_c}}\right)^2 - 1\right)\left(\left(\frac{u_{\tau_w}}{u_{\tau_c}}\right)^2 - 1\right), \tag{158}$$

  where $\mathcal{H}$ is the Heaviside function and

$$u_{\tau_c} \equiv \sqrt{\frac{\tau_c}{\rho}} \quad \text{and} \quad u_{\tau_w} \equiv \sqrt{\frac{\tau_w}{\rho}} \tag{159}$$

  denote the critical and actual wall shear velocities, defined as suggested in (156).

- The approach of Einstein (1950) [11] is stochastic. A statistically averaged wall shear stress is not considered here, it is rather assumed that turbulent fluctuations will push the particles in motion. The pick-up rate is expressed as

$$E = \psi_E\, \rho_s\, (\Delta g \mathfrak{d})^{0.5}\; P\,, \tag{160}$$

  in which ψ_E is a universal constant, and P is the fraction of time during which a sediment particle is suspended by the flow. Note that this relation contains no critical shear stress. While for small wall shear stress P is negligibly small, for sufficiently large wall shear stress P will rapidly reach its saturation value. In the present application we consider P simply a constant (for a given grain size range α) and the erosion will occur just as the shear stress exceeds its critical value.

[27] More generally, a criterion marking the onset of erosion is an equation of the form

$$f(I_{\boldsymbol{\sigma}},\, II_{\boldsymbol{\sigma}_E},\, III_{\boldsymbol{\sigma}_E}) = 0 \quad (*)$$

between the first stress invariant and the second and third stress deviator invariants at the basal surface. A dependence on $I_{\boldsymbol{\sigma}}$ describes a possible influence of the (mean) pressure; that on $II_{\boldsymbol{\sigma}_E}$ accounts for the significance of shearing, but the role of $III_{\boldsymbol{\sigma}_E}$ is presently not clear. In the form (∗) the erosion inception is very much reminiscent of the onset criterion of yield in the theories of plasticity.

- YALIN [53] determined the erosion rate from statistically averaged flow parameters. If the critical shear stress is exceeded, particles are entrained. The number of eroded particles rises linearly with the wall shear velocity. The erosion rate is computed by

$$E = \psi_Y \rho_s u_{\tau_w} . \tag{161}$$

  The constant ψ_Y should be determined by experiment.

It is evident from the above formulae that VAN RJIN's and EINSTEIN's erosion rates depend on the particle size, and for this reason can and should be restricted for a given grain size distribution curve to a single α-class of grain sizes. This makes YALIN's formula inapplicable to mathematical erosion processes which differentiate α-classes by grain size. KRAFT et al. [23] also remark that 'YALIN and VAN RJIN assumed in their formula that the number of eroded particles increases with increasing wall shear velocity'. ALAN and KENNEDY (see e.g. YALIN (1985) [54]) in their experiments demonstrated that the flow near the sediment bed is fully saturated when a certain wall shear velocity is reached, and the erosion rate converges to a certain value and does not rise further. With this in mind, only the approach of EINSTEIN does justice to these observations.

The above formulae have formally been written for a single particle diameter. Here, we interpret them as being applicable to the narrow range of particle diameters of class α. Let us summarize the salient formulae with this identification:

- Dimensionless α-particle diameter (see (151))

$$\mathfrak{d}_\alpha^\star = \mathfrak{d}_\alpha \left(\frac{g}{\nu^2 \Delta} \right)^{1/3} ; \tag{162}$$

- Dimensionless critical shear stress according to YALIN and DA SILVA [55] for class α and interpreted in the spirit of formula (156),

$$(\tau_c^*)_\alpha = Y_\alpha^* = 0.13(\mathfrak{d}_\alpha^\star)^{-0.392} \exp(-0.015(\mathfrak{d}_\alpha^\star)^2) + 0.045 \left[1 - \exp(-0.068(\mathfrak{d}_\alpha^\star)^2) \right] ; \tag{163}$$

- The pick-up rate for class α is given, according to VAN RIJN [46], by

$$E_\alpha = 0.0003(\mathfrak{d}_\alpha^\star)^{0.3} \tilde{T}_\alpha^{1.5} \rho_s \left(\Delta\, g \mathfrak{d}_\alpha \right)^{0.5} , \tag{164}$$

  where, from (158) and (159),

$$\begin{aligned} \tilde{T}_\alpha &\equiv \mathcal{H} \left(\left(\frac{u_{\tau_w}}{u_{\tau_c}} \right)^2 - 1 \right) \left(\left(\frac{u_{\tau_w}}{u_{\tau_c}} \right)^2 - 1 \right) \\ &= \mathcal{H} \left(\frac{\tau_w}{\tau_c} - 1 \right) \left(\frac{\tau_w}{\tau_c} - 1 \right) = \mathcal{H} \left(\frac{\tau_w}{\tau_c^* \Delta \rho g \mathfrak{d}_\alpha} - 1 \right) \left(\frac{\tau_w}{\tau_c^* \Delta \rho g \mathfrak{d}_\alpha} - 1 \right) ; \end{aligned} \tag{165}$$

- According to EINSTEIN [11],

$$E_\alpha = \psi_E \rho_s \left(\Delta\, g \mathfrak{d}_\alpha \right)^{0.5} P_\alpha , \quad P_\alpha = \text{constant} . \tag{166}$$

Subsequently we shall employ (162)–(165).

4.2.3 Detritus layer as a singular material surface

The basal surface, separating the particle laden fluid and the rigid bed from which sediment can be eroded and to which washload is deposited, will be conceived as a surface with its own material properties intended to model the thin detritus layer. As for the bulk material in layer I, the surface detritus will be treated as a mixture of class I. Thus, as dynamic boundary conditions in Model 2 we formulate the averaged balance laws of mass for the sediments of classes α and the detritus-mixture as a whole, as well as the the momentum balance law for the mixture as a whole, the master equation being (132).

The surface is defined by

$$F \equiv -b(x,y,t) + z = 0\,, \tag{167}$$

or, parametrically with $\xi^1 \equiv x$, $\xi^2 \equiv y$,

$$\boldsymbol{x} = x\boldsymbol{e}_1 + y\boldsymbol{e}_2 + b(x,y,t)\boldsymbol{e}_3 \equiv \boldsymbol{r}(x,y,t)\,, \quad (\boldsymbol{e}_3 \equiv \boldsymbol{e}_z)\,. \tag{168}$$

With definition (167) of F, $\boldsymbol{n}_b = \operatorname{grad} F/\|\operatorname{grad} F\|$ points *into* the fluid domain and satisfies (110) with

$$\boldsymbol{\tau}_1 \equiv \frac{\partial \boldsymbol{r}}{\partial x} = \boldsymbol{e}_1 + \frac{\partial b}{\partial x}\,\boldsymbol{e}_3\,, \quad \boldsymbol{\tau}_2 \equiv \frac{\partial \boldsymbol{r}}{\partial y} = \boldsymbol{e}_2 + \frac{\partial b}{\partial y}\,\boldsymbol{e}_3\,.$$

We have

$$\boldsymbol{n}_b = c\left(-\frac{\partial b}{\partial x}\,\boldsymbol{e}_1 - \frac{\partial b}{\partial y}\,\boldsymbol{e}_2 + \boldsymbol{e}_3\right)\,, \quad c \equiv \left[1 + \left(\frac{\partial\, b}{\partial\, x}\right)^2 + \left(\frac{\partial\, b}{\partial\, y}\right)^2\right]^{-1/2}\,.$$

Corresponding to (168), the surface velocity $\boldsymbol{w}$ is given by, see (115),

$$\boldsymbol{w} = \frac{\partial b}{\partial t}\,\boldsymbol{e}_3\,,$$

so that, with respect to the basis $\{\boldsymbol{\tau}_1, \boldsymbol{\tau}_2, \boldsymbol{n}_b\}$, $\boldsymbol{w}$ has the representation[28]

$$\boldsymbol{w} = c\,\frac{\partial b}{\partial x}\,\mathcal{U}_b\,\boldsymbol{\tau}_1 + c\,\frac{\partial b}{\partial y}\,\mathcal{U}_b\,\boldsymbol{\tau}_2 + \mathcal{U}_b\,\boldsymbol{n}_b\,, \quad \mathcal{U}_b = c\,\frac{\partial\, b}{\partial\, t}\,. \tag{169}$$

The displacement speed $\mathcal{U}_b$ is interpreted as *erosion/deposition rate* or *entrainment rate* and for it we will give a law according to the discussion in Sec. 4.2.2. So, we may keep

[28] To prove this, we write

$$\boldsymbol{w} = \alpha\boldsymbol{\tau}_1 + \beta\boldsymbol{\tau}_2 + \mathcal{U}_b\boldsymbol{n}_b = \frac{\partial\, b}{\partial\, t}\boldsymbol{e}_3\,.$$

If the above expressions for $\boldsymbol{\tau}_1$ and $\boldsymbol{\tau}_2$ are substituted this yields

$$\boldsymbol{w} = \left(\alpha - c\mathcal{U}_b\frac{\partial\, b}{\partial\, x}\right)\boldsymbol{e}_1 + \left(\beta - c\mathcal{U}_b\frac{\partial\, b}{\partial\, y}\right)\boldsymbol{e}_2 + \left(\alpha\frac{\partial\, b}{\partial\, x} + \beta\frac{\partial\, b}{\partial\, y} + c\mathcal{U}_b\right)\boldsymbol{e}_3 = \frac{\partial\, b}{\partial\, t}\boldsymbol{e}_3\,,$$

implying

$$\alpha = c\mathcal{U}_b\frac{\partial\, b}{\partial\, x}\,, \quad \beta = c\mathcal{U}_b\frac{\partial\, b}{\partial\, y}\,.$$

Table 6: Elements for the averaged surface balance relation (132) when referring to the detritus mixture and Model 2 ($\langle\cdot\rangle$ are omitted)

$f_{\mathcal{S}}$	$\boldsymbol{\phi}^{f_{\mathcal{S}}}$	$\pi^{f_{\mathcal{S}}}$	$s^{f_{\mathcal{S}}}$	f	$\boldsymbol{\phi}^{f}$
μ_α	$\mathbf{0}$	0	0	$\rho_\alpha = \rho\, c_\alpha$	$\boldsymbol{\phi}^{\rho_\alpha} = \boldsymbol{J}_\alpha - \rho\, c_\alpha \boldsymbol{w}^s_\alpha$
$\mu \equiv \sum_\alpha \mu_\alpha + \mu_f$	$\mathbf{0}$	0	0	ρ	$\boldsymbol{\phi}^{\rho} = 0$
$\mu \boldsymbol{v}_{\mathcal{S}} \equiv \sum_\alpha \mu_\alpha \boldsymbol{v}_{\mathcal{S}\alpha} + \mu_f \boldsymbol{v}_{\mathcal{S}f}$	$-\boldsymbol{R}_{\mathcal{S}}$	0	$\mu \boldsymbol{g}$	$\rho \boldsymbol{v}$	$\boldsymbol{\phi}^{\rho \boldsymbol{v}} = p\boldsymbol{I} - \boldsymbol{R}$

in mind that $\mathcal{U}_b$ is a known quantity. In particular, we note that $(169)_2$ stands for the determination of the basal elevation function b once $\mathcal{U}_b$ is known.

With the identification of the fields $f_{\mathcal{S}}$, $\boldsymbol{\phi}^{f_{\mathcal{S}}}$, $\pi^{f_{\mathcal{S}}}$, $s^{f_{\mathcal{S}}}$, $\boldsymbol{\phi}^{f}$ and f in equation (133) as stated in Table 6, it can be shown (see Appendix C) that the surface mass balance law takes the forms:

- For the sediment classes α, $\alpha = 1, \dots, N$,

$$\begin{aligned}\frac{\partial \mu_\alpha}{\partial t} + (\mu_\alpha \boldsymbol{v}_{\mathcal{S}\alpha})^{\mathfrak{a}}{}_{;\mathfrak{a}} - \frac{\partial \mu_\alpha}{\partial \xi^{\mathfrak{a}}}\, w^{\mathfrak{a}} - 2\mu_\alpha\, \mathcal{U}_b K = \\ (-\boldsymbol{\phi}^{\rho_\alpha} \cdot \boldsymbol{n}_b)^+ - (\rho\, c_\alpha\, \boldsymbol{v} \cdot \boldsymbol{n}_b)^+ - \left(\rho_\alpha^{\text{bed}} - (\rho c_\alpha)^+\right) \mathcal{U}_b\,;\end{aligned} \tag{170}$$

- For the mixture

$$\frac{\partial \mu}{\partial t} + (\mu \boldsymbol{v}_{\mathcal{S}})^{\mathfrak{a}}{}_{;\mathfrak{a}} - \frac{\partial \mu}{\partial \xi^{\mathfrak{a}}}\, w^{\mathfrak{a}} - 2\mu\, \mathcal{U}_b K = -(\rho\, \boldsymbol{v} \cdot \boldsymbol{n}_b)^+ - (\rho^{\text{bed}} - \rho^+)\mathcal{U}_b\,. \tag{171}$$

Here the (+)-sign indicates the water side of $\mathcal{S}_b$ and μ_α, μ, as well as the other quantities in (170), (171) are functions of $(\xi^1 \equiv x, \xi^2 \equiv y, t)$. Moreover, the components w^1, w^2 of the surface velocity $\boldsymbol{w}$ are given by

$$w^1 = c\, \frac{\partial b}{\partial x}\, \mathcal{U}_b\,, \quad w^2 = c\, \frac{\partial b}{\partial y}\, \mathcal{U}_b\,,$$

see (169). In deducing (170), (171) it is assumed that the motion of the basal surface is not subject to turbulent fluctuations, implying that $\langle \boldsymbol{n}_b \rangle = \boldsymbol{n}_b$, $\langle K \rangle = K$, $\langle \boldsymbol{w} \rangle = \boldsymbol{w}$ and $\langle \mathcal{U}_b \rangle = \mathcal{U}_b$.

The balance laws of mass, (170) and (171), contain unknown velocity components tangential to the surface $\mathcal{S}$ of the constituent classes α and the mixture. These velocities need be determined and for this determination essentially two procedures are at our disposal, namely

- We complement these laws with momentum equations for the surface flows of μ_α ($\alpha = 1, ..., N$) and μ. These laws then allow determination of the momenta $\mu_\alpha \boldsymbol{v}_{\mathcal{S}\alpha}$ and $\mu \boldsymbol{v}_{\mathcal{S}}$ (or $\mu_f \boldsymbol{v}_{\mathcal{S}f}$). This defines a surface mixture of class II.

- We are less ambitious and introduce instead diffusion mass fluxes of the α-class sediments,

$$\boldsymbol{j}_{\mathcal{S}\alpha} \equiv \mu_\alpha \left(\boldsymbol{v}_{\mathcal{S}\alpha} - \boldsymbol{v}_{\mathcal{S}} \right) , \tag{172}$$

  for which closure relations are postulated, while the barycentric velocity is determined from the surface momentum balance law for the mixture as a whole. This defines a mixture of class I.

As already mentioned, we follow this second route. Note that, since $\boldsymbol{v}_{\mathcal{S}\alpha} \cdot \boldsymbol{n}_b = \boldsymbol{v}_{\mathcal{S}} \cdot \boldsymbol{n}_b$ $(= \mathcal{U}_b)$, the diffusive surface mass flux is parallel to $\mathcal{S}_b$:

$$\boldsymbol{j}_{\mathcal{S}\alpha} = \boldsymbol{j}_{\mathcal{S}\alpha\parallel} \quad \Longrightarrow \quad \mu_\alpha \boldsymbol{v}_{\mathcal{S}\alpha\parallel} = \boldsymbol{j}_{\mathcal{S}\alpha} + \mu_\alpha \boldsymbol{v}_{\mathcal{S}\parallel} \,.$$

So, with definition (172) of $\boldsymbol{j}_{\mathcal{S}\alpha}$ we rewrite equation (170) as

$$\begin{aligned} &\frac{\partial \mu_\alpha}{\partial\, t} + \left(\mu_\alpha \boldsymbol{v}_{\mathcal{S}}\right)^{\mathfrak{a}}{}_{;\mathfrak{a}} - \frac{\partial \mu_\alpha}{\partial \xi^{\mathfrak{a}}} w^{\mathfrak{a}} - 2\mu_\alpha \,\mathcal{U}_b K = \\ &\qquad - \left(\boldsymbol{j}_{\mathcal{S}\alpha}\right)^{\mathfrak{a}}{}_{;\mathfrak{a}} + \left(-\boldsymbol{\phi}^{\rho_\alpha} \cdot \boldsymbol{n}_b\right)^+ - \left(\rho\, c_\alpha\, \boldsymbol{v} \cdot \boldsymbol{n}_b\right)^+ - \left(\rho_\alpha^{\mathrm{bed}} - \left(\rho c_\alpha\right)^+\right) \mathcal{U}_b \,. \end{aligned} \tag{173}$$

Now, the (averaged) surface momentum balance equation for the detritus mixture follows from (132) with the choices stated in Table 6, where $\boldsymbol{R}_{\mathcal{S}}$ is the surface Reynolds stress tensor, see (240), which can be represented as

$$\boldsymbol{R}_{\mathcal{S}} = \underbrace{S^{\mathfrak{ab}} \boldsymbol{\tau}_{\mathfrak{a}} \otimes \boldsymbol{\tau}_{\mathfrak{b}}}_{\text{in-plane surface stress}} + \underbrace{S^{\mathfrak{a}} (\boldsymbol{\tau}_{\mathfrak{a}} \otimes \boldsymbol{n}_b + \boldsymbol{n}_b \otimes \boldsymbol{\tau}_{\mathfrak{a}})}_{\text{surface shear } \perp \text{ to } \mathcal{S}} + \underbrace{S \boldsymbol{n}_b \otimes \boldsymbol{n}_b}_{\text{normal surface pressure}} . \tag{174}$$

Splitting this surface momentum balance law into a tangential component and a normal component to $\mathcal{S}_b$, we obtain the following results (see the derivation in Appendix D):

- Tangential surface momentum balance for the detritus mixture ($\mathfrak{a}, \mathfrak{b} = 1, 2$),

$$\begin{aligned} \frac{\partial \mu v^{\mathfrak{a}}_{\mathcal{S}}}{\partial t} + \left(\mu v^{\mathfrak{a}}_{\mathcal{S}} v^{\mathfrak{b}}_{\mathcal{S}} - S^{\mathfrak{ab}} \right)_{;\mathfrak{b}} + \mu v^{\mathfrak{b}}_{\mathcal{S}} \frac{\partial w^{\mathfrak{a}}}{\partial \xi^{\mathfrak{b}}} - \mu w^{\mathfrak{b}} \frac{\partial v^{\mathfrak{a}}_{\mathcal{S}}}{\partial \xi^{\mathfrak{b}}} - \mu \mathcal{U}_b g^{\mathfrak{ab}} \frac{\partial \mathcal{U}_b}{\partial \xi^{\mathfrak{b}}} - v^{\mathfrak{a}}_{\mathcal{S}} w^{\mathfrak{b}} \frac{\partial \mu}{\partial \xi^{\mathfrak{b}}} - \\ \left(2\mu \mathcal{U}_b v^{\mathfrak{b}}_{\mathcal{S}} - S^{\mathfrak{b}} \right) b_{\mathfrak{bc}} g^{\mathfrak{ca}} - 2K \left(\mu \mathcal{U}_b v^{\mathfrak{a}}_{\mathcal{S}} - S^{\mathfrak{a}} \right) = \\ -(-p\boldsymbol{I} + \boldsymbol{R})^+ \boldsymbol{n}_b \cdot \boldsymbol{\tau}^{\mathfrak{a}} + \left((\rho \boldsymbol{v})^+ \cdot \boldsymbol{\tau}^{\mathfrak{a}} \right) \left(\boldsymbol{v}^+ \cdot \boldsymbol{n}_b - \mathcal{U}_b \right) + (-p\boldsymbol{I} + \boldsymbol{R})^- \boldsymbol{n}_b \cdot \boldsymbol{\tau}^{\mathfrak{a}} + \mu \boldsymbol{g} \cdot \boldsymbol{\tau}^{\mathfrak{a}} ; \end{aligned} \tag{175}$$

- Normal surface momentum balance for the detritus mixture,

$$\begin{aligned} \frac{\partial \mu \mathcal{U}_b}{\partial t} + \left(\mu \mathcal{U}_b v^{\mathfrak{a}}_{\mathcal{S}} - S^{\mathfrak{a}} \right)_{;\mathfrak{a}} + \mu (v^{\mathfrak{a}}_{\mathcal{S}} - w^{\mathfrak{a}}) \frac{\partial \mathcal{U}_b}{\partial \xi^{\mathfrak{a}}} - w^{\mathfrak{a}} \mathcal{U}_b \frac{\partial \mu}{\partial \xi^{\mathfrak{a}}} - 2K \left(\mu \mathcal{U}_b^2 - S \right) = \\ -(-p\boldsymbol{I} + \boldsymbol{R})^+ \boldsymbol{n}_b \cdot \boldsymbol{n}_b + \left((\rho \boldsymbol{v})^+ \cdot \boldsymbol{n}_b \right) \left(\boldsymbol{v}^+ \cdot \boldsymbol{n}_b - \mathcal{U}_b \right) + (-p\boldsymbol{I} + \boldsymbol{R})^- \boldsymbol{n}_b \cdot \boldsymbol{n}_b + \mu \boldsymbol{g} \cdot \boldsymbol{n}_b \,. \end{aligned} \tag{176}$$

Note that (176) describes the evolution of the speed of displacement $\mathcal{U}_b$. However, we have chosen to prescribe $\mathcal{U}_b$ by giving an erosion/deposition law, so that (176) will be next omitted.[29] Equations (171), (173) and (175) stand for the determination of the surface fields μ, μ_α and $\boldsymbol{v}_{\mathcal{S}\|}$. However, there are quantities therein which must be prescribed, and this is dealt with in the next subsection.

4.2.4 Boundary conditions at the bed

Equations (171), (173) and (175) must be complemented by closure relations for the diffusive fluxes $\boldsymbol{j}_{\mathcal{S}\alpha}$, the stresses $S^{\mathfrak{ab}}$, $S^{\mathfrak{a}}$, and for the bulk quantities c_α^+, ρ^+, $\boldsymbol{v}^+$, $(\boldsymbol{\phi}^{\rho_\alpha})^+ \cdot \boldsymbol{n}_b$, $(-p\boldsymbol{I} + \boldsymbol{R})^{\pm}\boldsymbol{n}_b \cdot \boldsymbol{\tau}^{\mathfrak{a}}$. Thus, we make the following assumptions:

- For $\boldsymbol{j}_{\mathcal{S}\alpha}$ we assume the Fick law

$$\boldsymbol{j}_{\mathcal{S}\alpha} = -D_\alpha \nabla_{\mathcal{S}} \mu_\alpha \iff (\boldsymbol{j}_{\mathcal{S}\alpha})^{\mathfrak{a}} = -D_\alpha \, g^{\mathfrak{ab}} \frac{\partial \mu_\alpha}{\partial \xi^{\mathfrak{b}}} ,$$

  where D_α [$\mathrm{m}^2\,\mathrm{s}^{-1}$] are the surface mass diffusivities. This parameterization ignores cross dependencies analogous to those in $(50)_4$.

- The shear stresses $S^{\mathfrak{a}}$ are assumed to be negligibly small, because they represent physically thickness integrated shear forces perpendicular to $\mathcal{S}$ and the thickness is infinitely small. For the surface parallel stresses $S^{\mathfrak{ab}}$ we assume

$$S^{\mathfrak{ab}} = S^{\mathfrak{ab}}_{\text{elastic}} + S^{\mathfrak{ab}}_{\text{viscous}} , \tag{177}$$

  where

$$\begin{aligned} S^{\mathfrak{ab}}_{\text{elastic}} &= -p(\mu)\, g^{\mathfrak{ab}} , \\ S^{\mathfrak{ab}}_{\text{viscous}} &= \zeta_{\mathcal{S}} \operatorname{tr}(\boldsymbol{D}_{\mathcal{S}})\, g^{\mathfrak{ab}} + 2\nu_{\mathcal{S}} \left[D_{\mathcal{S}}^{\mathfrak{ab}} - \tfrac{1}{2}\operatorname{tr}(\boldsymbol{D}_{\mathcal{S}})\, g^{\mathfrak{ab}} \right] . \end{aligned} \tag{178}$$

  p is an elastic pressure depending on the surface mass density (and also on the temperature in non-isothermal processes), $\zeta_{\mathcal{S}}$ is an aerial viscosity analogous to the bulk viscosity in three dimensions, $\nu_{\mathcal{S}}$ is a surface shear viscosity which operates on the surface deviator of $\boldsymbol{D}_{\mathcal{S}}$, and $\boldsymbol{D}_{\mathcal{S}}$ is the surface rate of deformation tensor,

$$\boldsymbol{D}_{\mathcal{S}} \equiv \tfrac{1}{2} \Big(\boldsymbol{P} \left(\nabla_{\mathcal{S}} \boldsymbol{v}_{\mathcal{S}} \right) + \left(\nabla_{\mathcal{S}} \boldsymbol{v}_{\mathcal{S}} \right)^T \boldsymbol{P} \Big) = D_{\mathcal{S}}^{\mathfrak{ab}} \boldsymbol{\tau}_{\mathfrak{a}} \otimes \boldsymbol{\tau}_{\mathfrak{b}} . \tag{179}$$

  In (179), $\nabla_{\mathcal{S}}$ is the surface gradient and $\boldsymbol{P}$ is the projection operator onto the tangent plane to $\mathcal{S}$:

$$\nabla_{\mathcal{S}} \boldsymbol{u} \equiv \frac{\partial \boldsymbol{u}}{\partial \xi^{\mathfrak{a}}} \otimes \boldsymbol{\tau}^{\mathfrak{a}} , \quad \boldsymbol{P} \equiv \boldsymbol{\tau}_{\mathfrak{a}} \otimes \boldsymbol{\tau}^{\mathfrak{a}} ,$$

[29] Developing a model with the consideration of (176) requires further assumptions on S, $(-p\boldsymbol{I}+\boldsymbol{R})^+\boldsymbol{n}_b \cdot \boldsymbol{n}_b$, $(-p\boldsymbol{I} + \boldsymbol{R})^-\boldsymbol{n}_b \cdot \boldsymbol{n}_b$. We prefer to give an erosion/deposition law and so omit (176).

where $\boldsymbol{u}$ is a vector field defined on $\mathcal{S}$. With $\boldsymbol{u} = u^{\mathfrak{a}}\boldsymbol{\tau}_{\mathfrak{a}} + u\boldsymbol{n}$, we deduce

$$\boldsymbol{P}\nabla_{\mathcal{S}}\boldsymbol{u} \equiv u^{\mathfrak{a}}_{\ ;\mathfrak{b}}\boldsymbol{\tau}_{\mathfrak{a}} \otimes \boldsymbol{\tau}^{\mathfrak{b}}\,,$$

so that definition of $\boldsymbol{D}_{\mathcal{S}}$ implies the following expression for the components $D_{\mathcal{S}}^{\mathfrak{ab}}$:

$$D_{\mathcal{S}}^{\mathfrak{ab}} = \tfrac{1}{2}\left(u^{\mathfrak{a}}_{\ ;\mathfrak{c}}\,g^{\mathfrak{cb}} + u^{\mathfrak{b}}_{\ ;\mathfrak{c}}\,g^{\mathfrak{ca}}\right)\,.$$

Note that $\mathrm{tr}(\boldsymbol{D}_{\mathcal{S}}) = D_{\mathcal{S}}^{\mathfrak{ab}}g_{\mathfrak{ab}} = (\boldsymbol{D}_{\mathcal{S}})^{\mathfrak{a}}_{\ \mathfrak{a}}$. If one assumes $\zeta_{\mathcal{S}} = 0$ the correspondingly reduced equation $(178)_2$, viz.,

$$\left(S^{\mathfrak{ab}}_{\text{viscous}}\right)_{\text{Stokes}} = 2\nu_{\mathcal{S}}\left[D_{\mathcal{S}}^{\mathfrak{ab}} - \tfrac{1}{2}\,\mathrm{tr}(\boldsymbol{D}_{\mathcal{S}})\,g^{\mathfrak{ab}}\right]\,, \tag{180}$$

corresponds to the STOKES approximation of $(178)_2$. Note, since no 'areal preservance' is implemented, the tensor on the right-hand side of $(178)_2$ is (still) the deviator of the surface stretching.

A closure relation for $p(\mu)$ is still needed. The intuitive understanding is that surface pressure can only build under areal compaction but not dilatation. Moreover, with increasing density μ, compaction will be more and more inhibited, or the corresponding pressure more and more increased. So,

$$p(\mu) = \mathcal{H}\left(-\mathrm{tr}(\boldsymbol{D}_{\mathcal{S}})\right)\mathsf{P}(\mu). \tag{181}$$

Three choices for P are

$$\begin{aligned}
\mathsf{P}(\mu) &= p_1\tan\left(\frac{\pi}{2}\frac{\mu}{\mu_0}\right)\,, \quad \mu > 0\,,\\
\mathsf{P}(\mu) &= \begin{cases} 2p_1\dfrac{\mu}{\mu_0} & \mu < \mu_0\,,\\[1ex] \in [2p_1,\infty) & \mu = \mu_0\,,\end{cases}\\
\mathsf{P}(\mu) &= p_1'\mu + \frac{p_2'}{n}\mu^n = \left(p_1' + \frac{p_2'}{n}\mu^{n-1}\right)\mu\,,
\end{aligned} \tag{182}$$

where p_1, $p'_{1,2} > 0$ and $n > 1$. For $(182)_{1,2}$, $p(\mu_0) = \infty$, so preventing μ from going beyond μ_0. Such a limit is not built into $(182)_3$, but selecting n large, produces physically effectively the same (for the graphs of $(182)_{1,2,3}$ see Fig. 10). These proposals account for the fact that with $\mu > 0$ also $p > 0$; furthermore, the larger μ is, the larger will be the pressure. Relations $(182)_{1,2}$ incorporate a densest packing condition, $(182)_3$ does not, which is more realistic since grains can escape perpendicular to $\mathcal{S}$. This completes the postulation of the stress parameterization for $S^{\mathfrak{ab}}$.

- The sliding laws

$$(-p\boldsymbol{I} + \boldsymbol{R})^+\boldsymbol{n}_b - \left((-p\boldsymbol{I} + \boldsymbol{R})^+\boldsymbol{n}_b\cdot\boldsymbol{n}_b\right)\boldsymbol{n}_b = \rho^+\mathcal{C}_1\|\boldsymbol{v}^+_{\|} - \boldsymbol{v}_{\mathcal{S}\|}\|\left(\boldsymbol{v}^+_{\|} - \boldsymbol{v}_{\mathcal{S}\|}\right)\,, \tag{183}$$

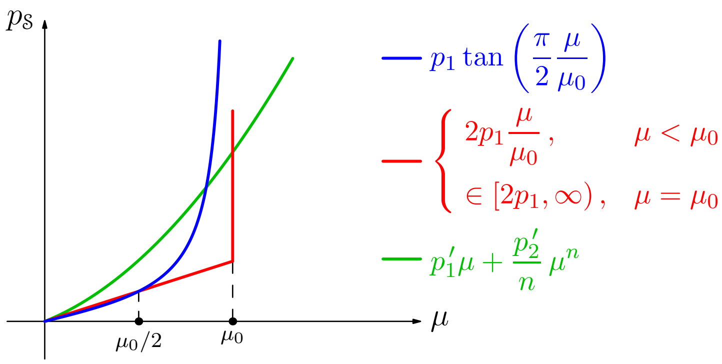

Figure 10: Pressure p as a function of μ for the 3 choices in (182)

$$(-p\boldsymbol{I} + \boldsymbol{R})^{-}\boldsymbol{n}_b - \big((-p\boldsymbol{I} + \boldsymbol{R})^{-}\boldsymbol{n}_b \cdot \boldsymbol{n}_b\big)\, \boldsymbol{n}_b = \rho^{\text{bed}}\mathcal{C}_2\|\boldsymbol{v}_{\mathcal{S}\|}\|\, \boldsymbol{v}_{\mathcal{S}\|}\,, \tag{184}$$

with the (dimensionless) drag coefficients $\mathcal{C}_1$, $\mathcal{C}_2 > 0$, will determine $(-p\boldsymbol{I}+\boldsymbol{R})^{\pm}\boldsymbol{n}_b\cdot\boldsymbol{\tau}^{\mathfrak{a}}$ in (175). In the Boussinesq approximation ρ^+ may be replaced by $\rho^* = \rho(4°\text{C})$; and in the shallow water approximation, $\boldsymbol{v}_{||}$ reduces to the horizontal component of $\boldsymbol{v}$, $\boldsymbol{v}_H$, so that (183) reads

$$(\tau_{xz}, \tau_{yz}) = \rho^*\mathcal{C}_1\sqrt{(u^+ - u_{\mathcal{S}})^2 + (v^+ - v_{\mathcal{S}})^2}\,((u^+ - u_{\mathcal{S}}), (v^+ - v_{\mathcal{S}})).$$

- For $(\boldsymbol{\phi}^{\rho_\alpha})^+ \cdot \boldsymbol{n}_b$ we simply evaluate $\boldsymbol{\phi}^{\rho_\alpha}$ on $\mathcal{S}_b$:

$$(\boldsymbol{\phi}^{\rho_\alpha})^+ \cdot \boldsymbol{n}_b = \boldsymbol{\phi}^{\rho_\alpha}|_{z=b(x,y,t)} \cdot \boldsymbol{n}_b\,.$$

- Now we refer to $\boldsymbol{v}^+$, ρ^+, c_α^+.

First, for the velocity $\boldsymbol{v}^+$ it is natural to request a kinematic condition of sliding or no-slip. When expressed in terms of the linear velocity profile across the thickness of the diffusive interface, see Fig. 11, this request implies

$$\boldsymbol{v}^+ = \Xi v_s^{\mathfrak{a}}\boldsymbol{\tau}_{\mathfrak{a}} + \mathcal{U}_b\boldsymbol{n}\,, \quad \Xi \in [1, 2]\,. \tag{185}$$

Now, the velocity tangential to $\mathcal{S}_b$ at the 'upper' interface of this thin layer is twice the barycentric tangential surface velocity $\boldsymbol{v}_{\mathcal{S}\|}$. If a plug flow profile is assumed, then the sliding velocity is $\|\boldsymbol{v}_{\|}^+ - \boldsymbol{v}_{\mathcal{S}\|}\|$. So, $\Xi \in [1, 2]$, but $\Xi = 2$ is the likelier value. These considerations lead to the above representation (185).

Second, since

$$\rho^+ = \textstyle\sum_\alpha \underbrace{\nu_\alpha^+\rho_s}_{\rho_\alpha^+} + \underbrace{\left(1 - \sum_\alpha\nu_\alpha^+\right)\rho_f}_{\tilde{\rho}_f^+}\,, \quad \rho_\alpha^+ = \rho^+c_\alpha^+ \longrightarrow \nu_\alpha^+ = \frac{\rho^+}{\rho_s}\,c_\alpha^+\,, \tag{186}$$

where ν_α is the solid volume fraction of α constituent and ρ_f is the true density of the fluid, we find

$$\rho^+ = \frac{\rho_f}{1 - \sum_\alpha c_\alpha^+ \left(1 - \frac{\rho_f}{\rho_s}\right)} \,. \tag{187}$$

So, according to $(186)_1$, (187), ρ^+ is known, once $\sum_\alpha \nu_\alpha^+$ or $\sum_\alpha c_\alpha^+$ is known. We postulate closure conditions for c_α or ν_α ($\alpha = 1, \ldots, N$).

Third, to postulate a phenomenological relation for c_α^+ or ν_α^+ is the hardest, because it is physically not obvious. In such a situation it is probably easiest to formulate a surface balance law for c_α^+ as stated in (133), viz.,

$$\frac{\partial\, c_\alpha^+}{\partial\, t} + \left(c_\alpha^+ \boldsymbol{v}_\parallel^+ + \boldsymbol{\phi}^{c_\alpha^+}\right)^{\mathfrak{a}}_{;\,\mathfrak{a}} - \frac{\partial\, c_\alpha^+}{\partial\, \xi^{\mathfrak{a}}}\, w^{\mathfrak{a}} - 2 c_\alpha^+ \mathcal{U}_b K = \pi^{c_\alpha^+} \,. \tag{188}$$

In this equation the jump terms of the bulk quantities are absent as is the supply term. For none of them the introduction would be justified. Moreover, $\boldsymbol{\phi}^{c_\alpha^+}$ is the flux of c_α^+ (parallel to $\mathcal{S}_b$),

$$\left(\boldsymbol{\phi}^{c_\alpha^+}\right)^{\mathfrak{a}} = -d_{c_\alpha^+} \left(c_\alpha^+\right)_{;\,\mathfrak{b}} g^{\mathfrak{a}\mathfrak{b}} \,, \tag{189}$$

in which $d_{c_\alpha^+}$ are diffusivities, and cross dependences on the concentrations c_β^+ ($\beta \neq \alpha$) have been ignored. If one considers the evolution of c_α^+ to be non-diffusive, then $\boldsymbol{\phi}^{c_\alpha^+} = \boldsymbol{0}$, and (188) becomes a pure evolution equation for c_α^+. The production rate density is assumed to depend on quantities in the slurry at $\mathcal{S}_b$ and of the moving interface,

$$\pi^{c_\alpha^+} = \hat{\pi}^{c_\alpha^+} (\mathfrak{d}_\alpha, c_\alpha^+, Re_\alpha^+, \mu_\alpha, \|\boldsymbol{v}_\parallel^+ - \boldsymbol{v}_{\mathcal{S}\parallel}\|, \ldots) \,, \tag{190}$$

such that $\pi^{c_\alpha^+}|_{\text{equil}} = 0$. Equilibrium conditions are characterized by uniform and time independent c_α^+ and $\mathcal{U}_b = 0$, so that the left-hand side of (189) vanishes. It transpires that appropriate selection of $\hat{\pi}^{c_\alpha^+}$ is crucial.

We now incorporate into (171), (173) the *entrainment-erosion* and *deposition* rates for which specialists in sediment transport substitute parameterizations. The mass flow from below into the basal bed is identified as entrainment, erosion or pick-up rate, and from the moving bed to the base as deposition rate. With

$$\rho^{\text{bed}} \equiv \sum_{\alpha=1}^{N} \rho_\alpha^{\text{bed}} + \rho_f^{\text{bed}} \,,$$

they are, obviously, given by

$$\mathcal{M}_b^\alpha \equiv -\mathcal{U}_b\, \rho_\alpha^{\text{bed}}, \quad \mathcal{M}_b^f \equiv -\mathcal{U}_b\, \rho_f^{\text{bed}}, \quad \mathcal{M}_b \equiv -\mathcal{U}_b\, \rho^{\text{bed}} \,, \tag{191}$$

from which we easily deduce

$$\mathcal{M}_b^\alpha = \frac{\rho_\alpha^{\text{bed}}}{\rho^{\text{bed}}}\, \mathcal{M}_b, \quad \mathcal{M}_b^f = \frac{\rho_f^{\text{bed}}}{\rho^{\text{bed}}}\, \mathcal{M}_b \,. \tag{192}$$

Positive (negative) $\mathcal{U}_b$ [negative (positive) $\mathcal{M}_b$] corresponds to deposition (erosion). The result (192) implies that we are not free to select closure relations for $\mathcal{M}_b^{\alpha,f}$ independently and evaluate $\mathcal{M}_b$ from these via

$$\mathcal{M}_b = \sum_{\alpha=1}^{n} \mathcal{M}_b^{\alpha} + \mathcal{M}_b^{f} .$$

On the contrary, we must postulate a closure relation for $\mathcal{M}_b$ and evaluate $\mathcal{M}_b^{\alpha,f}$ from $(192)_{1,2}$ via the known grain size distribution and the corresponding densities $\rho_{\alpha,f}^{\mathrm{bed}}$ just below $\mathcal{S}_b$. Erosion and deposition occur below the detritus layer. It is convenient to write

$$\mathcal{M}_b = \mathcal{M}_b^{\mathrm{eros}} - \mathcal{M}_b^{\mathrm{dep}} , \tag{193}$$

and to independently postulate representations for erosion and deposition. On the basis of the concepts of 'erosion inception' and 'erosion amount' we now postulate

$$\begin{aligned} \mathcal{M}_b^{\mathrm{eros}} &= \sum_{\alpha=1}^{N^*} (c_\alpha)^{\mathrm{bed}} (E_\alpha)^{\mathrm{eros}} \quad \text{(erosion)} , \\ \mathcal{M}_b^{\mathrm{dep}} &= -\rho^+ \sum_{\alpha} c_\alpha^+ \left(w_\alpha^{s+} \boldsymbol{e}_z \cdot \boldsymbol{n}_b + \mathcal{U}_b \right) \quad \text{(deposition)} , \end{aligned} \tag{194}$$

where N^* follows from the evaluation of the critical shear stress according to formula (153):

$$N^* = \max_{\alpha=1,\dots,N} \left\{ \alpha \;\middle|\; (\tau_c^*)_\alpha < \frac{(II_{\boldsymbol{\sigma}_E})^{1/2}}{\Delta\rho g \mathfrak{d}_\alpha} \right\}_{\mathcal{S}_b} . \tag{195}$$

Here $II_{\boldsymbol{\sigma}_E}$ is the second stress deviator invariant in the basal material evaluated at the basal surface. The parameterization for $\mathcal{M}_b^{\mathrm{dep}}$ makes use of the terminal velocity of a particle in an ambient fluid field, $\boldsymbol{w}_\alpha^{s+}$, see (9) and (10). For particle class α this yields the mass flow $-\rho_\alpha^+ \boldsymbol{w}_\alpha^{s+} \cdot \boldsymbol{n}_b$ towards the basal surface. However, this surface itself moves with the displacement speed $\mathcal{U}_b$ in the direction of $\boldsymbol{n}_b$. Thus, the mass flow of class-α particles is $-\rho_\alpha^+ (\boldsymbol{w}_\alpha^{s+} \cdot \boldsymbol{n}_b + \mathcal{U}_b)$. Summation over all α-classes now yields the total depositing mass flow

$$\mathcal{M}_b^{\mathrm{dep}} = -\sum_{\alpha} \rho_\alpha^+ \left(\boldsymbol{w}_\alpha^{s+} \cdot \boldsymbol{n}_b + \mathcal{U}_b \right) \overset{\boldsymbol{w}_\alpha^s = w_\alpha^s \boldsymbol{e}_z}{=} -\rho^+ \sum_{\alpha} c_\alpha^+ \left(w_\alpha^{s+} \boldsymbol{e}_z \cdot \boldsymbol{n}_b + \mathcal{U}_b \right) ,$$

which is $(194)_2$, and where expression (69) is to be substituted for w_α^s. When the shallowness approximation is justified then $\boldsymbol{e}_z \cdot \boldsymbol{n}_b \approx 1$.

With (191) and (192) the mass balance relations (173) and (171) can be respectively written as

$$
\begin{aligned}
&\frac{\partial \mu_\alpha}{\partial t} + (\mu_\alpha \boldsymbol{v}_{\mathcal{S}})^{\mathfrak{a}}{}_{;\mathfrak{a}} - \frac{\partial \mu_\alpha}{\partial \xi^{\mathfrak{a}}}\, w^{\mathfrak{a}} - 2\mu_\alpha\, \mathcal{U}_b K = \\
&\qquad - (\boldsymbol{j}_{\mathcal{S}\alpha})^{\mathfrak{a}}{}_{;\mathfrak{a}} + (-\boldsymbol{\phi}^{\rho_\alpha} \cdot \boldsymbol{n}_b)^+ - \rho_\alpha^+ \Big(\underbrace{\boldsymbol{v}^+ \cdot \boldsymbol{n}_b - \mathcal{U}_b}\Big) + \frac{\rho_\alpha^{\text{bed}}}{\rho^{\text{bed}}} \mathcal{M}_b\,,
\end{aligned}
\tag{196}
$$

$$
\frac{\partial \mu}{\partial t} + (\mu \boldsymbol{v}_{\mathcal{S}})^{\mathfrak{a}}{}_{;\mathfrak{a}} - \frac{\partial \mu}{\partial \xi^{\mathfrak{a}}}\, w^{\mathfrak{a}} - 2\mu\, \mathcal{U}_b K = -\rho^+ \Big(\underbrace{\boldsymbol{v}^+ \cdot \boldsymbol{n}_b - \mathcal{U}_b}\Big) + \mathcal{M}_b\,, \tag{197}
$$

for $\alpha = 1, \ldots, N$. In these relations the underbraced term vanishes when the normal component of the barycentric velocity follows the displacement speed $\mathcal{U}_b$ of $\mathcal{S}_b$. If $\mathcal{M}_b$ is known as a function of space and time on $\mathcal{S}_b$, (196) and (197) are field equations for μ_α and μ. Of course, also $\mathcal{U}_b$ must be known; it is determined by $(191)_3$, (193), (194).

Equation (197) states that the time rate of change of the specific surface mass μ grows by the mass flow from the slurry, $[(\boldsymbol{v}^+ \cdot \boldsymbol{n}_b - \mathcal{U}_b) < 0]$ and by the erosion rate ($\mathcal{M}_b > 0$) from below. (Note, $\mathcal{M}_b$ contains both erosion and deposition, but $\mathcal{M}_b > 0$ is a net erosion.) For $\mu \equiv 0$ the two contributions on the right-hand sides of (196), (197) must balance. Equation (196) allows an analogous inference, but for constituent α a diffusive flow normal to $\mathcal{S}_b$ is added to this balance.

For the boundary condition of heat we proceed as for the traction boundary condition. In fact, we impose either a Dirichlet or Neumann condition on the slurry side of $\mathcal{S}_b$. The simplest procedure is to impose

$$
T(x,y,z,t)\big|_{z=b(x,y,t)} = \Theta(x,y,t)\,,
$$

where $\Theta(x,y,t)$ is the temperature profile at the deepest position of the lake domain which is subject to the study. As an alternative the Neumann condition

$$
\kappa \frac{\partial T}{\partial \boldsymbol{n}_b} = Q_\perp(x,y,z,t)\big|_{z=b(x,y,t)}\,,
$$

where $Q_\perp$ is the geothermal heat, can also be used.

There remains the formulation of boundary conditions along the lake shore and at the corresponding boundary lines on the surface $\mathcal{S}$.

For the domain of the particle laden fluid It is convenient to think that the lake domain is divided into a number of layers which are bounded by fixed horizontal surfaces. Identify the layers by the subscript k and let h_k be their thicknesses. In each layer we think the corresponding portion of basal surface to be replaced by a vertical wall. For $k = 1$ this wall defines the mathematical shore line. Along the vertical walls fields of unit vectors $\boldsymbol{N}_k$ can be introduced which lie in horizontal planes parallel to the (x,y)-plane. If no detritus moves, then $\boldsymbol{v}_{\mathcal{S}}^k = 0$ and $\mu_{\mathcal{S}}^k = 0$, and boundary conditions are given by

$$
(h_k \rho_k \boldsymbol{v}_k) \cdot \boldsymbol{N}_k = \begin{cases} 0\,, & \text{for impermeable wall,} \\ \mathfrak{M}_k\,, & \text{for discharge into ground;} \end{cases}
$$

$$(h_k \boldsymbol{J}_k^\alpha) \cdot \boldsymbol{N}_k = \begin{cases} 0 \ , & \text{for impermeable wall,} \\ \mathfrak{M}_k^\alpha \ , & \text{for discharge of } \alpha\text{- mass into ground;} \end{cases}$$

$$(h_k \boldsymbol{Q}_k^{\epsilon,h}) \cdot \boldsymbol{N}_k = \begin{cases} 0 \ , & \text{for no heat loss,} \\ Q_k^{\text{geoth}} \ , & \text{for prescribed heat flow,} \end{cases} \qquad \text{or} \quad T_k = T_k^{\text{geoth}}.$$

The usual boundary conditions are those describing the ground as impermeable surface; else $\mathfrak{M}_k$ and $\mathfrak{M}_k^\alpha$ must be prescribed, which requires a model for the ground.

For the boundaries of the sediment 'layer' For the detritus layer the boundary value problem is that on a curved surface, which is bounded by a closed loop, most of which can be identified with the mathematical shore line. Because of the Fick-type diffusive constitutive relations for the constituent mass fluxes $\boldsymbol{j}_{\mathcal{S}\alpha}$ and the NAVIER-STOKES-type stress parameterizations for $S^{\mathfrak{a}b}$ closure conditions are analogous to those of the three-dimensional case. However no boundary condition must be formulated for the surface heat flow in our case, because energy considerations have been left unspecified. So, let $\mathcal{C}$ be a loop along the mathematical shore line (including a segment of the river bank and across the tributary). Define by $\boldsymbol{h}$ the unit vector field along $\mathcal{C}$ which is tangent to $\mathcal{S}$ and perpendicular to $\mathcal{C}$. With $\boldsymbol{v}_\mathcal{S}$, the barycentric surface velocity vector, and $\boldsymbol{j}_{\mathcal{S}\alpha}$ the surface mass flux, we may now write

$$\boldsymbol{j}_{\mathcal{S}\alpha} \cdot \boldsymbol{h} = \begin{cases} 0 \ , & \text{along } \mathcal{C} \text{ where } \boldsymbol{v}_\mathcal{S} = \boldsymbol{0}, \\ -\mathfrak{m}_\mathcal{S}^\alpha \ , & \text{along } \mathcal{C}\text{, where wash-load enters the lake from the tributary ;} \end{cases}$$

$$(\mu \boldsymbol{v}_\mathcal{S}) \cdot \boldsymbol{h} = \begin{cases} 0 \ , & \text{at the shore segments where } \boldsymbol{v}_\mathcal{S} \text{ is tangential to the shore,} \\ -\left(\sum_\alpha \mathfrak{m}_\mathcal{S}^\alpha + \mathfrak{m}^f\right) , & \text{at the river cross section.} \end{cases}$$

5 Transformation of the surface mass distribution into a detritus layer thickness

From a practical point of view the surface mass densities of the sediment classes μ_α $(\alpha = 1, \ldots, N)$ are not very useful variables. Better is the determination of the thickness h of the detritus layer; so, let us assume

$$\mu = \rho_s \nu_{\text{mean}}\, h \,, \quad \nu_{\text{mean}} \equiv \sum_\alpha \nu_{\text{mean}}^\alpha \,,$$

where ρ_s is the true density of the sand, and ν_{mean}^α are mean values of the solid volume fractions of the sediment classes $\alpha = 1, \ldots, N$ in the detritus layer. Note that $\nu_{\text{mean}} =$

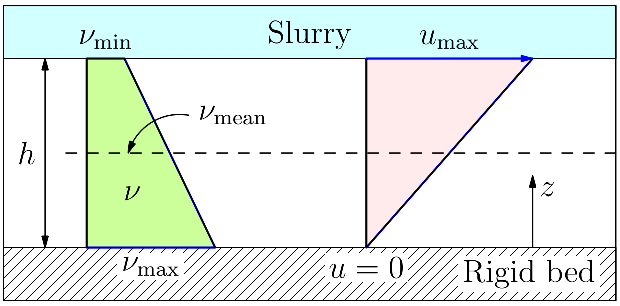

Figure 11: Detritus layer with thickness h. Distribution of the volume fraction and detritus velocity as functions of z.

$(1-n)$, where n is the average porosity within the detritus layer. Subsequently, the thickness of the detritus layer follows from

$$h = \frac{\mu}{\rho_s \nu_{\rm mean}}\,, \tag{198}$$

and our aim is to provide a model for $\nu_{\rm mean}$[30].

First, we consider that the detritus layer has linear volume fraction and velocity distributions across its thickness. The expectations are that the linear volume fraction through the layer has a maximum at the bottom and a minimum at the top. Similarly, the layer velocity vanishes at the bottom and reaches a maximum at the top surface, $u_{\rm max}$, see Fig. 11. So, their distributions are given by

$$\nu = \frac{\nu_{\rm min}-\nu_{\rm max}}{h}\,z + \nu_{\rm max}, \quad u = \frac{u_{\rm max}}{h}\,z\,. \tag{199}$$

As the figure shows, the layer may become instable if it is sufficiently sheared from above. A Richardson number dependence of the mean volume fraction in an arbitrary detritus layer (i.e., not necessarily as in Fig. 11) is then suggested.

So, still referring to Fig. 11, we define

$$Ri = \frac{-\dfrac{1}{\rho_{\rm mean}}\dfrac{{\rm d}\rho}{{\rm d}z}\,g}{\left(\dfrac{{\rm d}u}{{\rm d}z}\right)^2} = \frac{-\dfrac{1}{\nu_{\rm mean}}\dfrac{{\rm d}\nu}{{\rm d}z}\,g}{\left(\dfrac{{\rm d}\,u}{{\rm d}z}\right)^2} = \left\{\frac{2(\nu_{\rm max}-\nu_{\rm min})}{\nu_{\rm max}+\nu_{\rm min}}\right\}\frac{gh}{u_{\rm max}^2}\,, \tag{200}$$

where $\nu_{\rm mean} \equiv (\nu_{\rm max}+\nu_{\rm min})/2$ has been used. For particular values of $\nu_{\rm min}$, $\nu_{\rm max}$, $u_{\rm max}$, the Richardson number Ri is a function of the thickness h: $Ri = Ri(h)$. Now, our assumption for the mean volume fraction in an arbitrary detritus layer is

$$\nu_{\rm mean} = \nu_{\rm mean}(Ri(h))\,.$$

[30] If we assume $\mu_\alpha = \rho_s \nu^\alpha_{\rm mean} h$, then the mean volume fractions $\nu^\alpha_{\rm mean}$ are known once the height h is known: $\nu^\alpha_{\rm mean} = \mu_\alpha/(\rho_s h)$; or, equivalently, if $\nu_{\rm mean}$ is known, see (198): $\nu^\alpha_{\rm mean} = (\mu_\alpha/\mu)\nu_{\rm mean}$. For the detritus layer the mean volume fractions $\nu^\alpha_{\rm mean}$ are practically better quantities than the surface densities μ_α.

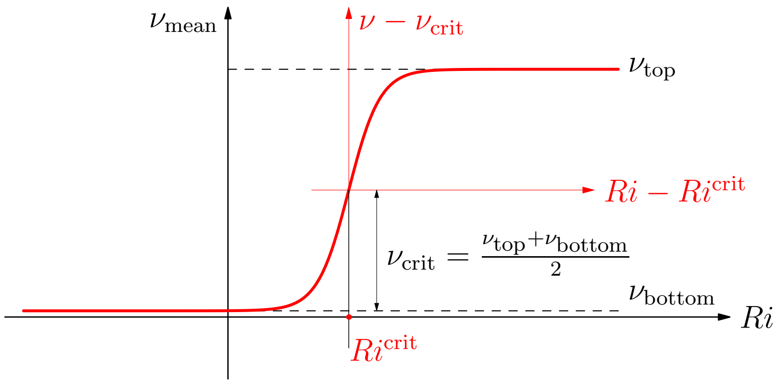

Figure 12: Qualitative behaviour of the mean volume fraction ν_{mean} of the mixture.

When inserted into (198), this yields an equation for the determination of h:

$$\frac{\mu}{\rho_s h} = \nu_{\text{mean}}(Ri(h))\,. \tag{201}$$

Moreover, with an obvious reminiscence to the KELVIN-HELMHOLTZ instability of a linearly stratified viscous fluid under simple shear MILES [28] (1967), we suppose a *Ri*-dependence as shown in Fig. 12. This function can qualitatively and quantitatively be given as

$$\begin{aligned}\nu_{\text{mean}} &= \tfrac{1}{2}(\nu_{\text{top}} + \nu_{\text{bottom}}) + a\tanh\left(b(Ri - Ri^{\text{crit}})\right)\,,\\ a = \tfrac{1}{2}(\nu_{\text{top}} - \nu_{\text{bottom}})\,,\quad b &= \tfrac{1}{\varepsilon}\,\text{atanh}\left\{\frac{2s\,\nu_{\text{top}} - (\nu_{\text{top}} + \nu_{\text{bottom}})}{\nu_{\text{top}} - \nu_{\text{bottom}}}\right\}\,.\end{aligned} \tag{202}$$

Here, $0 < \varepsilon < 1$, $0 \ll s < 1$, and a, b are so adjusted that

$$\begin{aligned}
Ri &\to \infty & &\longrightarrow & \nu_{\text{mean}} &= \nu_{\text{top}}\,,\\
Ri &\to -\infty & &\longrightarrow & \nu_{\text{mean}} &= \nu_{\text{bottom}}\,,\\
Ri &= Ri^{\text{crit}} & &\longrightarrow & \nu_{\text{mean}} &= \nu_{\text{crit}} \equiv \tfrac{1}{2}(\nu_{\text{top}} + \nu_{\text{bottom}})\,,\\
Ri &= Ri^{\text{crit}} + \varepsilon & &\longrightarrow & \nu_{\text{mean}} &= s\,\nu_{\text{top}}\,.
\end{aligned}$$

The modeler can pick values for ν_{top}, ν_{bottom}, Ri^{crit}, ε and s. Suggestions are given in Table 7. Obviously, for a Newtonian fluid Ri^{crit} is the value of the RICHARDSON number below which instability sets in.

With the parameterization (202), relation (201) becomes a nonlinear equation for h, which is easily seen to possess a unique solution. An iterative solution h is best found as

$$h^{(m+1)} = \frac{\mu}{\rho_s \nu_{\text{mean}}(Ri(h^{(m)}))}\,,\qquad h^{(0)} = \frac{2\mu}{\rho_s(\nu_{\text{top}} + \nu_{\text{bottom}})}\,,$$

Table 7: Suggested values for the parameters in equation (202).

$\nu_{\text{top}} = 0.8$	$Ri^{\text{crit}} = 0.25$	$\nu_{\text{bottom}} = 0.02$	$\varepsilon = 0.02$	$s = 0.98$

and computations are interrupted when

$$\left| h^{(m+1)} - h^{(m)} \right| \ll 1 \,.$$

This computation must be performed for all x, y and each time step t.

6 Discussion and Conclusion

In this article transport of sediments in suspension and in the detritus layer of an alluvial river-lake (or ocean) system was analyzed from a perspective of global processes, taking place in the lake or ocean basin, on the one hand, and in the moving or stagnant detritus layer at the bottom of the water body, on the other hand. These two regimes interact at their common boundary via erosion of sediments from the basal surface or as deposition of wash-load to the rigid bed. The suspended sediment fractions are transported by the wind-induced barotropic or baroclinic circulation of the homogeneous or density stratified lake or ocean water. These sediment fractions are carried into the lake as wash loads from river inlets. The bed-load detritus, on the other hand, is carried into the estuarine environment of the lake and contributes thereby its deposition to deltaic formations. In the vicinity of the river mouth both sediment formations are subjected to a new flow regime, which is governed by large scale circulation dynamics, in which the current speeds are generally smaller. This leads to an enhanced sedimentation of the coarser grain fractions and associated aggradation with progressing delta formations.

Whereas on decadal time scales the important regions of such land aggradation in oceans is restricted to estuarine zones, these zones may in lakes extend over substantial portions of the basins or the entire lake. This is particularly so for artificial reservoirs and mountainous terrain. Rigorous models on this complex detritus-particle-laden fluid interaction are still missing. It was our intention to present in this memoir the foundation for a class of such models as a basis for later use in attempts of software developments for sediment transport of this sort.

To this end, the lake domain was divided into two regions, the actual water domain with suspended (non)-buoyant particles, called also slurry, and the detritus layer with moving sediments, also a solid-fluid mixture, but very thin. Because of its thinness, this layer was collapsed into an infinitely thin moving and deforming surface, covered by a mixture of the N sediment classes α $(= 1, \ldots, N)$ and a fluid. This mixture moves along the surface, with each surface having its own tangential velocity, and thus intermixing with the others by surface parallel diffusion. However, further mass exchanges with the slurry above and the ground below takes also place as erosion and deposition processes.

The mathematical description of this local interaction problem turned out to be rather subtle, even in the simplest possible form as dealt with here.

In *domain I*, the governing field equations for the lake as a particle laden fluid are handled as a continuous mixture of class I, i.e., the balance laws of mass are formulated for the sediment classes α $(= 1, \dots, N)$ and the mixture as a whole, but balances of linear momentum and energy are only formulated for the mixture as a whole. This is done for a nearly density preserving fluid, whose density changes due to variations of the temperature, mineralization and pressure but also the distribution of the wash-load. The formulation is also complicated by the presence of turbulence. As a consequence, a considerable number of approximate models exists, all of which are claimed to be relevant to describe the three-dimensional circulation dynamics, including dispersion of the suspended wash-load. They differ in certain terms but the differences are seldom explained in the context of their physical implications. We have tried to close this gap.

Two model families were presented. In *model family 1*, referenced as generalized BOUSSINESQ models, two subfamilies were distinguished:

- In the *classical* BOUSSINESQ *assumption* variations of the density are ignored, except in the gravity term. This implies that the velocity field is solenoidal. This property is preserved also when turbulence averaging is performed and averaged equations are looked at.

- A *generalized* BOUSSINESQ *fluid* is defined by a mixture-density composition, $\rho = \rho_0(z)+\rho_d(\boldsymbol{x},t)$, in which $\rho_d(\boldsymbol{x},t)$ is ignored everywhere except in the gravity term. In this case the mass flux or momentum density $\rho_0\boldsymbol{v}(\boldsymbol{x},t)$ is solenoidal. This property is also preserved in the turbulent-averaged equations.

Model family 2 is based on the assumption of small turbulent density variations; it was coined by us

- *Small density fluctuation assumption.* It is based on the assumption that approximations are only introduced after the turbulent averaging operations have been performed with the compressible governing equations. Then, with $\rho = \langle\,\rho\,\rangle + \rho'$, every correlation term $\langle\,\rho' a\rangle$ is ignored. This assumption implies that the averaged mass balance of the mixture is preserved, see (39). So, acoustic waves can be studied in a turbulent fluid as can the influence of the pressure dependence of the equation of state, both effects which may be significant in very deep lakes.

A further popular approximation is the Shallow Water Approximation (SWA), in which the ratio of typical depth to length scales is used as a perturbation parameter $\mathcal{A}$ and the lowest order approximation to the reduced equations in the limit $\mathcal{A} \to 0$ is constructed. This implies that the vertical momentum balance reduces to a force balance between the gravity force and the vertical pressure gradient. This approximation is known as the *hydrostatic pressure assumption.* Moreover, the divergence of the stress deviator, and the divergences of the heat flux and the species mass fluxes reduce to

$$\frac{\partial\,\tau_{xz}}{\partial\,z}, \quad \frac{\partial\,\tau_{yz}}{\partial\,z}, \quad \frac{\partial\,Q_z^{\epsilon,h}}{\partial\,z}, \quad \frac{\partial\,\mathfrak{J}_z^{\alpha}}{\partial\,z},$$

whilst all other terms drop out. Both assumptions are today regarded as critical. An in-between compromise, which is sometimes used, still employs the hydrostatic pressure assumption but accounts for the horizontal stress, heat flux and species mass flux gradients. The modern trend, however, abandons the SWA altogether. These formulations are known as *non-hydrostatic models*. They are certainly needed in the aftermaths of incessant heavy rain fall with strong detritus and wash-load discharge from a river into the river-mouth region, when strong up- and down-welling are likely to occur, see Fig. 13. In such systems it may be advantageous to employ nesting, where a simpler model is used for the circulation dynamics of the entire lake, and the river-inlet environs are analyzed with a more complex model subject to the current, pressure, temperature, etc., input along the open boundary. A word of caution or alertness concerns the formulation of the heat equation (first law of

Figure 13: Sediment laden water in the forefront of the estuary mouth of the river Rhine (Alpen-Rhein) at Fussach near Bregenz, Austria. The picture demonstrates that up-welling and down-welling processes must be active, indicating that the Shallow Water Approximation in computational software should not be applied. A full non-hydrostatic three dimensional model is required. Copyright: 'Tino Dietsche - airpics4you.ch'

thermodynamics), which has consistently been given in two different forms, one in which the caloric potential is the HELMHOLTZ free energy (and the energy equation is written in terms of this free energy), and a second one, where the potential is the free enthalpy. As explained in the appendix, if ρ and T are the independent thermodynamic variables, then the heat equation is based on the free energy formulation, and, strictly in this case, the thermal equation of state has the form $p = p(\rho, T)$. Alternatively, if p and T are the independent thermodynamic variables, then $\rho = \rho(p, T)$ is the appropriate thermal equation of state and the energy is expressed in terms of the free enthalpy. In applications confusion may arise, since for most situations the thermal equation of state is given as $\rho = \rho(T)$ without a pressure dependence. In these cases it is irrelevant which energy equation is employed, the enthalpy formulation would be logical. Luckily it does not matter, since numerical values for the specific heats c_v and c_p are nearly the same.

Closure relations of the flux terms in the slurry have consistently been proposed as being of gradient type. A critical point in this formulation concerns only the constituent mass fluxes $\mathfrak{J}_\alpha$, defined in (8). These mass fluxes are written as compositions of two contributions, (i) a diffusive flux due to the difference of the velocity of particles of the same class relative to a representative particle velocity within this same sediment class plus a slip velocity of this representative particle of class α to the barycentric velocity of the mixture at the same position, which is fundamentally related to the free fall velocity of the representative particle in still water. Even though this latter choice is questionable in its own right,[31] this kind of parameterization tries to explicitly account for the convective motion of the non-buoyant particles and the diffusive nature of the analogous process due to particle size differences in the same sediment class.

Domain II is in reality a very thin layer of a granular fluid mixture with N sediment classes and an interstitial fluid at saturation. This system has been collapsed in our theoretical formulation into a moving singular surface with surface particles being equipped with surface masses, momenta, etc. This procedure is tantamount to replacing a mixture layer and its top and bottom boundary by a sharp interface, which is equipped with surface mass and evolves under the influence of the sedimentation and erosion processes. As a first approach, we have assumed this interface to be a material surface, being aware that in reality it is nourished from above and below by settling and eroding particles. Essential in this approach was the surface balance law (132), which is based on the transport theorem (130), valid for material surfaces.

The complications with the above described boundary conditions are connected with the fact that N surface sediment classes are introduced, which each may have its own motion tangential to the deforming surface, whose motion is defined by the kinematic equation of motion. If on either side of the deforming surface simple constituent continua are present, the possible surface material is also a simple constituent continuum. Then, the subtle issue is that the geometric motion of the surface from its reference state to its present state and given by the kinematic equation of the surface moving with the velocity $\boldsymbol{w}$, is not the same as the motion of a material body, geometrically-kinematically constrained to the surface, but free to move and deform tangentially to the surface with the material velocity $\boldsymbol{v}_{\mathcal{S}}$. The two are related by (see Fig. 10)

$$\boldsymbol{v}_{\mathcal{S}} = \dot{\xi}^{\mathfrak{a}} \boldsymbol{\tau}_{\mathfrak{a}} + \boldsymbol{w} \quad \longrightarrow \quad \boldsymbol{v}_{\mathcal{S}} \cdot \boldsymbol{n} = \boldsymbol{w} \cdot \boldsymbol{n} \,,$$

were $(\xi^1, \xi^2) \in \tilde{\Delta}$ is the coordinate cover of the moving surface $\mathcal{S}$ and $\boldsymbol{\tau}_{\mathfrak{a}}$ are the base vectors $\boldsymbol{\tau}_{\mathfrak{a}} = \partial \boldsymbol{r} / \partial \xi^{\mathfrak{a}}$, with $\boldsymbol{x} = \boldsymbol{r}(\xi^1, \xi^2, t)$. With these prerequisites the derivation of the

[31] The determination of the velocity of a particle in a moving and perhaps accelerating fluid field relative to the velocity of the fluid at the same position before the latter was inserted in the fluid, is a complex topic of fluid dynamics which does not, in general, agree with the free fall velocity.

local surface balance law for a physical quantity (132) from the corresponding global form (129) due to SLATTERY et al. (2007) [40] is more general than corresponding equations of earlier surface models for which $\boldsymbol{v}_{\mathcal{S}} = \boldsymbol{w}$ was assumed, see e.g. MÜLLER (1985) [30], or for which $\boldsymbol{w} = \mathcal{U}\boldsymbol{n}$ is assumed, see e.g. ALTS and HUTTER (1988) [2]–[5] and references therein. The more general equation has then served as master equation for the derivation of the physical balance laws for the surface-detritus-water mixture involving among others, the surface mass densities μ_α, μ and velocities $\boldsymbol{v}_{\mathcal{S}\alpha}$, $\boldsymbol{v}_{\mathcal{S}}$ ($\alpha = 1, \dots, N$), such that $\boldsymbol{v}_{\mathcal{S}\alpha} \cdot \boldsymbol{n}_b = \boldsymbol{v}_{\mathcal{S}} \cdot \boldsymbol{n}_b = \mathcal{U}_b$. These equations also contain the surface jump quantities from the bulk fields which represent, for mass balance physically the deposition and erosion rates and, for momentum balance laws the traction and impulse jump quantities. Parameterization of erosion consisted of two statements, (i) a criterion defining the onset of erosion of sediments of grain class α and (ii) a statement of the amount of eroded material. Reviews for both have been provided.

A conceptually decisive decision in connection with the detritus motion is whether a surface mixture theory of class II ought to be pursued or a less complicated mixture model of class I should be employed. The latter makes only use of the balance law of momentum for the mixture as a whole, but mass balances of all constituents, and it is technically simpler. The constituent surface velocities have been eliminated by introducing the diffusive surface-mass flux

$$\boldsymbol{j}_{\mathcal{S}\alpha} \equiv \mu_\alpha(\boldsymbol{v}_{\mathcal{S}\alpha} - \boldsymbol{v}_{\mathcal{S}}) = \mu_\alpha(\boldsymbol{v}_{\mathcal{S}\alpha} - \boldsymbol{v}_{\mathcal{S}})_{\parallel}$$

as a new variable of the sediment class α and writing a FICK-type constitutive relation for it. If the class α-velocity needs to be computed, this can a posteriori be done by

$$\boldsymbol{v}_{\mathcal{S}\alpha\parallel} = \frac{1}{\mu_\alpha}\boldsymbol{j}_{\mathcal{S}\alpha} + \boldsymbol{v}_{\mathcal{S}\parallel}\,.$$

The surface mixture momentum balance law entailed the parameterization of the surface parallel stress components S^{ab}, which were postulated as a two-dimensional linear viscous fluid with areal compressibility (but vanishing resistance to expansion). This avoids build-up of cohesion.

Further closure relations were needed in the form of detritus interface sliding laws from above and below and values of the particle concentrations c_α^+ ($\alpha = 1, \dots, N$) immediately above the detritus interface. These are N statements, which were postulated in terms of surface balance laws (188), each involving a FICKian gradient postulate for its flux quantity and N production terms. These balance relations for the boundary value of c_α^+ are likely the most esoteric feature of the model and call for the application and the use of the entropy principle and experiments to constraining the coefficients. A last set of relations completing the theory are explicit relations for the erosion and deposition rates, (194).

To treat the dynamics of the detritus layer by concepts of sharp interfaces is a simplification. In reality the detritus region is a thin layer of finite thickness, which is sheared by the bottom near flow of the wind induced motion of the lake water. By mimicking the thin detritus region as a sheared layer with linear volume fraction and velocity distributions across the layer and assuming the mean volume fraction in this layer to depend on the RICHARDSON number with stable and unstable regimes, the detritus layer thickness can be evaluated, see (198), and its transition from stable (and thin) to unstable (and thick) regimes be estimated.

To summarize, this theory of sediment transport in alluvial systems is fairly substantial but the modeler has some freedom to adjust its complexity somewhat by selecting the number of sediment classes when approximating the grain size distribution curve. There is also some flexibility in selecting the model equations for the lake circulation flow as a slurry and in the application of sub-structuring techniques by dividing the lake domain in subdomains with and without detritus transport. However, apart from these simplifications and some variation in the constitutive postulates the presented equations likely constitute the minimum complexity accounting for the essential physics. Further extensions are possible and have transpired in the derivation of the model. For instance, in (176) the momentum equation perpendicular to the moving detritus interface was presented, but it was ignored. Paired with additional closure statements involving jumps of bulk fields across $\mathcal{S}$, this equation is interpreted as an evolution equation for the displacement speed $\mathcal{U}_b$. When used, it would make postulation of deposition and entrainment rates obsolete. This fact would give sediment transport theories a completely different structure from what it has been so far. Moreover, the entire concept could also be pursued with a mixture of class II with all of its consequences. Presently the most urgent activities would be validation of the model by parameter identification, development of software for its use and application to realistic cases, such as that shown in Figs. 1, 2, 13.

Appendix

A Implications from the Second Law of Thermodynamics

This appendix gives a justification for the approximation (44). The results which are presented can be taken from any book on thermodynamics, e.g. Hutter (2003) [16]. The basis of the considerations is the so-called GIBBS relation of a heat conducting fluid,

$$\mathrm{d}\eta = \frac{1}{T}\left(\mathrm{d}\epsilon - \frac{p}{\rho^2}\,\mathrm{d}\rho\right), \tag{203}$$

in which η is the entropy, T the KELVIN temperature, ϵ the internal energy, p the pressure and ρ the fluid density; (203) is a consequence of the second law of thermodynamics. Solving (203) for $\mathrm{d}\epsilon$,

$$\mathrm{d}\epsilon = T\mathrm{d}\eta + \frac{p}{\rho^2}\,\mathrm{d}\rho\,, \tag{204}$$

identifies ϵ as a function of η and ρ, so that, alternatively and with $\epsilon = \hat{\epsilon}(\eta,\rho)$,

$$\mathrm{d}\epsilon = \frac{\partial\,\hat{\epsilon}}{\partial\,\eta}\,\mathrm{d}\eta + \frac{\partial\,\hat{\epsilon}}{\partial\,\rho}\,\mathrm{d}\rho\,. \tag{205}$$

Comparison of (204) and (205) implies

$$T = \frac{\partial \hat{\epsilon}}{\partial \eta}\,, \quad p = \rho^2\, \frac{\partial \hat{\epsilon}}{\partial \rho}\,. \tag{206}$$

The internal energy, interpreted as a function of entropy η and density ρ, is a thermodynamic potential for the absolute temperature and the pressure.

With the functions

$$\begin{aligned} \psi &= \epsilon - T\eta \quad \text{HELMHOLTZ free energy,} \\ h &= \epsilon + \frac{p}{\rho} \quad \text{enthalpy,} \\ g &= h - T\eta \quad \text{GIBBS free energy,} \end{aligned} \tag{207}$$

(these are LEGENDRE transformations) the GIBBS relation (204) takes the alternative forms

$$\begin{aligned} \mathrm{d}\psi &= -\eta \mathrm{d}T + \frac{p}{\rho^2}\,\mathrm{d}\rho \quad \longrightarrow \quad \psi = \hat{\psi}(T,\rho)\,, \\ \mathrm{d}h &= -T\mathrm{d}\eta + \frac{1}{\rho}\,\mathrm{d}p \quad \longrightarrow \quad h = \hat{h}(\eta,p)\,, \\ \mathrm{d}g &= -\eta \mathrm{d}T + \frac{1}{\rho}\,\mathrm{d}p \quad \longrightarrow \quad g = \hat{g}(T,p)\,. \end{aligned} \tag{208}$$

With the indicated different dependencies and the obvious potential properties, analogous to (206), we have

$$\begin{aligned} \eta &= -\frac{\partial \hat{\psi}}{\partial T}\,, \quad p = \rho^2 \frac{\partial \hat{\psi}}{\partial \rho}\,, \\ T &= -\frac{\partial \hat{h}}{\partial \eta}\,, \quad \frac{1}{\rho} = \frac{\partial \hat{h}}{\partial p}\,, \\ \eta &= -\frac{\partial \hat{g}}{\partial T}\,, \quad \frac{1}{\rho} = \frac{\partial \hat{g}}{\partial p}\,, \end{aligned} \tag{209}$$

and the integrability conditions

$$\begin{aligned} -\frac{\partial \eta}{\partial \rho} &\equiv \frac{\partial}{\partial T}\left(\frac{p}{\rho^2}\right) \quad \text{for} \quad \hat{\psi}(T,\rho)\,, \\ -\frac{\partial T}{\partial p} &\equiv \frac{\partial}{\partial T}\left(\frac{1}{\rho}\right) \quad \text{for} \quad \hat{h}(T,p)\,, \\ -\frac{\partial \eta}{\partial p} &\equiv \frac{\partial}{\partial T}\left(\frac{1}{\rho}\right) \quad \text{for} \quad \hat{g}(T,p)\,. \end{aligned} \tag{210}$$

Internal energy formulation

If we regard T and ρ as the independent thermodynamic variables, then according to $(207)_1$ we have

$$\epsilon = \psi - T\frac{\partial \psi}{\partial T} = -T^2 \frac{\partial}{\partial T}\left(\frac{\psi}{T}\right)\,, \tag{211}$$

and therefore,

$$\begin{aligned} \rho\frac{\mathrm{d}\epsilon}{\mathrm{d}\,t} &= \rho\, c_v \frac{\mathrm{d}T}{\mathrm{d}\,t} + \rho\, c_{T\rho}\frac{\mathrm{d}\rho}{\mathrm{d}\,t}\,, \\ c_v &:= -\frac{\partial}{\partial T}\left(T^2 \frac{\partial}{\partial T}\left(\frac{\hat\psi}{T}\right)\right) = \frac{\partial\,\hat\epsilon}{\partial\,T}\,, \\ c_{T\rho} &:= -T^2\frac{\partial}{\partial T}\left(\frac{\partial\,\hat\psi/\partial\,\rho}{T}\right) = \frac{\partial\,\hat\epsilon}{\partial\,\rho}\,. \end{aligned} \tag{212}$$

With the separation assumption

$$\psi = \hat\psi_T(T) + \hat\psi_\rho(\rho)\,, \tag{213}$$

$c_v = \hat{c}_v(T)$ and $c_{T\rho} = \hat{c}_{T\rho}(\rho) = \mathrm{d}\hat\psi_\rho/\mathrm{d}\,\rho$. Therefore, $(212)_1$ can be written as

$$\rho\frac{\mathrm{d}\epsilon}{\mathrm{d}\,t} = \rho\,\hat{c_v}(T)\frac{\mathrm{d}\,T}{\mathrm{d}\,t} + \underbrace{\rho\frac{\mathrm{d}\hat\psi_\rho}{\mathrm{d}\,\rho}\frac{\mathrm{d}\,\rho}{\mathrm{d}\,t}}_{\text{nearly }0} \approx \rho\hat{c}_v(T)\frac{\mathrm{d}\,T}{\mathrm{d}\,t}\,. \tag{214}$$

The second term on the right-hand side of (214) can be ignored since density veriations in a nearly incompressible fluid are minute.

Enthalpy formulation If we regard T and p as the independent thermodynamic variables, the Gibbs free energy is the thermodynamic potential and the enthalpy the adequate internal energy function. In view of (208) we now have

$$h = g - T\frac{\partial\,g}{\partial\,T} = -T^2\frac{\partial}{\partial\,T}\left(\frac{g}{T}\right)\,, \tag{215}$$

and therefore,

$$\begin{aligned} \rho\frac{\mathrm{d}h}{\mathrm{d}\,t} &= \rho\, c_p \frac{\mathrm{d}T}{\mathrm{d}\,t} + \rho\, c_{Tp}\frac{\mathrm{d}p}{\mathrm{d}\,t}\,, \\ c_p &:= -\frac{\partial}{\partial T}\left(T^2 \frac{\partial}{\partial T}\left(\frac{\hat g}{T}\right)\right) = \frac{\partial\,\hat h}{\partial\,T}\,, \\ c_{Tp} &:= -T^2\frac{\partial}{\partial T}\left(\frac{1}{T}\frac{\partial\,g}{\partial\,p}\right) = \frac{\partial\,\hat h}{\partial\,p}\,. \end{aligned} \tag{216}$$

With the separation assumption

$$h = \hat g_T(T) + \hat g_p(p)\,, \tag{217}$$

$c_p = \hat{c}_p(T)$ and $c_{Tp} = \hat{c}_{Tp}(p) = \mathrm{d}\hat{g}_p/\mathrm{d}\,p$. Therefore, $(203)_1$ can be written as

$$\rho\frac{\mathrm{d}h}{\mathrm{d}\,t} = \rho\,\hat{c}_p(T)\frac{\mathrm{d}\,T}{\mathrm{d}\,t} + \underbrace{\rho\frac{\mathrm{d}\hat{g}_p}{\mathrm{d}\,p}\frac{\mathrm{d}\,p}{\mathrm{d}\,t}}_{\text{nearly }0} \approx \rho\hat{c}_p(T)\frac{\mathrm{d}T}{\mathrm{d}\,t}\,. \tag{218}$$

Here the second term on the right-hand side can be ignored, since $\mathrm{d}\hat{g}_p/\mathrm{d}p$ must be very small, the growth of the enthalpy due to a pressure rise cannot be large as its working is due to dilatational deformations, which are small.

Parameterizations Because the temperature range of lake or ocean water is small, $0°\mathrm{C} \leqslant T \leqslant 50°\mathrm{C}$, the coefficients c_v and c_p exhibit a constrained variability and may well be assumed to be constant or linear functions of T. This then suggests to use

- for constant specific heats,

$$\epsilon = \int_{T_0}^{T} c_v(\bar{T})\,\mathrm{d}\bar{T} = c_v^0(T - T_0) + \epsilon_0\,, \quad h = \int_{T_0}^{T} c_p(\bar{T})\,\mathrm{d}\bar{T} = c_p^0(T - T_0) + h_0\,, \tag{219}$$

- for specific heats as linear functions of T:

$$\begin{aligned} \epsilon &= \int_{T_0}^{T} [c_v^0 + c_v'(\bar{T} - T_0)]\,\mathrm{d}\bar{T} = c_v^0(T - T_0) + \frac{1}{2}c_v'(T - T_0)^2 + \epsilon_0\,, \\ h &= \int_{T_0}^{T} [c_p^0 + c_p'(\bar{T} - T_0)]\,\mathrm{d}\bar{T} = c_p^0(T - T_0) + \frac{1}{2}c_p'(T - T_0)^2 + h_0\,. \end{aligned} \tag{220}$$

The expressions (214), (218) (219), (220) provide a thermodynamic justification of relations (44).

B Turbulent closure by Large Eddy Simulation

Large Eddy Simulation (LES) is another popular approach for simulating turbulent flows. In this technique the large, geometry-dependent eddies are explicitly accounted for by using a subgrid-scale (SGS) model. Equations (76)–(80) are now interpreted as resolved field equations obtained by applying a non-statistical filter to the NAVIER-STOKES equations.[32]

The effect of the small eddies on the resolved filtered field is included in the SGS-parameterization of the stress $\boldsymbol{R}$, given by (52) but by

$$\boldsymbol{R} = 2\rho\nu_{SGS}\boldsymbol{D}, \quad \mathrm{tr}\,\boldsymbol{D} = 0\,, \tag{221}$$

where ν_{SGS} is the SGS-turbulent viscosity,

$$\nu_{SGS} \equiv (C_s\Delta)^2 \left(\mathrm{tr}\,(2\boldsymbol{D}^2)\right)^{1/2}\,. \tag{222}$$

[32]Such a filter need not to fulfil the condition $\langle\langle\cdot\rangle\rangle = \langle\cdot\rangle$, where $\langle\cdot\rangle$ is the filter operation.

This parameterization is due to SMAGORINSKY (1963) [41]. C_s is a dimensionless coefficient, called SMAGORINSKY constant, and Δ is a length scale, equal to the local grid spacing. Thus, (221) with (222) is the classical viscous power law relating stress and stretching. According to KRAFT et al. [23], the above 'model is found to give acceptable results in LES of homogeneous and isotropic turbulence. With $C_s \approx 0.17$ according to LILLY (1967) [25], it is too dissipative [...] in the near wall region because of the excessive eddy-viscosity arising from the mean shear (MOIN & KIM (1982) [29]). The eddy viscosity predicted by SMAGORINSKY is nonzero in laminar flow regions; the model introduces spurious dissipation which damps the growth of small perturbations and thus restrains the transition to turbulence (PIOMELLI & ZANG (1991) [33]).

The limitations of the SMAGORINSKY model have led to the formulation of more general SGS models. The best known of these newer models may be the dynamic SGS (DSGS) model of GERMANO et al. (1991) [12]. In this model C_s is not a fixed constant but is calculated as a function of position and time, $C_s(\mathbf{x}, t)$, which vanishes near the boundary with the correct behaviour (PIOMELLI (1993) [32], [23]).

The parameterisations for the energy flux, $\boldsymbol{Q}_\epsilon$ and constituent mass fluxes, $\boldsymbol{J}_\alpha$, are the same as stated in $(52)_{2,3}$, however, with ν_{SGS} evaluated as given in (222). It is also evident from this presentation that the $(k - \varepsilon)$ - equations are not needed.

C Justification for (150)

In this appendix we provide a derivation of formula (150) for erosion inception on the basis of dimensional analysis. We consider sediment transport at a lake basal surface. It is rather intuitive that the erosion inception will likely depend on a stress (the shear stress) on the lake side of the basal surface, τ_c, the true densities, ρ_s, ρ_f, of the sediment grains and the fluid, the solid concentration, c_s, gravity acceleration, g, mixture kinematic viscosity, ν, and the nominal diameter, $\mathfrak{d}$, of the sediment corn, all evaluated at the base. So, inception of sediment transport can likely be described by an equation of the form

$$f(\tau_c, \rho_s, \rho_f, g, \mathfrak{d}, \nu, c_s) = 0 \,. \tag{223}$$

The dimensional matrix of the above 7 variables has rank 3; so, there are 4 dimensionless π-products, which we choose as follows:

$$\pi_1 = \frac{\tau_c}{\Delta \rho \, g \, \mathfrak{d}} \,, \quad \pi_2 = \frac{\rho_s}{\rho_f} \,, \quad \pi_3 = c_s \,, \quad \pi_4 = \left(\frac{g}{\Delta \nu^2} \right)^{1/3} \mathfrak{d} \,, \tag{224}$$

where ρ is the mixture density and $\Delta \equiv (\rho_s/\rho - 1)$. Here, τ_c has been scaled with the 'submerged' density $(\rho_s - \rho)$. Furthermore, it is not difficult to see that for small c_s the mixture density in (224) may approximately be replaced by ρ_f. We may thus write

$$f(\pi_1, \pi_2, \pi_3, \pi_4) = 0 \quad \text{or} \quad \frac{\tau_c}{\Delta \, \rho \, g \mathfrak{d}} = \tilde{f}(\pi_2, \pi_3, \pi_4) \,. \tag{225}$$

The number of variables is now reduced from 7 to 4, a dramatic reduction. However, even further reduction is possible. For sediment transport in the geophysical environment

π_2 is very nearly a constant on the entire Globe, and π_3 is very small ($\leqslant 10^{-2}$); so, the π_3-dependence may be dropped (i.e. expressed in a Taylor series expansion of π_3 and restricted to the term $\tilde{f}(\pi_2, 0, \pi_4)$). Thus, we may assume

$$\theta_c \equiv \frac{\tau_c}{\Delta\,\rho\, g\mathfrak{d}} = \tilde{f}(Re_c^*) = \tilde{f}(\mathfrak{d}^*)\,, \quad \pi_4 = Re_c^* = \mathfrak{d}^* \equiv \left(\frac{g}{\Delta\,\nu^2}\right)^{1/3} \mathfrak{d}\,. \tag{226}$$

This derivation assumes that only a single sediment fraction is present. It is important to note that the viscosity ν of the mixture is present in the variables describing the erosion inception. If it is dropped, then $\tilde{f}$ in (226) reduces to a constant and

$$\tau_c = \text{const.} \times \Delta\,\rho\, g\mathfrak{d}^*\,,$$

which is not supported by experiments. Omitting g as a governing parameter is disastrous, because π_1 and π_4 are then missing as π-products. In this case $\tilde{f}(\pi_2, \pi_3) = 0$ is simply meaningless.

D Justification for (170), (171) and (175), (176)

Justification for (170)**,** (171): For the constituent masses, noting that

$$\rho_\alpha(\boldsymbol{v}_\alpha - \boldsymbol{w}) = \underbrace{\rho_\alpha(\boldsymbol{v}_\alpha - \boldsymbol{v})}_{\equiv \mathfrak{J}_\alpha,\ \text{see eq. (8)}} + \rho_\alpha(\boldsymbol{v} - \boldsymbol{w})\,,$$

the non-averaged balance (133), in which $f_{\mathbb{S}} = \mu_\alpha$, $\boldsymbol{\phi}^{f_{\mathbb{S}}} = \boldsymbol{0}$, $f = \rho_\alpha$, $\boldsymbol{v} = \boldsymbol{v}_\alpha$, $\boldsymbol{\phi}^f = \boldsymbol{0}$, can be written as

$$\frac{\partial \mu_\alpha}{\partial\, t} + (\mu_\alpha \boldsymbol{v}_{\mathbb{S}\alpha})^{\mathfrak{a}}{}_{;\mathfrak{a}} - \frac{\partial \mu_\alpha}{\partial \xi^{\mathfrak{a}}}\, w^{\mathfrak{a}} - 2\mu_\alpha\, \mathcal{U}_b K = -[\![\mathfrak{J}_\alpha + \rho_\alpha(\boldsymbol{v} - \boldsymbol{w})]\!] \cdot \boldsymbol{n}_b\,. \tag{227}$$

Analogously, for the fluid we deduce

$$\frac{\partial \mu_f}{\partial\, t} + \big(\mu_f \boldsymbol{v}_{\mathbb{S}f}\big)^{\mathfrak{a}}{}_{;\mathfrak{a}} - \frac{\partial \mu_f}{\partial \xi^{\mathfrak{a}}}\, w^{\mathfrak{a}} - 2\mu_f\, \mathcal{U}_b K = -[\![\mathfrak{J}_f + \tilde{\rho}_f(\boldsymbol{v} - \boldsymbol{w})]\!] \cdot \boldsymbol{n}_b\,, \tag{228}$$

where $\mathfrak{J}_f \equiv \tilde{\rho}_f(\boldsymbol{v}_f - \boldsymbol{v})$, with $\tilde{\rho}_f$ and $\boldsymbol{v}_f$ the mass density and velocity of the fluid ($\tilde{\rho}_f = \rho - \sum_\alpha \rho_\alpha$). Now we sum equations (227) and (228) over all constituents. Using relation

$$\sum_\alpha \mathfrak{J}_\alpha + \mathfrak{J}_f = \boldsymbol{0}\,, \tag{229}$$

and definitions

$$\mu \equiv \sum_\alpha \mu_\alpha + \mu_f\,, \quad \mu \boldsymbol{v}_{\mathbb{S}} \equiv \sum_\alpha \mu_\alpha \boldsymbol{v}_{\mathbb{S}\alpha} + \mu_f \boldsymbol{v}_{\mathbb{S}f} \tag{230}$$

for the mixture surface density μ and mixture velocity $\boldsymbol{v}_{\mathbb{S}}$, we obtain the mass balance for the mixture by summation of (227) and (228):

$$\frac{\partial \mu}{\partial\, t} + (\mu \boldsymbol{v}_{\mathbb{S}})^{\mathfrak{a}}{}_{;\mathfrak{a}} - \frac{\partial \mu}{\partial \xi^{\mathfrak{a}}}\, w^{\mathfrak{a}} - 2\mu\, \mathcal{U}_b K = -[\![\rho(\boldsymbol{v} - \boldsymbol{w})]\!] \cdot \boldsymbol{n}_b\,. \tag{231}$$

We now average equations (227) and (228). In so doing we assume that the interface does not perform any fluctuations, whence necessarily $\langle\, \boldsymbol{n}_b \,\rangle = \boldsymbol{n}_b$, $\langle\, K \,\rangle = K$, $\langle\, \boldsymbol{w} \,\rangle = \boldsymbol{w}$ and $\langle \mathcal{U}_b \rangle = \mathcal{U}_b$. Thus, for the averaged equations we get

$$
\begin{aligned}
&\frac{\partial \langle \mu_\alpha \rangle}{\partial t} + \left(\langle \mu_\alpha \rangle \langle\, \boldsymbol{v}_{\mathcal{S}\alpha} \,\rangle\right)^{\mathfrak{a}}{}_{;\mathfrak{a}} + \left(\langle\, \mu'_\alpha \, (\boldsymbol{v}_{\mathcal{S}\alpha})' \,\rangle\right)^{\mathfrak{a}}{}_{;\mathfrak{a}} - \frac{\partial \langle \mu_\alpha \rangle}{\partial \xi^{\mathfrak{a}}} \, w^{\mathfrak{a}} - 2 \langle \mu_\alpha \rangle \mathcal{U}_b K \\
&\qquad = -[\![\langle\, \mathfrak{J}_\alpha \rangle + \langle\, \rho'_\alpha \boldsymbol{v}' \,\rangle + \langle\, \rho_\alpha \,\rangle (\langle\, \boldsymbol{v} \,\rangle - \boldsymbol{w})]\!] \cdot \boldsymbol{n}_b \,,
\end{aligned} \tag{232}
$$

$$
\begin{aligned}
&\frac{\partial \langle \mu_f \rangle}{\partial t} + \left(\langle \mu_f \rangle \langle\, \boldsymbol{v}_{\mathcal{S}f} \,\rangle\right)^{\mathfrak{a}}{}_{;\mathfrak{a}} + \Big(\langle\, \mu'_f \, (\boldsymbol{v}_{\mathcal{S}f})' \,\rangle\Big)^{\mathfrak{a}}{}_{;\mathfrak{a}} - \frac{\partial \langle \mu_f \rangle}{\partial \xi^{\mathfrak{a}}} \, w^{\mathfrak{a}} - 2 \langle \mu_f \rangle \mathcal{U}_b K \\
&\qquad = -[\![\langle\, \mathfrak{J}_f \rangle + \langle\, \tilde{\rho}'_f \boldsymbol{v}' \,\rangle + \langle\, \tilde{\rho}_f \,\rangle (\langle\, \boldsymbol{v} \,\rangle - \boldsymbol{w})]\!] \cdot \boldsymbol{n}_b \,.
\end{aligned} \tag{233}
$$

If we sum (232) and (233), because of (229), (230) we obtain

$$
\begin{aligned}
&\frac{\partial \langle \mu \rangle}{\partial t} + \left(\langle \mu \rangle \langle\, \boldsymbol{v}_{\mathcal{S}} \,\rangle\right)^{\mathfrak{a}}{}_{;\mathfrak{a}} + \left(\langle\, \mu' \, (\boldsymbol{v}_{\mathcal{S}})' \,\rangle\right)^{\mathfrak{a}}{}_{;\mathfrak{a}} - \frac{\partial \langle \mu \rangle}{\partial \xi^{\mathfrak{a}}} \, w^{\mathfrak{a}} - 2 \langle \mu \rangle \mathcal{U}_b K \\
&\qquad = -[\![\underbrace{\langle\, \rho' \boldsymbol{v}' \,\rangle}_{\equiv\, \boldsymbol{\phi}^\rho \text{ in Table 6}} + \langle\, \rho \,\rangle (\langle\, \boldsymbol{v} \,\rangle - \boldsymbol{w})]\!] \cdot \boldsymbol{n}_b \,.
\end{aligned} \tag{234}
$$

Of course, (234) is the average of (231), and only two of (232)–(234) are independent. For computations of initial boundary value problems we recommend to use (232) and (234) and to infer $\langle \mu_f \rangle$ a posteriori from $\langle \mu_f \rangle = \langle \mu \rangle - \sum_\alpha \langle \mu_\alpha \rangle$.

It follows: with Reynolds averaging we have a non-vanishing mass flux in the mass balance (234). A Favre-type averaging would have to be performed. However, if ρ' is small on both sides of the basal surface we can drop $\langle\, \rho' \boldsymbol{v}' \,\rangle$ in (234). Moreover, with $\rho' \approx 0$, $\rho_\alpha = \rho c_\alpha$, decomposition (9) and definition of $\boldsymbol{J}_\alpha$ (see (43)), for the constituent class α the mass flux $\langle\, \mathfrak{J}_\alpha \rangle + \langle\, \rho'_\alpha \boldsymbol{v}' \,\rangle$ takes the form

$$
\langle\, \mathfrak{J}_\alpha \rangle + \langle\, \rho'_\alpha \boldsymbol{v}' \,\rangle = \boldsymbol{J}_\alpha - \rho \langle\, c_\alpha \rangle \langle \boldsymbol{w}^s_\alpha \rangle \,,
$$

which explains Table 6 for Model 2. The main text, formulae (170), (171) (as deduced from (232), (234)) and Table 6 show the averaged fields without the averaging operator $\langle \cdot \rangle$ and with negligible correlations

$$
\langle\, \mu'_\alpha \, (\boldsymbol{v}_{\mathcal{S}\alpha})' \,\rangle, \quad \langle\, \mu' \, (\boldsymbol{v}_{\mathcal{S}})' \,\rangle .
$$

Justification for (175) **and** (176): Now we consider (132), in which $f_{\mathcal{S}} = \mu_\alpha \boldsymbol{v}_{\mathcal{S}\alpha}$, $\boldsymbol{\phi}^{f_{\mathcal{S}}} = -\boldsymbol{\sigma}_{\mathcal{S}\alpha}$, $\pi^{f_{\mathcal{S}}} = 0$, $s^{f_{\mathcal{S}}} = \mu_\alpha \boldsymbol{g}$, $f = \rho_\alpha \boldsymbol{v}_\alpha$, $\boldsymbol{v} = \boldsymbol{v}_\alpha$, $\boldsymbol{\phi}^f = -\boldsymbol{\sigma}_\alpha$, for each $\alpha = 1, \dots, N$:

$$
\begin{aligned}
&\frac{\partial}{\partial t} (\mu_\alpha \boldsymbol{v}_{\mathcal{S}\alpha}) + \operatorname{Div} \left(\mu_\alpha \boldsymbol{v}_{\mathcal{S}\alpha} \otimes \boldsymbol{v}_{\mathcal{S}\alpha} - \boldsymbol{\sigma}_{\mathcal{S}\alpha}\right) - \frac{\partial}{\partial \xi^{\mathfrak{a}}} (\mu_\alpha \boldsymbol{v}_{\mathcal{S}\alpha}) \, w^{\mathfrak{a}} = \\
&\qquad -[\![\rho_\alpha \boldsymbol{v}_\alpha \otimes (\boldsymbol{v}_\alpha - \boldsymbol{w}) - \boldsymbol{\sigma}_\alpha]\!] \, \boldsymbol{n}_b + \mu_\alpha \boldsymbol{g} \,.
\end{aligned} \tag{235}
$$

A similar equation holds for the interstitial fluid:

$$\frac{\partial}{\partial t}\left(\mu_f \boldsymbol{v}_{\mathbb{S}f}\right) + \mathrm{Div}\left(\mu_f \boldsymbol{v}_{\mathbb{S}f} \otimes \boldsymbol{v}_{\mathbb{S}f} - \boldsymbol{\sigma}_{\mathbb{S}f}\right) - \frac{\partial}{\partial \xi^{\mathfrak{a}}}\left(\mu_f \boldsymbol{v}_{\mathbb{S}f}\right) w^{\mathfrak{a}} = \\ -[\![\tilde{\rho}_f \boldsymbol{v}_f \otimes (\boldsymbol{v}_f - \boldsymbol{w}) - \boldsymbol{\sigma}_f]\!]\, \boldsymbol{n}_b + \mu_f \boldsymbol{g}\,. \tag{236}$$

Summing (235), (236) and using definition (230) we obtain

$$\frac{\partial}{\partial t}\left(\mu \boldsymbol{v}_{\mathbb{S}}\right) + \mathrm{Div}\left(\mu \boldsymbol{v}_{\mathbb{S}} \otimes \boldsymbol{v}_{\mathbb{S}} - \boldsymbol{\sigma}_{\mathbb{S}}\right) - \frac{\partial}{\partial \xi^{\mathfrak{a}}}\left(\mu \boldsymbol{v}_{\mathbb{S}}\right) w^{\mathfrak{a}} = -[\![\rho \boldsymbol{v} \otimes (\boldsymbol{v} - \boldsymbol{w}) - \boldsymbol{\sigma}]\!]\, \boldsymbol{n}_b + \mu \boldsymbol{g}\,, \tag{237}$$

where the bulk, $\boldsymbol{\sigma}$, and surface, $\boldsymbol{\sigma}_{\mathbb{S}}$, mixture stress tensors are defined by

$$\rho \boldsymbol{v} \otimes \boldsymbol{v} - \boldsymbol{\sigma} \equiv \sum_{\alpha} \left(\rho_\alpha \boldsymbol{v}_\alpha \otimes \boldsymbol{v}_\alpha - \boldsymbol{\sigma}_\alpha\right) + \tilde{\rho}_f \boldsymbol{v}_f \otimes \boldsymbol{v}_{\mathbb{S}f} - \boldsymbol{\sigma}_f\,, \tag{238}$$

$$\mu \boldsymbol{v}_{\mathbb{S}} \otimes \boldsymbol{v}_{\mathbb{S}} - \boldsymbol{\sigma}_{\mathbb{S}} \equiv \sum_{\alpha} \left(\mu_\alpha \boldsymbol{v}_{\mathbb{S}\alpha} \otimes \boldsymbol{v}_{\mathbb{S}\alpha} - \boldsymbol{\sigma}_{\mathbb{S}\alpha}\right) + \mu_f \boldsymbol{v}_{\mathbb{S}f} \otimes \boldsymbol{v}_{\mathbb{S}f} - \boldsymbol{\sigma}_{\mathbb{S}f}\,. \tag{239}$$

Averaging (237) under the assumptions $\mu' \approx 0$, $\rho' \approx 0$, recalling definition $(43)_1$ of the Reynolds stress tensor $\boldsymbol{R}$ and introducing the laminar and turbulent surface mixture stress tensor $\boldsymbol{R}_{\mathbb{S}}$ according to

$$\boldsymbol{R}_{\mathbb{S}} \equiv \langle \boldsymbol{\sigma}_{\mathbb{S}} \rangle - \mu \langle \boldsymbol{v}'_{\mathbb{S}} \otimes \boldsymbol{v}'_{\mathbb{S}} \rangle\,, \tag{240}$$

we deduce (we omit the angular brackets)

$$\frac{\partial}{\partial t}\left(\mu \boldsymbol{v}_{\mathbb{S}}\right) + \mathrm{Div}\left(\mu \boldsymbol{v}_{\mathbb{S}} \otimes \boldsymbol{v}_{\mathbb{S}} - \boldsymbol{R}_{\mathbb{S}}\right) - \frac{\partial}{\partial \xi^{\mathfrak{a}}}\left(\mu \boldsymbol{v}_{\mathbb{S}}\right) w^{\mathfrak{a}} = \\ -[\![\rho \boldsymbol{v} \otimes (\boldsymbol{v} - \boldsymbol{w}) + p\boldsymbol{I} - \boldsymbol{R}]\!]\, \boldsymbol{n}_b + \mu \boldsymbol{g}\,, \tag{241}$$

which explains the last line in Table 6.

Next we want to write (241) using the components of vectors and tensors with respect to the local basis $\{\boldsymbol{\tau}_1, \boldsymbol{\tau}_2, \boldsymbol{n}_b\}$, which will give (175) and (176). To this end we use the formulae (for simplicity in this derivation we omit the lower index b in $\mathcal{U}_b$ and $\boldsymbol{n}_b$ referring to the basal surface)

$$\frac{\partial \boldsymbol{\tau}_{\mathfrak{a}}}{\partial \xi^{\mathfrak{b}}} = \Gamma^{\mathfrak{c}}_{\mathfrak{ab}} \boldsymbol{\tau}_{\mathfrak{c}} + b_{\mathfrak{ab}} \boldsymbol{n}\,, \quad \frac{\partial \boldsymbol{n}}{\partial \xi^{\mathfrak{a}}} = -b_{\mathfrak{ab}} \boldsymbol{\tau}^{\mathfrak{b}}\,, \quad \frac{\partial \boldsymbol{n}}{\partial t} = -g^{\mathfrak{ab}} \left\{\frac{\partial \mathcal{U}}{\partial \xi^{\mathfrak{a}}} + b_{\mathfrak{cb}} w^{\mathfrak{c}}\right\} \boldsymbol{\tau}_{\mathfrak{b}}\,, \\ \frac{\partial \boldsymbol{\tau}_{\mathfrak{a}}}{\partial t} = \frac{\partial \boldsymbol{w}}{\partial \xi^{\mathfrak{a}}} = \left\{\frac{\partial w^{\mathfrak{b}}}{\partial \xi^{\mathfrak{a}}} + w^{\mathfrak{c}} \Gamma^{\mathfrak{b}}_{\mathfrak{ca}} - \mathcal{U} b_{\mathfrak{ac}} g^{\mathfrak{cb}}\right\} \boldsymbol{\tau}_{\mathfrak{b}} + \left\{\frac{\partial \mathcal{U}}{\partial \xi^{\mathfrak{a}}} + w^{\mathfrak{b}} b_{\mathfrak{ba}}\right\} \boldsymbol{n}\,, \tag{242}$$

and for a scalar function f, vector fields $\boldsymbol{u}$, $\boldsymbol{v}$ and a second order tensor field $\boldsymbol{T}$ defined on the surface $\mathcal{S}$, the rules of differentiation[33]

$$\mathrm{Div}\,(f\boldsymbol{v}) = f\mathrm{Div}\,\boldsymbol{v} + \mathrm{Grad}\,f\cdot\boldsymbol{v}\,,\quad \mathrm{Div}\,(f\boldsymbol{T}) = f\mathrm{Div}\,\boldsymbol{T} + \boldsymbol{T}\mathrm{Grad}\,f\,,$$
$$\mathrm{Div}\,(\boldsymbol{u}\otimes\boldsymbol{v}) = v^{\mathfrak{a}}\frac{\partial\boldsymbol{u}}{\partial\xi^{\mathfrak{a}}} + (\mathrm{Div}\,\boldsymbol{v})\,\boldsymbol{u}\,,\quad \mathrm{Div}\,\boldsymbol{n} = -2K\,,\quad \mathrm{Div}\,(\boldsymbol{n}\otimes\boldsymbol{n}) = -2K\boldsymbol{n}\,, \tag{243}$$
$$\mathrm{Div}\,(\boldsymbol{n}\otimes\boldsymbol{\tau}_{\mathfrak{a}}) = -b_{\mathfrak{ab}}\boldsymbol{\tau}^{\mathfrak{b}} + \Gamma^{\mathfrak{b}}_{\mathfrak{ab}}\boldsymbol{n}\,,\quad \mathrm{Div}\,(\boldsymbol{\tau}_{\mathfrak{a}}\otimes\boldsymbol{n}) = -2K\boldsymbol{\tau}_{\mathfrak{a}}\,,$$

where

$$\mathrm{Grad}\,f \equiv \frac{\partial f}{\partial\xi^{\mathfrak{a}}}\boldsymbol{\tau}^{\mathfrak{a}}\,,\quad \mathrm{Div}\,\boldsymbol{v} \equiv \frac{\partial\boldsymbol{v}}{\partial\xi^{\mathfrak{a}}}\cdot\boldsymbol{\tau}^{\mathfrak{a}}\,,\quad \mathrm{Div}\,\boldsymbol{T} \equiv \frac{\partial\boldsymbol{T}}{\partial\xi^{\mathfrak{a}}}\boldsymbol{\tau}^{\mathfrak{a}}\,.$$

Thus, using the decomposition

$$\boldsymbol{v}_{\mathcal{S}} = \boldsymbol{v}_{\mathcal{S}\|} + \mathcal{U}\boldsymbol{n} = v^{\mathfrak{a}}\boldsymbol{\tau}_{\mathfrak{a}} + \mathcal{U}\boldsymbol{n}\,,$$

we obtain

$$\begin{aligned}\frac{\partial}{\partial t}(\mu\boldsymbol{v}_{\mathcal{S}}) = \frac{\partial\mu v^{\mathfrak{a}}}{\partial t}\boldsymbol{\tau}_{\mathfrak{a}} + \mu v^{\mathfrak{b}}\left\{\frac{\partial w^{\mathfrak{a}}}{\partial\xi^{\mathfrak{b}}} + w^{\mathfrak{c}}\Gamma^{\mathfrak{a}}_{\mathfrak{cb}} - \mathcal{U}b_{\mathfrak{bc}}g^{\mathfrak{ca}}\right\}\boldsymbol{\tau}_{\mathfrak{a}} - \\ \mu\mathcal{U}g^{\mathfrak{ab}}\left\{\frac{\partial\mathcal{U}}{\partial\xi^{\mathfrak{b}}} + b_{\mathfrak{bc}}w^{\mathfrak{c}}\right\}\boldsymbol{\tau}_{\mathfrak{a}} + \left\{\frac{\partial\mu\,\mathcal{U}}{\partial t} + \mu v^{\mathfrak{a}}\frac{\partial\mathcal{U}}{\partial\xi^{\mathfrak{a}}} + \mu b_{\mathfrak{ba}}v^{\mathfrak{a}}w^{\mathfrak{b}}\right\}\boldsymbol{n}\,.\end{aligned} \tag{244}$$

Then,

$$\begin{aligned}&\mathrm{Div}\,(\mu\boldsymbol{v}_{\mathcal{S}}\otimes\boldsymbol{v}_{\mathcal{S}}) = \\ &\mathrm{Div}\,(\mu\boldsymbol{v}_{\mathcal{S}\|}\otimes\boldsymbol{v}_{\mathcal{S}\|}) + \mathrm{Div}\,(\mu\mathcal{U}\boldsymbol{v}_{\mathcal{S}\|}\otimes\boldsymbol{n}) + \mathrm{Div}\,(\mu\mathcal{U}\boldsymbol{n}\otimes\boldsymbol{v}_{\mathcal{S}\|}) + \mathrm{Div}\,(\mu\mathcal{U}^2\boldsymbol{n}\otimes\boldsymbol{n}) = \\ &\mathrm{Div}\,(\mu\boldsymbol{v}_{\mathcal{S}\|}\otimes\boldsymbol{v}_{\mathcal{S}\|}) - \mu\mathcal{U}\,v^{\mathfrak{b}}\,b_{\mathfrak{bc}}\,g^{\mathfrak{ca}}\,\boldsymbol{\tau}_{\mathfrak{a}} + \mathrm{Div}\,(\mu\mathcal{U}\boldsymbol{v}_{\mathcal{S}\|})\,\boldsymbol{n} - 2\mu K\mathcal{U}\boldsymbol{v}_{\mathcal{S}}\,,\end{aligned} \tag{245}$$

and with the notations (174) for the components of $\boldsymbol{R}_{\mathcal{S}}$,

$$\mathrm{Div}\boldsymbol{R}_{\mathcal{S}} = \mathrm{Div}\,(S^{\mathfrak{ab}}\boldsymbol{\tau}_{\mathfrak{a}}\otimes\boldsymbol{\tau}_{\mathfrak{b}}) - \left\{S^{\mathfrak{c}}b_{\mathfrak{cb}}g^{\mathfrak{ba}} + 2KS^{\mathfrak{a}}\right\}\boldsymbol{\tau}_{\mathfrak{a}} + \{\mathrm{Div}\,(S^{\mathfrak{a}}\boldsymbol{\tau}_{\mathfrak{a}}) - 2SK\}\,\boldsymbol{n}\,. \tag{246}$$

Finally, we have

$$\frac{\partial}{\partial\xi^{\mathfrak{b}}}(\mu\boldsymbol{v}_{\mathcal{S}})\,w^{\mathfrak{b}} = w^{\mathfrak{b}}\left\{\frac{\partial\mu v^{\mathfrak{a}}}{\partial\xi^{\mathfrak{b}}} + \mu v^{\mathfrak{c}}\,\Gamma^{\mathfrak{a}}_{\mathfrak{cb}} - \mu\mathcal{U}\,b_{\mathfrak{bc}}g^{\mathfrak{ca}}\right\}\boldsymbol{\tau}_{\mathfrak{a}} + w^{\mathfrak{b}}\left\{\mu v^{\mathfrak{c}}\,b_{\mathfrak{cb}} + \frac{\partial\mu\mathcal{U}}{\partial\xi^{\mathfrak{b}}}\right\}\boldsymbol{n}\,. \tag{247}$$

Now, substituting (244)–(247) into (241) and separating the tangential and normal parts of the emerging relation yields (175) and (176).

[33] (243) can be easily deduced with the aid of (242).

E List of symbols

Roman Symbols

a	Parameter in the representation (202) of the volume fraction ν
A	Parameter arising in formula (61) for the particle drag coefficient $\mathcal{C}_{\mathfrak{d}_\alpha}$
$\boldsymbol{A}$	Unspecified symmetric second rank tensor
$\mathcal{A}_L$	$\equiv [H]/[L]$ Aspect ratio for lengths
$\mathcal{A}_V$	$\equiv [W]/[V]$ Aspect ratio for velocities
$\mathcal{A}$	$\equiv \mathcal{A}_L = \mathcal{A}_V$ Aspect ratio for lengths and velocities
b	Parameter in the representation (202) of the volume fraction ν
$b(x, y, t)$	z-coordinate of the basal surface: $z = b(x, y, t)$
$b_{\mathfrak{ab}}$	Coefficients of the second fundamental form of a surface
B	Parameter arising in formula (61) for the particle drag coefficient $\mathcal{C}_{\mathfrak{d}_\alpha}$
$\mathcal{B}^{\pm}$	Material body parts on the $\pm$ sides of a singular surface
$\mathcal{B}$	$\equiv g[\sigma][H]/[f][L][V] \approx 10^{-2} - 10^{2}$ Buoyancy parameter; material body
c	Function arising in the formula for the unit normal, $\boldsymbol{n}_b$, at the basal surface
c_α	Mass concentration (fraction) of sediment class α
$[c_\alpha]$	$\approx 10^{-3} - 10^{-1}$ Scale for mass concentration of sediment class α
c_k	Coefficient in the zeroth order parameterization of the turbulent kinetic energy k
c_v, c_p	Specific heats at constant volume and constant pressure, respectively
c_v^0, c_p^0	Constant specific heats
c_v', c_p'	Parameters in the linear representations (220) for specific heats
c_{T_ρ}	Specific heat at constant temperature in the energy formulation
c_{T_p}	Specific heat at constant temperature in the enthalpy formulation
$[c_v]$, $[c_p]$	$\approx 4200\ \mathrm{m^2\,s^{-2}\,K^{-1}}$ Typical values of the specific heats c_v and c_p
$\begin{cases} c_1, c_2, c_3 \\ c_k, c_\mu, c_\varepsilon \end{cases}$	'Universal' coefficients in the zeroth and first order parameterizations for $k - \varepsilon$
C_s	Smagorinsky coefficient

$\mathfrak{C}$	Closed double point free curve bounding a surface
$\mathcal{C}_1$, $\mathcal{C}_2$	Drag coefficients of basal sliding laws (183), (184)
C_d^{wind}	$\approx 2 \times 10^{-3}$ Wind drag coefficient
$\mathcal{C}_{\mathfrak{d}_\alpha}$	Drag coefficient for sediment class α with the mean diameter $\mathfrak{d}_\alpha$
$[d_{\min}, d_{\max})$	Range of particle diameters of sediment classes α, $\alpha = 1, \dots, N$
$[d_{\alpha-1}, d_\alpha)$	Range of nominal particle diameters of sediment class α
$\mathfrak{d}$, $\mathfrak{d}_\alpha$	Nominal mean diameter of sediment grains and in class α:
	$\mathfrak{d}$, $\mathfrak{d}_\alpha \in [d_{\alpha-1}, d_\alpha)$
$\mathfrak{d}^*$, $\mathfrak{d}_\alpha^*$	$\equiv (\Delta\, g/\nu^2)^{1/3}\, \mathfrak{d}(\mathfrak{d}_\alpha)$ Dimensionless mean particle diameter of class α
D_α	Surface mass diffusivities
$D^{(T)}$	$\equiv \chi_\ell^{(T)} + \dfrac{\nu_t}{\sigma_T}$ Laminar + turbulent thermal mass flux diffusivity
$D^{(c_\alpha)}$	$\equiv \chi_\ell^{(c_\alpha)} + \dfrac{\nu_t}{\sigma_{c_\alpha}}$ Laminar + turbulent species mass flux diffusivity
$\mathfrak{D}^{(T)}$	$\equiv D^{(T)}/[f][H^2] \approx 10^{-4} - 10^0$ Dimensionless thermal diffusivity
$\mathfrak{D}^{(c_\alpha)}$	$\equiv D^{(c_\alpha)}/[f][H^2] \approx 10^{-4} - 10^0$ Dimensionless species mass diffusivity
$\boldsymbol{D}$	Rate of strain-rate (strain rate, stretching) tensor of the mixture
$\boldsymbol{D}_{\mathcal{S}}$	Surface rate of strain-rate tensor of the detritus surface mixture
$\boldsymbol{e}_1, \boldsymbol{e}_2, \boldsymbol{e}_3$	Unit vectors in the x, y, z-directions
$\boldsymbol{e}_z$	$\equiv \boldsymbol{e}_3$ Unit vector in the z-direction
E	Relative error for settling velocities of different authors
E, E_α	Erosion (entrainment) rate of sediments α from the base
f	$\equiv 2\Omega \sin\varphi$ First CORIOLIS parameter;
	specific density of an unspecified physical bulk quantity
$\tilde{f}$	$\equiv 2\Omega \cos\varphi$ Second CORIOLIS parameter
$f_{\mathcal{S}}$	Specific density of an unspecified physical surface quantity
F	Function identifying a singular surface by $F(\boldsymbol{x}, t) = 0$
$\mathfrak{F}$	$\equiv [V^2]/[c_v][\Delta T] \approx 10^{-7} - 10^{-1}$ Pressure work parameter
$[f]$	$\approx 10^{-4}\,\text{s}^{-1}$ CORIOLIS parameter

$1/[f]$	Time scale
g	Gravity constant; GIBBS free energy ($\equiv h - T\eta$)
$\boldsymbol{g}$	Gravity vector
$g_{\mathfrak{ab}}$	Coefficients of the first fundamental form of a surface
$g^{\mathfrak{ab}}$	Components of the inverse matrix of $(g_{\mathfrak{ab}})$
$\mathcal{G}$	$\equiv g[H]/[f^2][L^2] \approx 10^0 - 10^3$ Squared velocity ratio
h	Specific enthalpy ($\equiv \epsilon + p/\rho$); thickness of the detritus layer
h_0	Reference specific enthalpy
$\boldsymbol{h}$	Unit vector tangent to a surface $\mathcal{S}$ and normal to the closed curve $\mathcal{C}$ bounding $\mathcal{S}$
$\mathcal{H}$	Heaviside function
$[H]$	$\approx 10^1 - 10^3\,\mathrm{m}$ Vertical length scale
$\boldsymbol{j}_\alpha$	$\equiv \rho c_\alpha(\boldsymbol{v}_\alpha - \boldsymbol{v}^s_\alpha)$
	Diffusive flux of sediment class α vs. a representative particle in the class α
$\boldsymbol{\mathfrak{J}}_\alpha$	$\equiv \rho c_\alpha(\boldsymbol{v}_\alpha - \boldsymbol{v})$
	Diffusive flux of sediment class α with respect to the barycentric motion
$\boldsymbol{\mathfrak{J}}_f$	$\equiv \tilde{\rho}_f(\boldsymbol{v}_f - \boldsymbol{v})$
	Diffusive flux of the bearer fluid with respect to the barycentric motion
$\boldsymbol{J}_\alpha$	Laminar + turbulent specific species mass flux of sediment class α:
	$\equiv \langle \boldsymbol{j}_\alpha \rangle + \rho_0 \langle c'_\alpha \boldsymbol{v}' \rangle - \rho_0 \langle c'_\alpha \boldsymbol{w}^{s'}_\alpha \rangle$ in BOUSSINESQ model,
	$\equiv \langle \boldsymbol{j}_\alpha \rangle + \rho \langle c'_\alpha \boldsymbol{v}' \rangle - \rho \langle c'_\alpha \boldsymbol{w}^{s'}_\alpha \rangle$ in Model 2
k	Specific turbulent kinetic energy
K	$\equiv \frac{1}{2} g^{\mathfrak{ab}} b_{\mathfrak{ab}}$ Mean curvature of a surface
$\boldsymbol{L}$	$\equiv \operatorname{grad} \boldsymbol{v}$ Spatial velocity gradient
$\boldsymbol{L}^T$	Transpose of $\boldsymbol{L}$
$[L]$	$\approx 10^4 - 10^6\,\mathrm{m}$ Horizontal length scale
$\mathcal{M}, \mathcal{M}^\pm$	Mass flow through a singular surface (in (126))
$\mathcal{M}_b^{\mathrm{eros/dep}}$	Erosion and deposition mass flow through the basal surface
$\mathcal{M}_b, \mathcal{M}_b^{\alpha/f}$	Mass flow through the basal surface (in (191))

n	Average porosity within the detritus layer
$\boldsymbol{n}$	Unit normal vector to a surface
$\boldsymbol{n}_b$	The unit normal vector to the basal surface pointing into the flowing material
$\boldsymbol{n}_s$	The unit normal vector to the free surface pointing into atmosphere
N	Number of constituents α
N^*	Limit index for α determining $\mathfrak{d}_{N*}$ such that α classes for which $\mathfrak{d}_\alpha^* < \mathfrak{d}_{N*}$ are erosive sediment classes
$\mathcal{N}$	$\equiv \nu_t/[f][H^2] \approx 10^{-6} - 10^1$ Dimensionless kinematic turbulent viscosity
p	Mixture pressure
p^{atm}	Atmospheric pressure
p_d	Dynamic mixture pressure (see (22))
p_{st}	(Quasi)-static pressure (see (22))
P, P_α	Fraction of time during which a sediment particle is suspended by the flow; P - surface pressure function (in (181), (182))
$\mathcal{P}_x$, $\mathcal{P}_y$, $\mathcal{P}_z$	Cartesian components of the average pressure work $\boldsymbol{\mathcal{P}}$
$\mathcal{P}_\epsilon^{(T)}$	$\equiv [\phi^{(T)}]/\rho^*[f][c_v][\Delta T]$ Power working parameter
$\mathcal{P}_h^{(T)}$	$\equiv [\phi^{(T)}]/\rho^*[f][c_p][\Delta T]$ Power working parameter
$\mathcal{P}^{(c_\alpha)}$	$\equiv [\phi^{(c_\alpha)}]/\rho^*[f][c_\alpha]$ Dimensionless constituent mass production parameter
$\boldsymbol{\mathcal{P}}$	$\equiv \langle p' \boldsymbol{v}' \rangle$ Pressure velocity correlation
$\mathcal{P}_x$, $\mathcal{P}_y$, $\mathcal{P}_z$	Cartesian components of the pressure velocity correlation $\boldsymbol{\mathcal{P}}$
$\boldsymbol{q}$	Heat flux vector
$Q_{x,y,z}^{\epsilon,h}$	Cartesian components of the heat flux vectors $\boldsymbol{Q}_\epsilon$, $\boldsymbol{Q}_h$
$Q_\perp^{\text{atm}}$	$\equiv \boldsymbol{Q}_\perp^{\text{atm}} \cdot \boldsymbol{n}_s$ Atmospheric heat flux through the water surface
Q_{ir}^{atm}	Radiative atmospheric heat flow at the water surface
Q_{ir}^{water}	Radiative water heat flow at the water surface
Q_ℓ	Latent heat flow between water and air
Q_s	Sensible heat flow between water and air
$Q_\perp$	Geothermal heat from the rigid bed

$\boldsymbol{Q}_\epsilon$	Laminar +turbulent heat flux:
	$\equiv \langle \boldsymbol{q} \rangle + \rho_0 \langle \epsilon' \boldsymbol{v}' \rangle$ in generalized BOUSSINESQ model,
	$\equiv \langle \boldsymbol{q} \rangle + \rho \langle \epsilon' \boldsymbol{v}' \rangle$ in Model 2
$\boldsymbol{Q}_h$	Laminar +turbulent heat flux:
	$\equiv \langle \boldsymbol{q} \rangle + \rho_0 \langle h' \boldsymbol{v}' \rangle$ in generalized BOUSSINESQ model,
	$\equiv \langle \boldsymbol{q} \rangle + \rho \langle h' \boldsymbol{v}' \rangle$ in Model 2
$\boldsymbol{Q}_\perp^{\mathrm{atm}}$	Atmospheric heat flux vector through the water surface
$\boldsymbol{r}$	Position vector of a point on a surface
Re	$\equiv (w_\alpha^s \mathfrak{d}_\alpha)/\nu$ Particle REYNOLDS number of sediment class α
Re_c^*	$\equiv (u^* \mathfrak{d})/\nu$ Critical particle REYNOLDS number
Ri	RICHARDSON number
Ri^{crit}	Critical RICHARDSON number
$\mathcal{R}o$	$\equiv [V]/[f][L] \approx 10^{-4} - 10^0$ ROSSBY number
$R_{xx}, \ldots$	Components of $\boldsymbol{R}$ with respect to a Cartesian coordinate system
$\boldsymbol{R}$	Laminar + turbulent mixture stress tensor:
	$\equiv \langle \boldsymbol{\sigma}_E \rangle - \rho_0 \langle \boldsymbol{v}' \otimes \boldsymbol{v}' \rangle$ in generalized BOUSSINESQ model,
	$\equiv \langle \boldsymbol{\sigma}_E \rangle - \rho \langle \boldsymbol{v}' \otimes \boldsymbol{v}' \rangle$ in Model 2
$\boldsymbol{R}_{\mathcal{S}}$	$\equiv \langle \boldsymbol{\sigma}_{\mathcal{S}} \rangle - \mu \langle \boldsymbol{v}'_{\mathcal{S}} \otimes \boldsymbol{v}'_{\mathcal{S}} \rangle$ Laminar + turbulent surface mixture stress tensor
s	Constant salinity; parameter in the representation (202) of ν_{mean}
$s(x,y,t)$	z-coordinate of the free surface: $z = s(x,y,t)$
s^f	Supply rate density of the physical bulk quantity f
$s^{f_{\mathcal{S}}}$	Supply rate density of the physical surface quantity $f_{\mathcal{S}}$
$\mathcal{S}$	Surface
$\mathcal{S}_b$	Basal surface
$\mathcal{S}_s$	Free surface
t	Time
T	Temperature measured in KELVIN or Celsius scales
T_0	Reference temperature in energy/enthalpy constitutive relation (44)

T^* = 4°C Reference temperature in the law (46) of the water density ρ_w

$\tilde{T}$, $\tilde{T}_\alpha$ Function of shear velocities (in (158), (165))

u Mixture velocity component in the x-direction

u^* $\equiv (g\nu/\Delta)^{1/3}$ Critical shear velocity

$u_{\max}$ Maximum value of the velocity u within the detritus layer in the linear representation (199)

u_{τ_c} $\equiv \sqrt{\tau_c/\rho}$ Critical wall shear velocity

u_{τ_w} $\equiv \sqrt{\tau_w/\rho}$ Actual wall shear velocity

$\mathcal{U}$ $= \boldsymbol{w}\cdot\boldsymbol{n}$ Displacement speed of an unspecified singular surface

$\mathcal{U}_b$ Displacement speed of the basal surface

v Mixture velocity component in the y-direction

$\boldsymbol{v}$ Barycentric velocity vector

$\boldsymbol{v}_\alpha$ Velocity vector of sediment class α

$\boldsymbol{v}_f$ Fluid velocity

$\boldsymbol{v}^s_\alpha$ Velocity vector of a representative particle in sediment class α

$\boldsymbol{v}_H$ Horizontal component of the barycentric velocity at the basal surface $\mathcal{S}_b$

$\boldsymbol{v}^{\text{wind}}$ Wind velocity at the water surface

$\boldsymbol{v}^{\text{wind}}_H$ Horizontal component of the wind velocity at the water surface

$\boldsymbol{v}^{\mathcal{S}}$ Velocity of a material point moving on a surface

$\boldsymbol{v}^{\mathcal{S}}_\parallel$ Component of $\boldsymbol{v}^{\mathcal{S}}$ tangent to the surface

$\boldsymbol{v}^{\mathcal{S}}_\alpha$ Velocity of a sediment material point in class α which moves on the basal surface

$(\boldsymbol{v}^{\mathcal{S}}_\alpha)_\parallel$ Component of $\boldsymbol{v}^{\mathcal{S}}_\alpha$ tangent to the basal surface

$[V]$ $\approx 10^{-2} - 10^{1}\ \mathrm{m\,s^{-1}}$ Horizontal velocity scale

w Mixture velocity component in the z-direction

w^s_α Terminal fall velocity of a particle of sediment class α

w^1, w^2 Components of the surface velocity $\boldsymbol{w}$ with respect to $\boldsymbol{\tau}_1$, $\boldsymbol{\tau}_2$

$\boldsymbol{w}$ Surface velocity of a moving surface

$\boldsymbol{w}^s_\alpha$ $\equiv -(\boldsymbol{v}^s_\alpha - \boldsymbol{v})$ Negative of the relative velocity of a representative particle in sediment class α vs. the barycentric motion

$[W]$	Vertical velocity scale
x	x-coordinate of a Cartesian coordinate system
$\boldsymbol{x}$	Position vector in R^3
$\boldsymbol{X}$	Position vector of a surface material point in a reference configuration
y	y-coordinate of a Cartesian coordinate system
z	z-coordinate of a Cartesian coordinate system

Greek Symbols

α	Counting index for the sediment classes
$\tilde{\alpha}$	$= 6.493 \times 10^6\,\mathrm{K}^{-2}$ Thermal expansion coefficient of water
β	Parameter arising in the formula for w^s_α in equation (70)
$\lambda(\mu, k)$	Exponent coefficient in formula for Λ
$\Gamma^{\mathfrak{c}}_{\mathfrak{ab}}$	CHRISTOFFEL symbols
Δ	Ratio of submerged sediment density to water density ($\equiv \rho_s/\rho - 1$); local grid spacing scale in SMAGORINSKI viscosity (222)
$[\Delta T]$	$\approx 10^\circ$ C Temperature scale
ϵ	Specific internal energy
ϵ_0	Reference specific internal energy
ε	Turbulent specific energy dissipation ($\equiv 4\nu_\ell \langle II_{\boldsymbol{D}'}\rangle$); parameter in the representation (202) of the volume fraction ν
ε_0	Parameter in the boundary layer representation of ε
η	Specific entropy
θ	A tilt angle (see (11))
θ_c	Critical SHIELDS parameter (also called τ^*_c)
θ'_w	Root mean square turbulent fluctuation of wall shear stress
$\Theta(z,t)$	Temperature profile at the deepest position of the lake domain
κ	Thermal conductivity
$\lambda_{\alpha\beta}$	$(N \times N)$-matrix for species mass flux α due to sediment class β

μ	Dynamic viscosity of the bearer fluid;
	surface mass density of the mixture moving on the basal surface
μ_α	Surface mass density of sediments in class α moving on the basal surface
μ_f	Surface fluid mass density
$\mu_0,\ \mu_1$	Constant coefficients in (182)
ν	Kinematic viscosity of the bearer fluid $\equiv \mu/\rho$;
	volume fraction within the detritus layer
ν_{mean}	$\equiv \sum_\alpha \nu^\alpha_{\text{mean}}$ Mean averaged sediment volume fraction in the detritus layer
ν^α_{mean}	Mean averaged volume fraction of the sediments α in the detritus layer
$\nu_{\text{top/bottom}}$	Parameters in the representation (202) of the volume fraction ν
$\nu_{\text{min/max}}$	Minimum and maximum values of the volume fraction ν in the linear
	representation (199)
ν_{crit}	Critical sediments volume fraction in the detritus layer
ν_ℓ, ν_t	Laminar, turbulent kinematic viscosities of the mixture
ν_{SGS}	Smagorinski turbulent viscosity
$\xi^1,\ \xi^2$	Parameters on a surface
π^f	Specific production rate density of a physical bulk quantity f
$\pi^{f_\mathbb{S}}$	Specific production rate density of a physical surface quantity $f_\mathbb{S}$
π^k	Specific production rate density of turbulent kinetic energy
π^ε	Specific production rate density of turbulent dissipation
Π	$\equiv [f][L][V]/[c_p][\Delta T] \approx 10^{-7} - 10^{-2}$ Pressure work parameter
ρ_α	Mass density of constituent α
$\tilde{\rho}_f$	$\equiv n\rho_f$ Mass density of the interstitial fluid (porosity $\times$ true density)
ρ	$\equiv \sum_\alpha \rho_\alpha + \tilde{\rho}_f$ Mixture density
ρ_s	$\approx 2100\,\text{kg}\,\text{m}^{-3}$ Buoyancy corrected density of the suspended sediment
ρ_f	True mass density of the interstitial fluid
ρ^*	$= 1000\,\text{kg}\,\text{m}^{-3}$ Reference density of water at 4° C
ρ^{bed}	Mass density in the rigid bed immediately below the basal surface

ρ_α^{bed}	Mass density of particles in class α in the rigid bed immediately below the basal surface
ρ_f^{bed}	Mass density of fluid in the rigid bed immediately below the basal surface
$\rho_0(z)$	Steady density function describing vertical ground stratification
$\rho_d(\boldsymbol{x},t)$	$\equiv \rho - \rho_0(z)$ The excess of mixture density over the steady density $\rho_0(z)$
$\rho_w(T,s)$	Natural water density as function of temperature and salinity
σ	Standard deviation; dimensionless mixture density
$[\sigma]$	$\approx 10^{-3}$ Scale for density variations of water; density anomaly
σ_T	PRANDTL number of heat
σ_{c_α}	SCHMIDT number of species α
σ_k	PRANDTL number of turbulent kinetic energy
σ_ε	PRANDTL number of turbulent dissipation rate
$\boldsymbol{\sigma}$	(CAUCHY) stress tensor
$\boldsymbol{\sigma}_E$	Extra (CAUCHY) stress tensor of the mixture ((CAUCHY) stress deviator)
$\boldsymbol{\sigma}^{\text{atm}}$	(CAUCHY) stress tensor at the water surface
$\boldsymbol{\tau}_1$, $\boldsymbol{\tau}_2$	Tangent vectors to a surface
τ_c	Critical shear traction
τ_c^*, $(\tau_c^*)_\alpha$	$\equiv \tau_c/\Delta\rho\, g\, \mathfrak{d}\, (\mathfrak{d}_\alpha)$ Critical shear traction (dimensionless)
τ_w	Shear stress on the basal surface
$\boldsymbol{\tau}^{\text{wind}}$	Wind shear traction at the water surface
$\boldsymbol{\tau}_H^{\text{wind}}$	$= (\tau_{xz}^{\text{wind}}, \tau_{yz}^{\text{wind}})$ Horizontal shear traction components
φ	Latitude angle; angle of internal friction (water submerged)
ϕ_p	VAN RIJN's erosion rate per unit mass, area and time
$\phi^{(T)}$	Laminar + turbulent internal energy/enthalpy production rate density $\equiv \text{tr}\,\langle\boldsymbol{\sigma}_E\rangle\langle\boldsymbol{D}\rangle + \text{tr}\,\langle\boldsymbol{\sigma}_E'\boldsymbol{D}'\rangle - \langle p'\text{div}\,\boldsymbol{v}'\rangle$
$\phi^{(c_\alpha)}$	Production mass density of sediment class α
$[\phi^{(T)}]$	Scale for energy/enthalpy production density rate
$[\phi^{(c_\alpha)}]$	Scale for production of mass density of tracer α

$\boldsymbol{\phi}^{f}$	Flux density of a physical bulk quantity f
$\boldsymbol{\phi}^{f_{\mathbb{S}}}$	Flux density of a physical surface quantity $f_{\mathbb{S}}$
$\boldsymbol{\phi}^{k}$	Flux of turbulent specific kinetic energy k
$\boldsymbol{\phi}^{\varepsilon}$	Flux of turbulent specific energy dissipation ε
$\chi_{\ell}^{(T)}, \chi_{\ell}^{(c_\alpha)}$	Laminar kinematic heat/species mass diffusivities
$\boldsymbol{\chi}$	Function describing the motion of a material point on a surface
ψ	$\equiv \epsilon - T\eta$ HELMHOLTZ free energy
$\psi^{\mathfrak{a}}{}_{;\,\mathfrak{b}}$	Covariant derivative of the surface vector field $\boldsymbol{\psi}$
ψ_E	Parameter in EINSTEIN's erosion rate formula
ψ_Y	Parameter in YALIN's erosion rate formula
ψ_Z	Parameter in ZANKE's critical shear stress
$\boldsymbol{\Omega}$, Ω	Angular velocity of the Earth

Miscellaneous Symbols

$\langle\,\cdot\,\rangle$	Turbulent averaging operator
$\langle\!\langle\,\cdot\,\rangle\!\rangle = \langle\,\cdot\,\rangle$	Statistical averaging property of the REYNOLDS filter
$\{\cdot\}$	$\langle\,\rho(\cdot)\,\rangle / \langle\rho\rangle$ FAVRE filter (barycentric)
$\langle\, f\,\rangle$	Turbulent average of f
f'	Turbulent fluctuation of f
$[\![\, f\,]\!]$	$\equiv f^{+} - f^{-}$ Jump of f across a singular surface
$I_{\boldsymbol{A}}$	$\equiv \mathrm{tr}\boldsymbol{A}$ First invariant of $\boldsymbol{A}$
$II_{\boldsymbol{A}}$	$\equiv \frac{1}{2}\left(I_{\boldsymbol{A}^2} - (I_{\boldsymbol{A}})^2\right)$ Second invariant of $\boldsymbol{A}$
$III_{\boldsymbol{A}}$	$\equiv \det \boldsymbol{A}$ Third invariant of $\boldsymbol{A}$
$II_{\boldsymbol{\sigma}'}^{\varepsilon,k}$	Parameters in the boundary layer representation of ε and k
$\nabla_{\mathbb{S}} f$, $\mathrm{Grad}\, f$	$\equiv \dfrac{\partial f}{\partial \xi^{\mathfrak{a}}}\,\boldsymbol{\tau}^{\mathfrak{a}}$ Surface gradient
Div	Surface divergence: $\mathrm{Div}\boldsymbol{v} \equiv \dfrac{\partial \boldsymbol{v}}{\partial \xi^{\mathfrak{a}}} \cdot \boldsymbol{\tau}^{\mathfrak{a}}$, $\quad \mathrm{Div}\,\boldsymbol{T} \equiv \dfrac{\partial \boldsymbol{T}}{\partial \xi^{\mathfrak{a}}}\,\boldsymbol{\tau}^{\mathfrak{a}}$

Acknowledgment The authors thank Prof. Rutschmann for publication of this work in his 'Mitteilungen'. They also thank Dr. F. Zunic and his crew for handling all editing details. While performing this work we have been self-supporting.

References

[1] Ahrens, J.P. A fall velocity equation. *J. Waterways, Port, Coastal and Ocean Engineering* **126**(2), 99-102 (2000)

[2] Alts, T. and Hutter, K. Continuum description of the dynamics and thermodynamics of phase boundaries between ice and water. Part I: Surface balance laws and their interpretation in terms of three dimensional balance laws averaged over the phase change boundary layer. *J. Non-Equilibrium Thermodyn.* **13**, 221-257 (1988)

[3] Alts, T. and Hutter, K. Continuum description of the dynamics and thermodynamics of phase boundaries between ice and water. Part II: Thermodynamics. *J. Non-Equilibrium Thermodyn.* **13**, 259-280 (1988)

[4] Alts, T. and Hutter, K. Continuum description of the dynamics and thermodynamics of phase boundaries between ice and water. Part III: Thermostatics and its consequences. *J. Non-Equilibrium Thermodyn.* **13**, 301-329 (1988)

[5] Alts, T. and Hutter, K. Continuum description of the dynamics and thermodynamics of phase boundaries between ice and water. Part IV: On thermostatic stability and well posedness. *J. Non-Equilibrium Thermodyn.* **14**, 1-22 (1989)

[6] Brown, P.P. and Lawler, D.F. Sphere drag and settling velocity revisited. *J. Environmental Engineering*, **129**(3), 222-231 (2003)

[7] Caamenen, B. Simple and general formula for the settling velocity of particles. *J. Hydraulic Engineering*, **133**(2), 229-233 (2007)

[8] Cheng, N.S. Simplified settling velocity formula for sediment particle. *J. Hydraul. Engineering*, **123**(2), 149-152 (1997)

[9] Concha, F. and Almendra, E.R. Settling velocities of particle systems: I Settling velocities of individual spherical partiles. *Int. J. Mineral Processing.* **5**(4), 349-367 (1979)

[10] Eglund, F. and Hansen, E. *A monograph on sediment transport in alluvial streams*, third Ed. Technical Press, Copenhagen (1972)

[11] Einstein, H.A. The bedload function for sediment transportation in open channel flow. *Technical Bulletin Nr 1026* U.S. Dept. Agriculture, Washington DC. (1950)

[12] Germano, M., Piolelli, U., Moin, P. and Cabiot, W.H. A dynamic subgrid-scale eddy viscosity model. *Phys. Fluids A* **3**(7), 1760-1765 (1991)

[13] Guo, J. Logarithmic matching and its application in computational hydraulics and sediment transport. *J. Hydraul. Research*, **40**(5), 555-565 (2002)

[14] Hanjalic, K. and Launder, B.E. A Reynolds stress model of turbulence in its application to thin shear flows. *J. Fluid Mech.* **52**, 609-638 (1972)

[15] Hutter, K. The physics of ice-water phase change surfaces In: CISM Lectures: *Modelling macroscopic phenomena at liquid boundaries*, Murdoch, I. and Kosinski, W., eds., Springer Verlag New York, Vienna (1992)

[16] Hutter, K. *Fluid und Thermodynamik, eine Einführung*. Springer Verlag Berlin etc. (2003)

[17] Hutter, K. and Jöhnk, K. *Continuum Methods of Physical Modeling*. Springer, Berlin, 635p (2004)

[18] Hutter, K., Wang, Y. and Chubarenko, I. *Physics of Lakes - Foundation of the Mathematical and Physical Background* Vol. I. Springer, Berlin, 434p (2011)

[19] Hutter, K., Wang, Y. and Chubarenko, I. *Physics of Lakes - Lakes as Oscillators* Vol. II, Springer, Berlin, 646p (2011)

[20] Jimenez, J.A. and Madsen, O.S. A simple formula to estimate settling velocity of natural sediments. *J. Waterways, Port, Coastal and Ocean Engineering* **129**(2), 70-78 (2003)

[21] Jones, W.P and Launder, B.E. The prediction of laminarisation with a two-equation model of turbulence. *J. Heat Mass Tranf.* **15**, 301-314 (1972)

[22] Julien, Y.P. *Erosion and Sedimentation*. Cambridge University Press, Cambridge (1995)

[23] Kraft, S. Wang, Y. and Oberlack, M. Large eddy simulation of sediment deformation in a turbulent flow by means of level set method. *J. Hydr. Eng.* ASCE, November 2011, 1-12 (2011)

[24] Launder, B.E and Spalding, D.B. The numerical computation of turbulent flow. *Comp. Meth. Appl. Mech. Eng.* **3**, 269-288 (1974)

[25] Lilly, D. K. The representation of small-scale turbulence in numerical simulation experiments. *Proc. IBM Scientific Computing Symp. Environ. Sci.*, 195-210 (1967)

[26] Luca, I., Fang, Ch. and Hutter, K. A thermodynamic model of turbulent motion in a granular material. *Continuum Mech. Thermodyn.* **16**, 363-390 (2004)

[27] McGauhay, P.H. Theory of Sedimentation. *J. of the American Water Works Assoc.* **48**, 437-448 (1956)

[28] Miles, J. W. On the stability of heterogeneous shear flows. *J. Fluid Mech.* **10**, 496-508 (1967)

[29] Moin, P. and Kim, J. Numerical investigation of turbulent channel flow. *J. Fluid Mech.*, **118**(1), 341-377 (1982)

[30] Müller, I. Thermodynamics, Pitman, London (1985)

[31] Munk, W. H. On the wind-driven ocean circulation *J. Meteorology*, **7**, 79 (1950)

[32] Piomelli, U. High Reynolds number calculations using the dynamic subgri-scale stress model. *Phys. Fluids A* **5**(6), 1484 (1993)

[33] Piomelli, U. and Zang, T. A. Large eddy simulation of transitional channel flow. *Comput. Phys. Commun.* **65**(1-3), 224-230 (1991)

[34] Prandtl, L. Neuere Ergebnisse der Turbulenzforschung. *Zeitschr. VDI* **77**, 105-113 (1933)

[35] Rodi, W. Examples of calculation methods for flow and mixing in stratified fluids. *J. Geophys. Res.* (C5), **92**, 5305-5328 (1987)

[36] Rodi, W. *Turbulence Models and Their Application in Hydraulics* IAHR Monograph Series. A.A. Balkema, Rotterdam/Brookfield (1993)

[37] Rotta, J.C. *Turbulente Strömungen, eine Einführung in die Theorie und ihre Anwendung*, Teubner, Stuttgart, 267 p (1972)

[38] She, K., Trim, L. and Pope, D. Fall velocities of natural sediment particles: A simple mathematical presentation of the fall velocity law. *J. Hydraul. Research*, **43**(2), 189-195 (2005)

[39] Shields, A. Anwendung der Ähnlichkeitsmechanik und der Turbulenzforschung. *Mitt. der Preussischen Versuchsanstalt für Wasser- und Schiffsbau*, Heft 26, Berlin (1936)

[40] Slattery, J. C., Sagis, L. and Oh, E.-S. Interfacial transport phenomena. 2^{nd} Ed., Springer (2007)

[41] Smagorinsky, J. General circulation experiments with the primitive equations I. The basic experiment. *Mon. Weather Rev.* **91**(3), 99-165 (1963)

[42] Song, Z., Wu, T., Xu, F. and Li, R. A simple formula for predicting settling velocity of sediment particles. *Water Science and Engineering*, **1**(1) 37-43 (2008) DOI:10.3882/j.issn.1674-2370.2008.01.005

[43] Soulsby, R.L. *Dynamics of Marine Sands.* Thomas Telford, London (1997)

[44] Thomas, T.Y. *Plastic Flow and Fracture in Solids.* Academic Press, New York, London (1961)

[45] Turton, R. and Clark, N.N. An explicit relationship to predict spherical particle terminal velocity. *Power Technol.* **53**(2), 1127-129 (1987)

[46] Van Rijn, L.C. Sediment pick-up functions. *J. Hydraul. Eng. ASCE* **110**(10), 1494-1502 (1984)

[47] Van Rijn, L.C. Sediment transport, Part II: Suspended load transport. *J. Hydraul. Eng. ASCE* **110**(11), 1613-1641 (1984)

[48] Van Rijn, L.C. Unified view of sediment transport by currents and waves. I: Initiation of motion, bed roughness, and bed-load transport. *J. Hydraul. Eng. ASCE* **133**(6), 649-667 (2007)

[49] Vetsch, D. *Numerical Simulation of Sediment Transport with Meshfree Methods.* Doctoral Dissertation, Laboratory of Hydraulics, Hydrology and Glaciology, Swiss Federal Institute of Technology, Zurich p. 200 (2012)

[50] Wang, Y. *Windgetriebene Strmungen in einem Rechteckbecken und im Bodensee.* PhD thesis, TH Darmstadt, Germany, Shaker Verlag, Aachen, ISBN 3-8265-1381-9. p. 432 (1996)

[51] Wilcox, D.C. Reassessment of the scale determining equation for advanced turbulence models. *AIAA J.* **26**(11), 1299-1310 (1988)

[52] Wilcox, D.C. *Turbulence modeling for CFD.* DWC Industries, Inc.,La Cañada, California, 2nd Edition (1998)

[53] Yalin, M.S. *Mechanics of sediment transport.* Second Edition Pergamon Press, Oxford, (1977)

[54] Yalin, M.S. On the determination of ripple geometry. *J. Hydraul. Eng.* **111**(8), 1148-1155 (1985)

[55] Yalin, M.S. and da Silva, A.M.F. *Fluvial processes.* IAHR International Association of Hydraulic Engineering and Research (2001)

[56] Zanke, U. Berechnung der Sinkgeschwindigkeiten von Sedimenten. *Mitt. des Franzius-Instituts für Wasserbau* **46**, 243 p (1977)

[57] Zanke, U.C.E. Zum Einfluss der Turbulenz auf den Beginn der Sedimentbewegung *Mitt. Institut für Wasserbau und Wasserwirtschaft* Techn. Hochschule Darmstadt p 120 (2001)

[58] Zhang, R.J *Sediment Dynamics in Rivers.* Water Resources Press (in Chinese) (1989)

[59] Zhu, L.J. and Cheng, N.S. *Settlement of settling particles.* River and Harbour Engineering Department, Nanjing Hydraulic Research Institute, Nanjing (in Chinese) (1993)